Journal of Oncology

Metastasis: Genetics, Mechanism, and Diagnostic and Therapeutic Strategies

Guest Editors: Mehmet Gunduz, Esra Gunduz, Levent Beder, Davut Pehlivan, Omer Faruk Hatipoglu, Sushant Kachhap, and Reidar Grenman

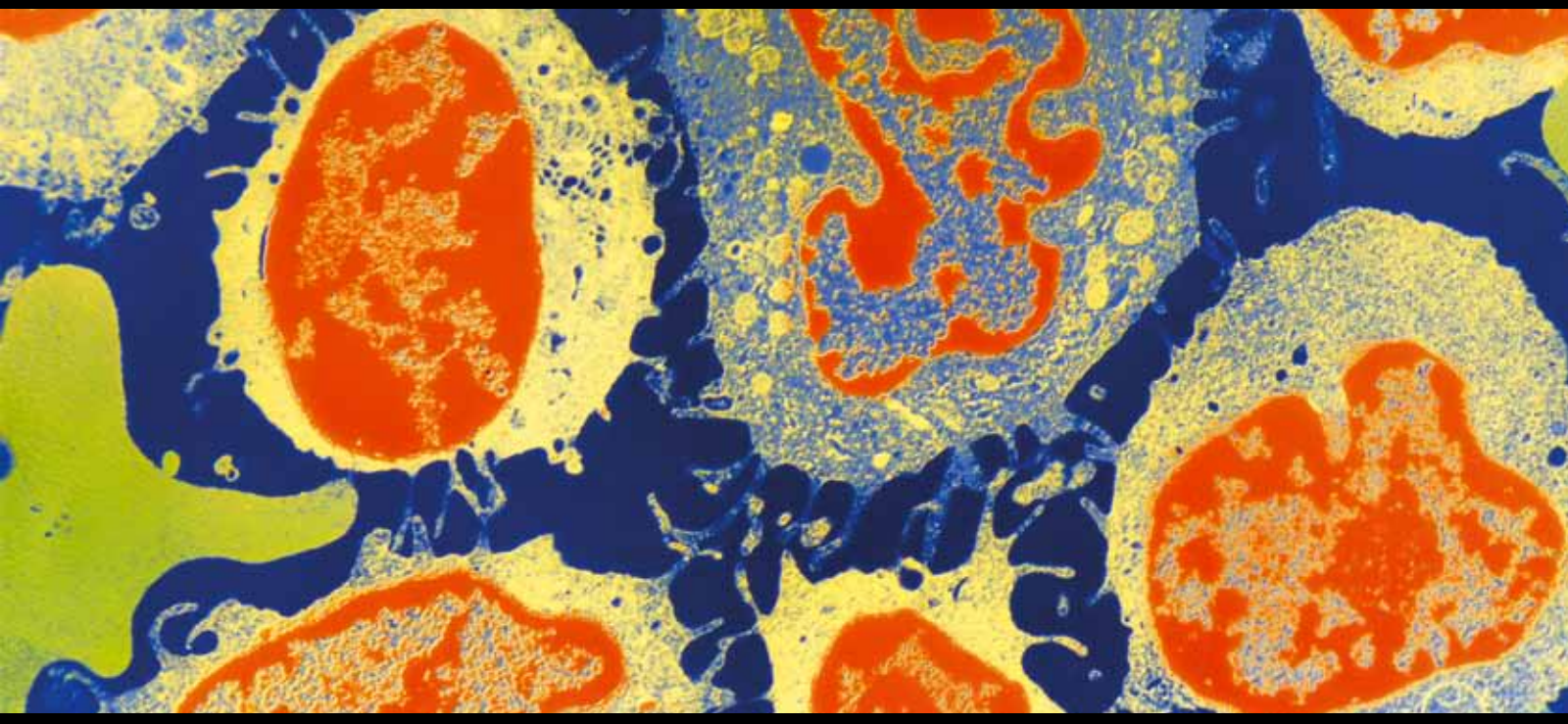

Metastasis: Genetics, Mechanism, and Diagnostic and Therapeutic Strategies

Journal of Oncology

Metastasis: Genetics, Mechanism, and Diagnostic and Therapeutic Strategies

Guest Editors: Mehmet Gunduz, Esra Gunduz, Levent Beder, Davut Pehlivan, Omer Faruk Hatipoglu, Sushant Kachhap, and Reidar Grenman

Editorial Board

Contents

Metastasis: Genetics, Mechanism, and Diagnostic and Therapeutic Strategies, Mehmet Gunduz, Esra Gunduz, Levent Beder, Davut Pehlivan, Omer Faruk Hatipoglu, Sushant Kachhap, and Reidar Grenman
Volume 2012, Article ID 390835, 2 pages

Metastatic Behavior in Melanoma: Timing, Pattern, Survival, and Influencing Factors, Faruk Tas
Volume 2012, Article ID 647684, 9 pages

Salivary Protein Profiles among HER2/neu-Receptor-Positive and -Negative Breast Cancer Patients: Support for Using Salivary Protein Profiles for Modeling Breast Cancer Progression, Charles F. Streckfus, Daniel Arreola, Cynthia Edwards, and Lenora Bigler
Volume 2012, Article ID 413256, 9 pages

Adamantyl Retinoid-Related Molecules Induce Apoptosis in Pancreatic Cancer Cells by Inhibiting IGF-1R and Wnt/β-Catenin Pathways, Lulu Farhana, Marcia I. Dawson, Jayanta K. Das, Farhan Murshed, Zebin Xia, Timothy J. Hadden, James Hatfield, and Joseph A. Fontana
Volume 2012, Article ID 796729, 14 pages

Dual Roles of *METCAM* in the Progression of Different Cancers, Guang-Jer Wu
Volume 2012, Article ID 853797, 13 pages

Angiogenesis in Paget's Disease of the Vulva and the Breast: Correlation with Microvessel Density, Patricia E. Ellis, Allan B. MacLean, L. F. Wong Te Fong, Julie C. Crow, and Christopher W. Perrett
Volume 2012, Article ID 651507, 6 pages

The Molecular Biology of Brain Metastasis, Gazanfar Rahmathulla, Steven A. Toms, and Robert J. Weil
Volume 2012, Article ID 723541, 16 pages

A Proposal of a Practical and Optimal Prophylactic Strategy for Peritoneal Recurrence, Masafumi Kuramoto, Shinya Shimada, Satoshi Ikeshima, Akinobu Matsuo, Hiroshi Kuhara, Kojiro Eto, and Hideo Baba
Volume 2012, Article ID 340380, 7 pages

Hindawi Publishing Corporation
Journal of Oncology
Volume 2012, Article ID 390835, 2 pages
doi:10.1155/2012/390835

Editorial

Metastasis: Genetics, Mechanism, and Diagnostic and Therapeutic Strategies

Mehmet Gunduz,[1] Esra Gunduz,[2] Levent Beder,[3] Davut Pehlivan,[4] Omer Faruk Hatipoglu,[5] Sushant Kachhap,[6] and Reidar Grenman[7]

[1] *Departments of Medical Genetics and Otorhinolaryngology, Faculty of Medicine, Fatih University, Istanbul, Turkey*
[2] *Department of Medical Genetics, Faculty of Medicine, Fatih University, Istanbul, Turkey*
[3] *Department of Otorhinolaryngology, Wakayama Medical University, Wakayamashi, Wakayama, Japan*
[4] *Department of Molecular and Human Genetics, Baylor College of Medicine, Houston, TX, USA*
[5] *Department of Molecular Biology and Biochemistry, Okayama University, Okayama, Japan*
[6] *Prostate Cancer/Genitourinary Program, The Sidney Kimmel Comprehensive Cancer Center, Baltimore, MD, USA*
[7] *Department of Otorhinolaryngology, University of Turku and Turku University Hospital, Turku, Finland*

Correspondence should be addressed to Mehmet Gunduz, mehmet.gunduz@gmail.com

Received 11 December 2012; Accepted 11 December 2012

Tumor masses are composed of heterogenic subpopulations of cancer cells, and cancer stem cell theory suggests that only a specific subpopulation of these cells has the ability to sustain cancer growth and metastatic activity, whereas all of the other cancer cells have only a limited growth potential or no growth potential at all. Based on this concept in the literature, to define the aggressiveness of a tumor, examination of the molecular characteristics of metastatic cell populations is a logical way to characterize cancer stem cells.

The general prognosis of patients with various cancer types has not improved significantly, despite major advances in early detection, surgical resection, and chemoradiation protocols. The poor outcome has mainly been attributed to local and distant lymph node metastasis as well as recurrence. The ability to assess or predict the presence of metastasis has significant prognostic relevance and treatment implications in the management of cancer. In order to decrease morbidity and mortality from cancer, it is necessary to gain a greater understanding of metastasis and define the molecular factors that contribute to this process.

In this special issue, metastatic behaviour of several cancer types is reviewed. One of them is an aggressive tumor type, though its incidence is low. F. Tas presented the clinical outcome of a relatively large number of melanoma cases, and over 200 patients were followed up for metastasis and survival. Due to its aggressive character, more than 30% of the melanoma cases were already metastatic when it was diagnosed first time. Most common metastatic organs were lung, liver, bone, and brain. In another lethal cancer type, in pancreatic cancer, L. Farhana et al. examined the effect of adamantly-retinoid-related (ARR) molecules in 3 pancreatic cancer cell lines. They found that two different ARR compounds inhibited not only the pancreatic cancer cell lines but also their cancer stem-cell-like populations (CD44+/CD24+ cells), and this inhibition was through suppression of IGF1R and Wnt/BCatenin pathways. Induction of apoptosis in the pancreatic cancer cell lines by ARR compounds suggested novel therapeutic agents for this chemotherapy-resistant cancer type. In another interesting study for early diagnostics, C. Streckfus et al. compared the salivary protein components of two different breast cancer patients group, one is positive for Her2 and the other is negative for this marker, but they are all in the same tumor stages (II). They performed a proteomic analysis of the saliva from the two groups by LC-MS/MS mass spectrometer. 71 proteins among 188 comparative saliva proteins were differentially expressed. There were 34 upregulated proteins, while 37 proteins were downregulated. In conclusion, they suggested that salivary gland proteins may be a real-time in vivo follow-up marker for breast cancer progression.

P. Ellis et al. examined angiogenesis in vulvar as well as breast Paget diseases. Using anti-Von Willebrand factor

antibody, microvessel density was determined in Paget diseases of Vulva and Breast. Increased microvessel density was demonstrated in Paget's disease of the breast with DCIS and with carcinoma alone compared to Paget's disease of the breast alone, suggesting that neovascularisation is an important process in the development of Paget's disease of the breast. Metastasis to the central nervous system (CNS) remains a major cause of morbidity and mortality in patients with systemic cancers. Various crucial interactions between the brain environment and tumor cells take place during development of the cancer at its new location. In one of the current papers in this issue, G. Rahmathulla et al. summarized the principal molecular and genetic mechanisms that underlie the development of brain metastasis (BrM) from aspects of migration-related events and molecules such as epithelial mesenchymal transition, interaction with tumor stroma, e-cadherin catenin complex, integrins, matrix metalloproteinases, urokinase-type plasminogen activator, CAI1, and tumor colonization. By this way, the authors tried to increase knowledge of the metastatic process leading to better detection and treatment of brain metastases.

METCAM, an integral membrane cell adhesion molecule (CAM) in the Ig-like gene superfamily, is capable of performing typical functions of CAMs, such as mediating cell-cell and cell-extracellular interactions, crosstalk with intracellular signaling pathways, and modulating social behaviors of cells. In this special issue, G. Wu et al. investigated many possible mechanisms mediated by this CAM during early tumor development and metastasis. METCAM-induced tumorigenesis has been studied in melanoma, prostate cancer, breast cancer, and ovarian cancer. In conclusion, they emphasized that preclinical trials using a fully humanized anti-METCAM antibody against melanoma growth and metastasis and using a mouse anti-METCAM monoclonal antibody against angiogenesis and tumor growth of hepatocarcinoma, leiomyosarcoma, and pancreatic cancer have been successfully demonstrated. Alternatively, small soluble peptides derived from METCAM may also be useful for blocking the tumor formation and tumor angiogenesis.

M. Kuramoto et al. focused on peritoneal metastasis, which often arises in patients with advanced gastric cancer and is well known as a miserable and ill-fated disease.

The authors suggested extensive intraoperative peritoneal lavage (EIPL) as a useful and practical adjuvant surgical technique for those gastric cancer patients who are likely to suffer from peritoneal recurrence. By this way, they tried to diagnose early and prevent peritoneal recurrences.

Metastasis and its molecular steps are still unclear, and their identification is crucial for curing the cancer. Recent and future developments in molecular medicine will allow to better understand metastatic process and early diagnose as well as treat the patients in a better way.

Mehmet Gunduz
Esra Gunduz
Levent Beder
Davut Pehlivan
Omer Faruk Hatipoglu
Sushant Kachhap
Reidar Grenman

Hindawi Publishing Corporation
Journal of Oncology
Volume 2012, Article ID 647684, 9 pages
doi:10.1155/2012/647684

Clinical Study

Metastatic Behavior in Melanoma: Timing, Pattern, Survival, and Influencing Factors

Faruk Tas

Institute of Oncology, Istanbul University, 34390 Istanbul, Turkey

Correspondence should be addressed to Faruk Tas, faruktas2002@yahoo.com

Received 10 October 2011; Accepted 24 April 2012

Academic Editor: Levent Beder

Metastatic melanoma (MM) is a fatal disease with a rapid systemic dissemination. This study was conducted to investigate the metastatic behavior, timing, patterns, survival, and influencing factors in MM. 214 patients with MM were evaluated retrospectively. Distant metastases (82%) were the most frequent for patients initially metastatic. The median and 1-year survival rates of initially MM patients were 10 months and 41%, respectively. The median time to metastasis for patients with localized disease was 28 months. The timing of appearance of metastases varied minimally; however, times to metastases for distant organs varied greatly. For the first metastatic pathway, more than half of the primary metastases were M1A (57%). These findings were in contrast to the results compared with those with metastatic in diagnosis ($P < 0.001$). The median and 1-year survival rates of all patients were 12 months and 49%, respectively. Outcome was higher in M1A than visceral metastases ($P < 0.001$). In conclusion, the fact that over half of all recurrences/metastases occurred within 3 years urges us to concentrate follow-up in the early time periods following diagnosis. Because the clinical behavior of MM is variable, the factors for survival consisting of site and number of metastases should be emphasized.

1. Introduction

Over several decades, the incidence of melanoma has steadily risen as incidence rates have increased by averages ranging from 3 to 8% per year and continue to rise nowadays. Melanoma represented estimated 5% and 4% of incidents of cancer in males and females in 2009 and it was the fifth and sixth most common type of cancer in males and females, respectively [1]. Now, presents a lifetime risk of one in 39 for men and one in 58 for women in the USA.

Melanoma is an aggressive and highly metastatic disease. Metastatic melanoma is a fatal disease with a rapid systemic dissemination. The 5-year survival rate is less than 15% in patients with metastatic disease. While the minority of patients, which constitute 4% of newly diagnosed melanoma patients [1], present with distant metastasis at initial diagnosis, the majority who present with early stage initially eventually develop metastatic disease as a consequence of disease progression. Approximately one-third of all melanoma patients will experience disease recurrence [2]. Although almost all organs can be involved, the most frequent target sites are the liver, bone, and brain. Despite recent advances in the understanding of oncogenic mechanisms and therapeutic interventions, the median survival in patients with metastatic disease does not go beyond 12 months.

In spite of the fact that factors that predict recurrence have been well described, few studies have investigated the natural history of melanoma, including factors that determine and influence type, pattern, and timing of recurrence/metastases of melanoma [2–6]. In this retrospective study, we analyzed the metastatic timing, patterns, and factors influencing metastasis and survival in patients with metastatic melanoma.

2. Material and Methods

Two hundred and fourteen patients with histologically confirmed melanoma, treated in our clinic with metastatic disease from 1997 to 2009, were evaluated retrospectively; 66 patients presented initially with metastatic disease, while 148 patients with early stage developed metastasis during treatment or follow-up.

All patients were evaluated and staged at the first visit by history, physical examination, CBC, serum biochemistry analysis, chest X-ray and CT imaging, cranial CT or MRI, whole-body scan and abdominal CT or USG (ultrasonography). The standard follow-up protocol was applied for all of the patients.

Time to metastasis was defined as the time period from the date of histological diagnosis to the time of appearance of metastasis. Overall survival was determined as the time elapsed between the time of histological diagnosis and the date of death or the last follow-up visit. The period from the date of relapse to death or the last follow-up day was referred to as the postrecurrence survival.

χ^2 tests were performed to test differences of frequencies. Overall and postrecurrence survival values were analyzed by the Kaplan-Meier method. Univariate analyses were performed by the log-rank tests. Statistical differences were accepted as significant at $P < 0.05$.

3. Results

The median age of 214 patients was 50 years (range: 22 to 86), and there was a predominance of males, 62% of subjects were men. Patient characteristics are summarized in Table 1. Sixty-six patients presented initially with metastatic disease, while 148 developed metastatic disease during follow-up for early stages. The distribution of metastatic involvement is shown in Table 2.

Table 1: Patient's characteristics.

Parameter	Metastasis at presentation (%)	Metastasis during follow-up (%)
	31	69
Gender		
Male	65	61
Female	35	39
Age		
Median (range)	50 (22–86)	49 (24–83)
Localization		
Axial	56	58
Extremity	44	42
Histology		
Nodular	50	51
Nonnodular	50	49
Breslow thickness		
<4mm	50	51
>4mm	50	49
Clark invasion		
I–III	5	18
IV-V	95	82
Ulceration		
No	36	17
Yes	64	83
Mitotic rate (/mm^2)		
Median (range)	3 (1–46)	4 (1–52)
Lymphocyte infiltration		
No	47	40
Yes	53	60
Regression		
No	83	85
Yes	17	15
Vascular invasion		
No	71	82
Yes	29	18
Neurotropism		
No	89	93
Yes	11	7

3.1. Metastases at Presentation. Totally 66 patients (31% of all patients) were diagnosed with metastatic disease at presentation.

The characteristics of the patients are shown in Table 1. The median age was 50 years, two-thirds of the patients were men, and their primary lesions were more axial sited (56%). The distributions of clinicopathologic forms (nodular versus nonnodular) and Breslow thickness (less versus more than 4 mm) were identical.

Slightly more than half (56%) of the patients presented with single metastases (Table 2). The distant metastases, 82% totally, combined with 67% for M1C and 15% for M1B, were the most frequent for initially metastatic patients, and distant skin, subcutaneous, or nodal metastases (M1A) were the least common (18%). For the involvement of distant organ other than the lung (M1C), liver was the most common site (48%) followed by the brain (29%) and bone (23%).

The distribution of metastatic behaviors, such as the number and site of metastases, was not different in relation to the parameters of the tumors and the patients.

The median and 1-year survival rates of initially metastatic patients were determined as 10 months and 41%, respectively (Figure 1). Survival in patients with single metastasis was higher than that in those with multiple metastases (median 12 versus 7 months, resp., $P = 0.07$). Likewise, as statistically insignificant, the patients with M1A had the higher and those with M1C had the lower survival rates ($P = 0.2$). However, there was no difference in distribution of visceral organ involvement with respect to organ site metastases ($P = 0.8$).

3.2. Metastases during Follow-Up. One hundred and forty-eight patients with cutaneous melanoma diagnosed at the stage of the primary tumor without detectable metastases subsequently developed metastases. The characteristics of the patients are shown in Table 1. Regarding patient and disease parameters, no difference was found between the patients who presented with metastases at diagnosis and these patients.

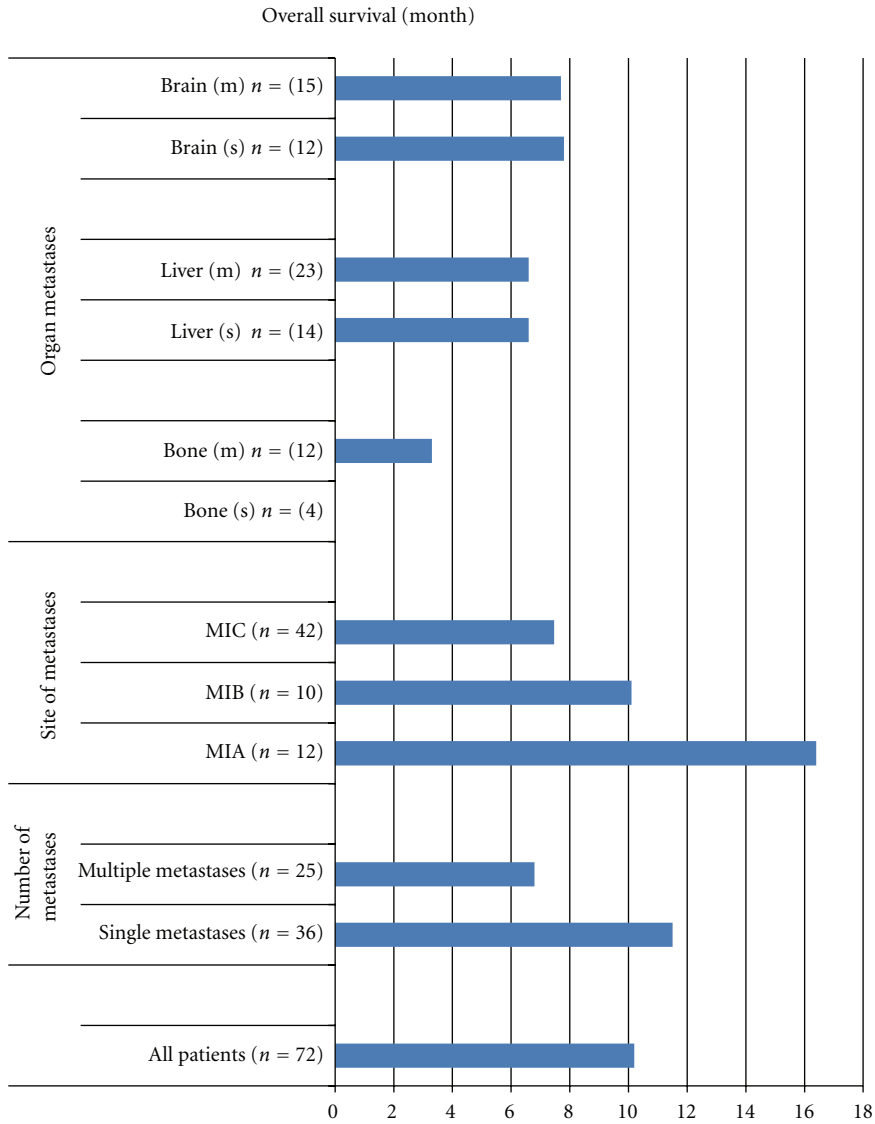

Figure 1: Overall survival rates of metastatic patients diagnosed at presentation. S: only single-organ metastasis; M: mixed with other distal organ metastases.

Table 2: Metastatic patterns of cases.

	Metastasis at presentation 66 (31%)	Metastasis during follow-up 148 (69%)	Secondary metastasis 72 (34%)
Number of involvements			
Single	37 (56%)	98 (66%)	45 (63%)
Multiple	29 (44%)	50 (34%)	27 (37%)
Stage IV			
M1A	12 (18%)	84 (57%)	18 (25%)
M1B	10 (15%)	19 (13%)	8 (11%)
M1C	44 (67%)	45 (30%)	46 (64%)
Stage M1C			
Bone	12 (23%)	18 (37%)	17 (31%)
Liver	25 (48%)	20 (42%)	14 (25%)
Brain	15 (29%)	10 (21%)	24 (44%)

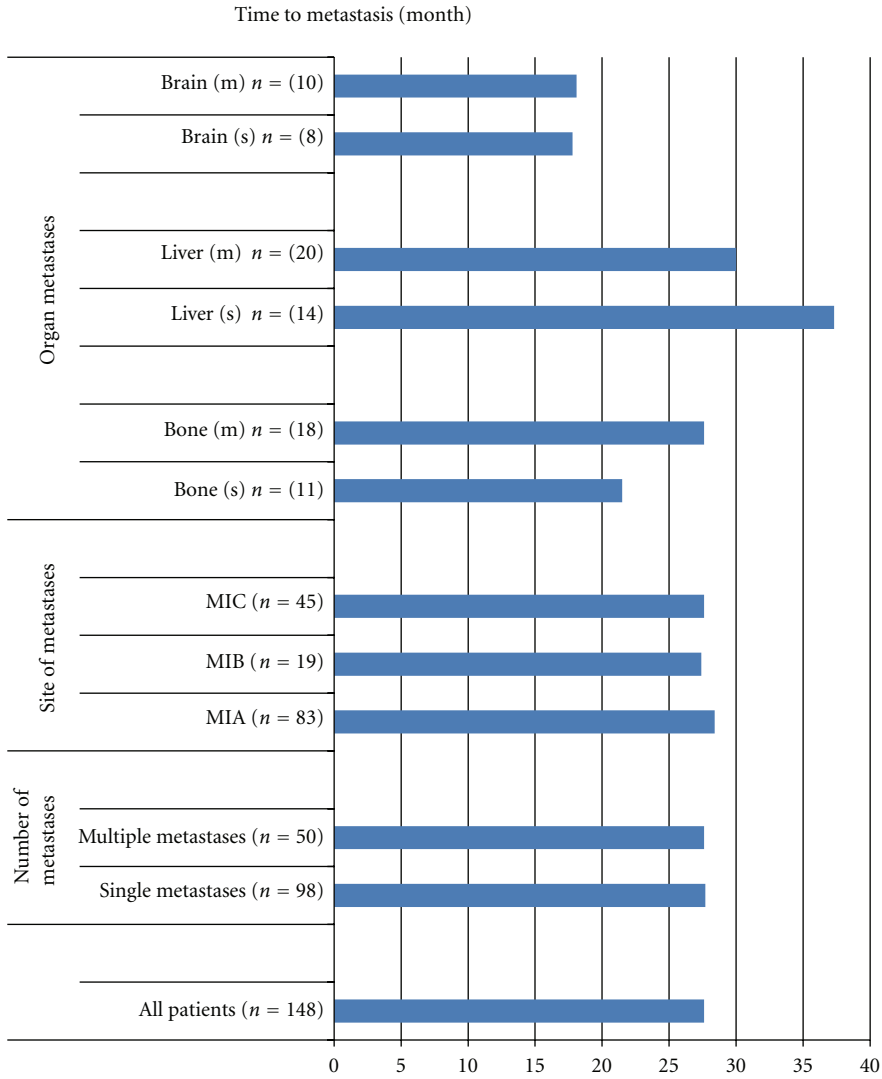

Figure 2: Time periods to metastases in metastatic patients with diagnosed during follow-up.

The median time to metastasis for the 148 patients with localized disease who developed metastases during follow-up was 28 months (Figure 2). The timing of appearance of metastases according to metastatic M1 stage varied minimally. Thus, the median times to metastases were 28, 27, and 28 months for patients with M1A, M1B, and M1C, respectively. Likewise, there is no difference for occurrence time of metastasis between single and multiple metastases. However, times to metastases for distal organs other than the lung varied greatly: the longer times for liver metastases, the shorter times for brain metastases, and the equal values for bone metastases.

Two-thirds of the patients had single metastatic disease (Table 2). The first metastatic pathway in relation to the primary tumor site showed that more than half of the primary metastases were distant skin, subcutaneous, or nodal metastases (M1A) (57%) followed by distant metastases other than the lung (M1C) (30%) and lung metastases (M1B) (13%). These findings were contrast to the results compared with those with metastatic in diagnosis ($P < 0.001$). The percentages of the liver (42%) and bone (37%) involvement were identical and more than cerebral metastasis (21%). When compared with the group containing the metastatic patients diagnosed at presentation, no difference was found.

The median survival and 1-year survival rates of all patients were 12 months and 49%, respectively (Figure 3). Single-organ metastasis showed significant survival advantages compared with multiple metastases (median 20 versus 6 months, resp., $P < 0.001$). Similarly, overall survival was found to be significantly higher in M1A than in M1B and M1C ($P < 0.001$). However, in contrary to this, there was no difference among distant organs with respect to site of organ involvement.

3.3. Secondary Metastases. In our study, 72 out of total 214 (34%) patients with metastatic melanoma went on to develop metastases twice during follow-up. With respect to gender and age of the patients, there was no difference

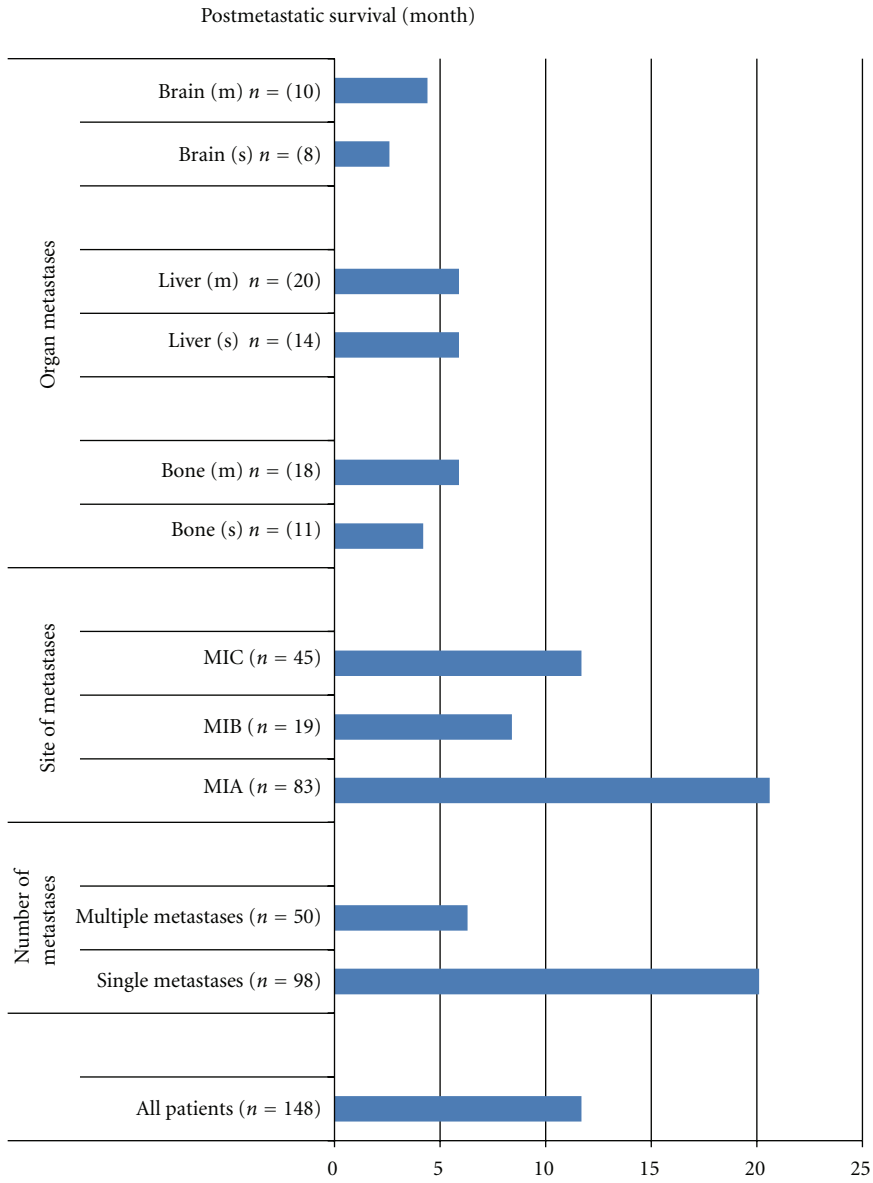

Figure 3: Postmetastatic survival values in metastatic patients diagnosed during follow-up.

among patients. Interestingly, patients with axial localization of primary melanoma (92%) presented mostly than those with extremity sites ($P < 0.001$).

The median time to development of second metastases from the time of first metastases was 11 months (Figure 4). The timing of appearance of metastases according to metastatic M1 stage varied greatly. Thus, the median times to development were 20 and 21 months for M1A and M1B, respectively, and M1C had highly lower times (9 months). However, in contrast, there were no differences for occurrence times among the M1C organs.

When we look at the occurrence from first metastases to second metastases, more transformations occurred among M1A to M1C (32%), M1A to M1A (21%), M1B to M1C, (17%), and M1C to M1C (15%) of patients (Table 3).

Table 3: Transformations of metastases from first to second.

From	To		
	M1A	M1B	M1C
M1A ($n = 45$)	15 (33%)	7 (16%)	23 (51%)
M1B ($n = 14$)	1 (7%)	1 (7%)	12 (86%)
M1C ($n = 13$)	2 (15%)	0 (0%)	11 (85%)

The development of M1C prominently occurred in consequence of 51% for M1A, 86% for M1B, and 85% for M1C.

The timing of appearances of metastases according to metastatic transformation varied The median times to secondary metastases development were 20 and 21 months

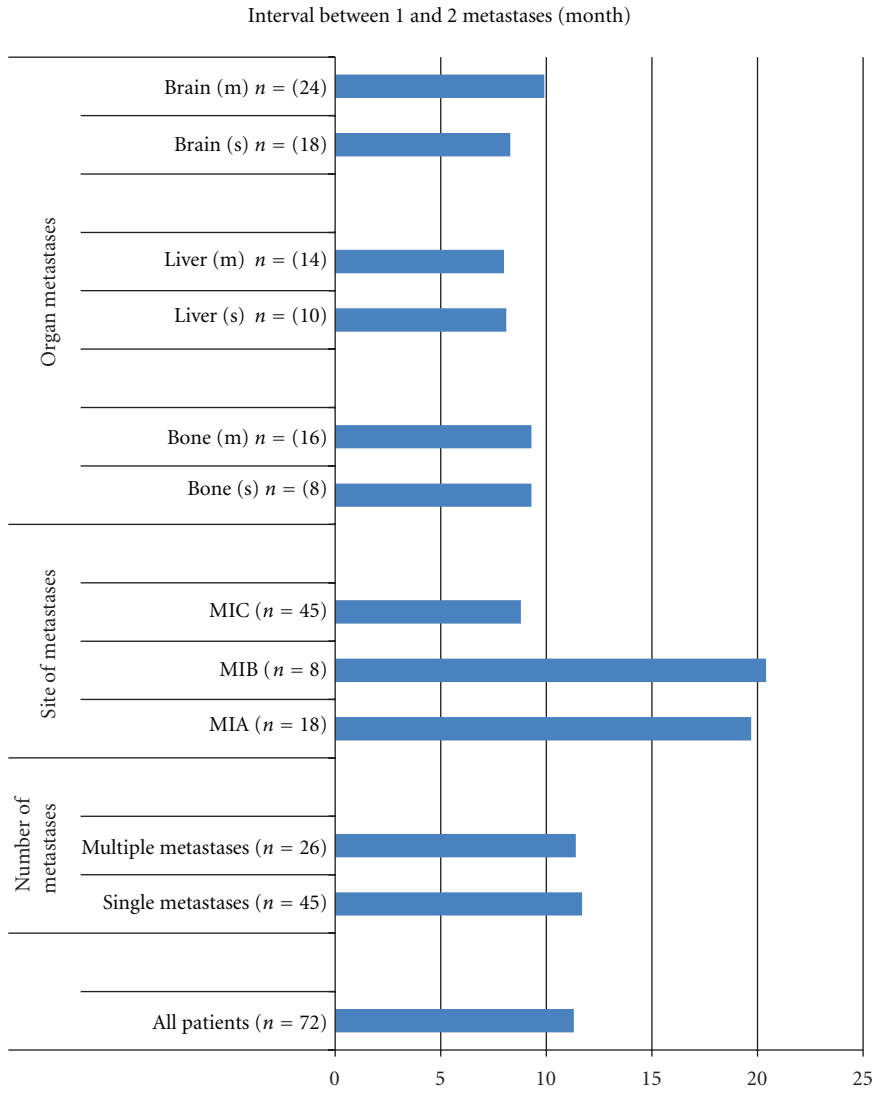

Figure 4: Intervals from the date of first metastases to the date of second metastases in metastatic patients who presented twice with metastatic disease.

for M1A to M1A and M1A to M1B, respectively, and 7 months for M1C to M1C (Figure 5).

Similar to former groups, the metastatic distribution was single metastatic area in nearly two-thirds of patients (Table 2). Identical to the patients with metastases at presentation, 75% of the patients who developed clinical metastases secondarily presented with distant metastases, combined with 64% for M1C plus 11% for M1B and distant skin, subcutaneous, or nodal metastases (M1A) developed in only one-fourth of patients (Table 2). In other words, these findings were in contrast with the data in metastases during follow-up ($P < 0.001$) and similar to the data regarding metastases at presentation (Figure 6).

In 44% of the patients the second metastases during follow-up developed in the brain. In the remaining half of the patients, bone (31%) and liver (25%) involvement carried out (Table 2). These values are statistically different from both metastasis at presentation ($P = 0.05$) and metastasis during follow-up ($P = 0.04$) (Figure 7). While bone metastases were distributed equally with respect to gender, liver (64% versus 36%, $P = 0.02$) and brain (79% versus 21%, $P = 0.04$) metastases were found more in females and males, respectively. No other correlation was found between the factors of patient/disease and the number/site of the metastases.

4. Discussion

Patients with metastatic melanoma generally have a poor prognosis; survival is limited and typically measured in months rather than years. In general, the duration of survival is less than a year, a median of nearly 6 to 8 months. The 1-year survival rate is 45%, and less than 10% will live for 5 years or more. Multivariate analyses of prognostic factors have identified several independent factors that predict survival in this poor prognosis group, including the site of

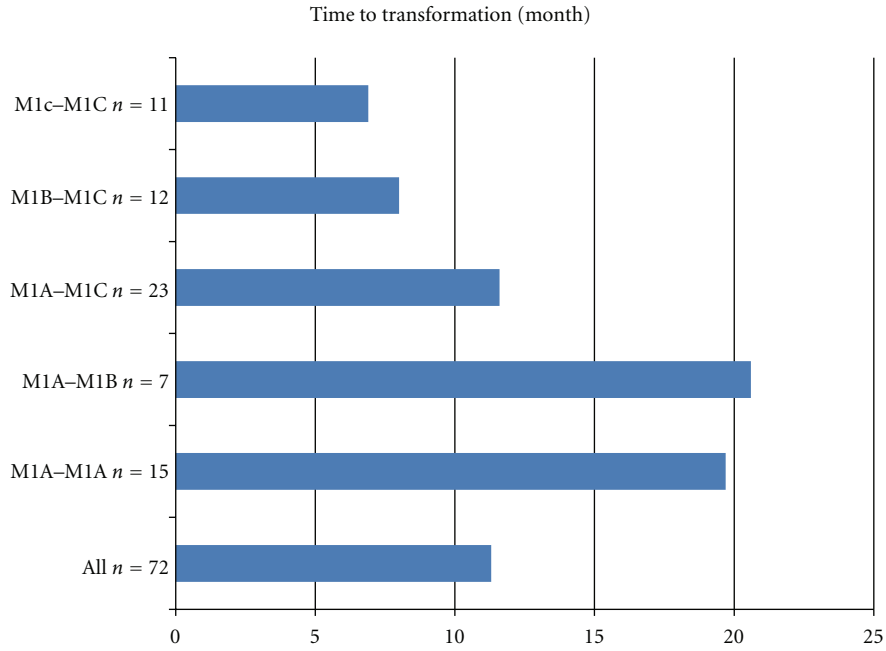

Figure 5: Intervals between initial metastases and secondary metastases.

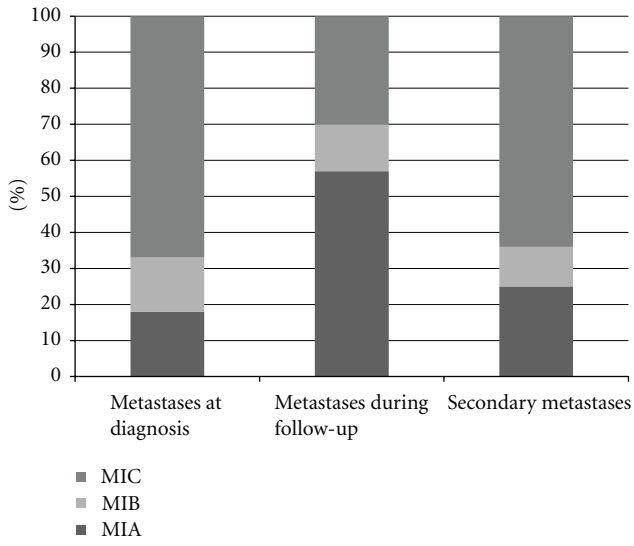

Figure 6: The distributions of M stages depend on time of metastasis presentation (%).

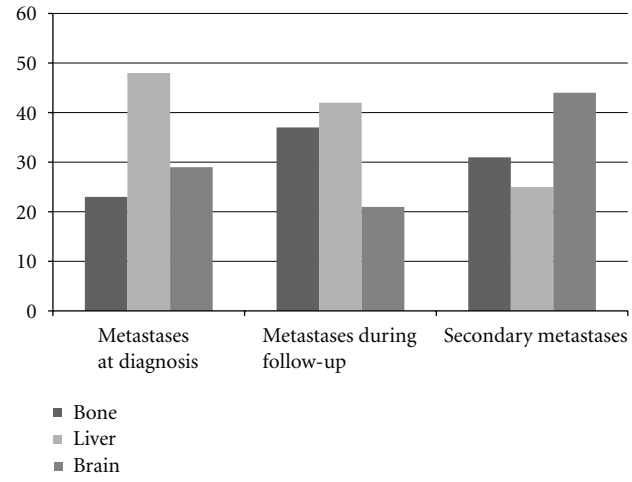

Figure 7: The distributions of distant organs depend on time of metastasis presentation (%).

the first metastases, number of metastatic sites, and duration of remission [2–4].

The site of distant metastasis is an important independent predictor of survival in patients with metastatic disease [3, 4]. In the 2002 AJCC melanoma database analysis, the greatest difference in survival was found showing that patients with locoregional, distant nodal, and soft tissue metastasis have a better survival rate than the patients with visceral metastasis [3, 7]. Additionally, patients in whom the lung was the only site of visceral metastasis had a better 1-year survival duration time compared with those with metastasis in other visceral sites. In the recent analysis of the AJCC melanoma database, separation of patients into three groups based on sites of disease produced the greatest splay in median survival [3, 8]. Patients with melanoma metastasis to visceral sites other than the lung (M1C) had a median survival of 7 months, those with lung metastases had a median survival of 12 months, and those with metastasis to nonvisceral sites (i.e., skin, subcutaneous tissue, and distant lymph nodes) had a median survival of 18 months. In general, patients who have visceral metastases to sites other than the lung, such as the liver, brain, or bone, do poorly with a median survival ranging from 3 to 6 months.

Patients with one distant metastatic site have a significantly improved outcome compared with those with two or more distant sites [3]. The number of metastatic sites was the most significant prognostic factor in patients with distant metastasis [9]. In this study, patients with one, two, three, or more sites of distant metastasis had a median survival duration of 7, 4, and 2 months, respectively. The 1-year survival rate was 36% for patients with one metastatic site, 13% for patients with two sites, and less than 1% for patients with three or more sites. In another study, the number of metastases, one versus more than one, was the strongest independent predictor of survival; the median survival times for groups were 23 months and 8 months, respectively [10]. In the 2008 stage IV collaborative melanoma database preliminary analysis, the number of metastatic sites was also associated with survival by both univariate and multivariate analyses [8]. In contrast to these studies, however, the number of metastatic sites was not a significant independent prognostic factor in the multivariate analysis of the studies [11]. This may suggest that certain sites of metastases have a dominant negative effect on survival. Patients whose initial site of metastases was the liver or brain had a median survival of only 4 months compared with patients whose initial sites were the skin and/or lymph nodes, who had a median survival of 15 months [4, 11].

Few patients with newly diagnosed melanoma have clinically evident distant metastases at the initial diagnosis [1, 4]. The majority of the metastatic patients who present with early stage initially eventually develop metastatic disease as a consequence of disease progression. Nearly one-third of all melanoma patients will experience disease recurrence [2]. For most patients without distant metastases, the time to recurrence/metastasis varies inversely with tumor stage at presentation. For patients with thicker tumors the risk of recurrence is the greatest in the first year after treatment and declines steadily over time [2, 4]. Most recurrences (55% to 79%) become evident by 2 years, whereas 65% to 85% are apparent by 3 years after the initial diagnosis of the primary tumor. In addition, the disease-free interval is considerably shorter in patients with ulcerated tumors [2, 4]. In general, patients with nodal metastases, stage III, have recurrences earlier than patients whose lymph nodes are negative. In addition, age of diagnosis can also influence the timing of distant metastases, that is, patients older than 50 years of age have been shown to relapse sooner than younger patients. The disease-free interval before the onset of distant metastasis was a significant prognostic factor in a multivariate analysis of studies [9, 11]. The stage of disease preceding distant metastasis was also identified as an important prognostic factor [11]. For patients who progressed directly from stage I or II disease, a disease-free interval of 34 months or longer was associated with prolonged survival, whereas for patients with a history of stage III melanoma, a disease-free interval of 18 months or longer was associated with prolonged survival.

Melanoma is well known for its ability to metastasize to virtually any organ or tissue, including some sites rarely seen with other solid tumors [4]. Nevertheless, some sites are more likely to harbor initial distant metastases. The initial sites of distant metastases are most commonly the skin, subcutaneous tissue, and lymph nodes, which occurred in 42% to 59% of patients in various studies. Visceral metastases were the initial sites of relapse in approximately 25% of all metastatic melanoma patients. The most common sites of visceral metastases were the lung (18–36%), brain (12–20%), liver (14–20%), and bone (11–17%).

In conclusion, lifetime follow-up of melanoma patients, particularly during the first three years, is necessary because the expected cure is rarely achieved after surgical excision and also given adjuvant treatment. The fact that over half of all recurrences/metastases occurred within 3 years urges us to concentrate follow-up in the early time periods following diagnosis. Generally, the prognosis of patients with metastatic melanoma is poor; however, because the clinical behavior of metastatic melanoma is variable, significant factors for survival consisting of site of metastasis and number of metastatic sites should be emphasized.

Conflict of Interests

The authors have no conflict of interests to declare.

References

[1] A. Jemal, R. Siegel, E. Ward, Y. Hao, J. Xu, and M. J. Thun, "Cancer statistics, 2009," *CA Cancer Journal for Clinicians*, vol. 59, no. 4, pp. 225–249, 2009.

[2] S.-J. Soong, R. A. Harrison, W. H. McCarthy, M. M. Urist, and C. M. Balch, "Factors affecting survival following local, regional, or distant recurrence from localized melanoma," *Journal of Surgical Oncology*, vol. 67, no. 4, pp. 228–233, 1998.

[3] J. E. Gershenwald, C. M. Balch, S. J. Soong, and J. F. Thompson, "Prognostic factors and natural history of melanoma," in *Cutaneous Melanoma*, C. M. Balch, A. N. Houghton, A. J. Sober, S. J. Soong, M. B. Atkins, and J. F. Thompson, Eds., pp. 35–64, Quality Medical Publishing, St. Louis, Mo, USA, 5th edition, 2009.

[4] M. B. Atkins, A. Hauschild, R. L. Wahl, and C. M. Balch, "Diagnosis of Stage IV melanoma," in *Cutaneous Melanoma*, C. M. Balch, A. N. Houghton, A. J. Sober, S. J. Soong, M. B. Atkins, and J. F. Thompson, Eds., pp. 573–602, Quality Medical Publishing, St. Louis, Mo, USA, 5th edition, 2009.

[5] F. Meier, S. Will, U. Ellwanger et al., "Metastatic pathways and time courses in the orderly progression of cutaneous melanoma," *British Journal of Dermatology*, vol. 147, no. 1, pp. 62–70, 2002.

[6] A. Tejera-Vaquerizo, M. V. Barrera-Vigo, I. Fernández-Canedo et al., "Longitudinal study of different metastatic patterns in the progression of cutaneous melanoma," *Actas Dermo-Sifiliograficas*, vol. 98, no. 8, pp. 531–538, 2007.

[7] C. M. Balch, S. J. Soong, J. E. Gershenwald et al., "Prognostic factors analysis of 17,600 melanoma patients: validation of the American Joint Committee on Cancer melanoma staging system," *Journal of Clinical Oncology*, vol. 19, no. 16, pp. 3622–3634, 2001.

[8] J. E. Gersenhenwald, D. L. Morton, J. F. Thompson et al., "Staging and prognostic factors for stage IV melanoma: initial results of an American Joint Committee on Cancer (AJCC) international evidence-based assessment of 4895 melanoma patients. Forty-fourth Annual Meeting of the American

Society of Clinical Oncology, Chicago, IL, May 2008," *Journal of Clinical Oncology* , vol. 26, supplement, abstract 9035, 2008.

[9] C. M. Balch, S. Soong, and T. M. Murad, "A multifactorial analysis of melanoma. IV. Prognostic factors in 200 melanoma patients with distant metastases (stage III)," *Journal of Clinical Oncology*, vol. 1, no. 2, pp. 126–134, 1983.

[10] H. B. Neuman, A. Patel, N. Ishill et al., "A single-institution validation of the AJCC staging system for stage IV melanoma," *Annals of Surgical Oncology*, vol. 15, no. 7, pp. 2034–2041, 2008.

[11] A. Barth, L. A. Wanek, and D. L. Morton, "Prognostic factors in 1,521 melanoma patients with distant metastases," *Journal of the American College of Surgeons*, vol. 181, no. 3, pp. 193–201, 1995.

Hindawi Publishing Corporation
Journal of Oncology
Volume 2012, Article ID 413256, 9 pages
doi:10.1155/2012/413256

Clinical Study

Salivary Protein Profiles among HER2/neu-Receptor-Positive and -Negative Breast Cancer Patients: Support for Using Salivary Protein Profiles for Modeling Breast Cancer Progression

Charles F. Streckfus, Daniel Arreola, Cynthia Edwards, and Lenora Bigler

Department of Diagnostic Sciences, UTHSC, Dental Branch, Behavioral and Biomedical Sciences Building, Rm. 5322, Houston, TX 77054, USA

Correspondence should be addressed to Charles F. Streckfus, charles.streckfus@uth.tmc.edu

Received 25 October 2011; Accepted 17 January 2012

Academic Editor: Esra Gunduz

Purpose. The objective of this study was to compare the salivary protein profiles from individuals diagnosed with breast cancer that were either HER2/neu receptor positive or negative. *Methods.* Two pooled saliva specimens underwent proteomic analysis. One pooled specimen was from women diagnosed with stage IIa HER2/neu-receptor-positive breast cancer patients ($n = 10$) and the other was from women diagnosed with stage IIa HER2/neu-receptor-negative cancer patients ($n = 10$). The pooled samples were trypsinized and the peptides labeled with iTRAQ reagent. Specimens were analyzed using an LC-MS/MS mass spectrometer. *Results.* The results yielded approximately 71 differentially expressed proteins in the saliva specimens. There were 34 upregulated proteins and 37 downregulated proteins.

1. Introduction

Clinicopathologic factors such as histological type, tumor size, tumor grade, hormone receptor status, lymph node involvement, and HER-2/neu overexpression are recognized as having prognostic use in breast cancer management. HER-2/neu (HER2), also known as c-*erb*B-2, is a biomarker assayed in tissue biopsies from women diagnosed with malignant breast tumors [1, 2]. Used primarily as a prognostic indicator, HER2/neu protein is overexpressed in approximately 20%–30% of malignant breast tumors and has been used in postoperative followup evaluation as an indicator of patient relapse [3–6].

The evolution of HER2 testing, first as a prognostic marker assay and later as a diagnostic test to determine eligibility for trastuzumab-targeted therapy, has expanded the role of traditional diagnostic pathology. Unlike most testing performed by anatomic pathologists, which serves as an adjunct to establishing a diagnosis, the results of HER2 testing stand alone in determining which patients are likely to respond to trastuzumab therapy. HER2 status may also predict sensitivity to certain cytotoxic drugs and antiestrogens [3–6].

Currently, two testing methods are approved by the Food and Drug Administration (FDA) for HER2 assessment in the laboratory [1, 2]. They are immunohistochemical analysis (IHC) and fluorescence *in situ* hybridization (FISH). Commercially available, FDA-approved HER2 assays are available for both methods. Immunohistochemical analysis and FISH have the advantage over other assay methods (i.e., those requiring homogenization) because they are morphologically driven. This allows for the direct evaluation of tumor cells, correlation with other morphologic features, and the ability to assay smaller patient samples such as needle core biopsy specimens [1, 2].

While clinical treatment choices are critical, the actual tests used to determine HER2 status have demonstrated a number of pitfalls. One such pitfall is the number of false negatives and false positives associated with the tests. This creates a treatment dilemma as it can result in situations

where patients requiring trastuzumab-targeted therapy may not receive it, while those receiving trastuzumab-targeted therapy should not receive it [6–8].

Not everyone is convinced that the problem is as simple as false negatives and false positives. One problem may be with the cutoff points that scientists have established to delineate between HER2 negative and positive in IHC testing. Data from several preclinical and clinical studies suggest that trastuzumab activity does not strictly require HER2 overexpression or gene amplification, as is currently thought. Instead, even tumor cells that express a lower level of the protein might respond to a trastuzumab-chemotherapy combination. Currently, tumors that have moderate amounts of HER2 protein would be scored as 1+ or 2+ on IHC tests and would be called negative because they are below the predetermined cutoff value for the test [1–8].

Even FISH testing, which is considered the "gold standard" for detecting gene amplification, has problems. The test measures the ratio between the area surrounding the HER2 gene on chromosome 17 and other parts of chromosome 17. That means a cell that has extra copies of chromosome 17, called polysomy 17, appears negative by FISH but actually has extra copies of HER2, and probably expresses more protein than a wild-type cell would [1, 2].

The inconsistency in the test may stem, in part, from heterogeneity of HER2 expression in the tumor sample. If so, then multiple tests on the same tumor could yield different results, even though the tests are working as designed. The testing problem has been a matter of discussion, and how it will be resolved remains unclear. However, clinicians and researchers agree that current technology to assess HER2 status needs improvement [1–8].

Therefore, the purpose of this study was twofold. The first objective was to compare salivary protein profiles among Her2-receptor-positive and -negative breast cancer patients and secondly, to support the theory for using salivary protein profile expression as a method for modeling breast cancer progression [9, 10].

2. Methods

2.1. Design. The investigators protein profiled three pooled, stimulated whole saliva specimens. One specimen consisted of pooled saliva from 10 stage IIa ($T_2N_0M_0$) HER2-receptor-status-positive invasive ductal carcinoma patients (IDC), and the second pooled specimen was from 10 subjects diagnosed with stage IIb ($T_2N_0M_0$), HER2-receptor-status-positive invasive ductal carcinoma. The cancer cohorts were estrogen, progesterone receptor status negative as determined by the pathology report. Histological grade was not available for this study. The subjects were matched for age and race and were nontobacco users.

The participating subjects were given an explanation about their participation rights, and they signed an IRB consent form. The saliva specimens and related patient data are nonlinked and bar-coded in order to protect patient confidentiality. This study was performed under the UTHSC IRB-approved protocol number HSC-DB-05-0394. All procedures were in accordance with the ethical standards of the UTHSC IRB and with the Helsinki Declaration of 1975, as revised in 1983.

2.2. Saliva Collection and Sample Preparation. Stimulated whole salivary gland secretion is based on the reflex response occurring during the mastication of a bolus of food. Usually, a standardized bolus (1 gram) of paraffin or a gum base (generously provided by the Wrigley Co., Peoria, IL) is given to the subject to chew at a regular rate. The individual, upon sufficient accumulation of saliva in the oral cavity, expectorates periodically into a preweighed disposable plastic cup. This procedure is continued for a period of five minutes. The volume and flow rate is then recorded along with a brief description of the specimen's physical appearance [9, 10]. The cup with the saliva specimen is reweighed and the flow rate determined gravimetrically. A protease inhibitor from Sigma Co. (St. Louis, MI, USA) is added along with enough orthovanadate from a 100 mM stock solution to bring its concentration to 1 mM. The treated samples were centrifuged for 10 minutes at top speed in a tabletop centrifuge. The supernatant was divided into 1 mL aliquots and frozen at −80.

2.3. Two-Dimensional Gel Analysis (2D DIGE)

2.3.1. Sample Preparation. 2D DIGE and protein ID was performed by Applied Biomics, Inc. (Hayward, CA). Proteins from the saliva were precipitated by methanol then resuspended in a 2D cell lysis buffer (30 mM Tris-HCl, pH 8.8, containing 7 M urea, 2 M thiourea, and 4% CHAPS). Protein concentration was measured using Bio-Rad protein assay method.

2.3.2. CyDye Labeling. For each sample, 30 ug of protein was mixed with 1.0 μL of diluted CyDye and kept in dark on ice for 30 min. Samples from each pair were labeled with Cy2 and Cy5, respectively. The labeling reaction was stopped by adding 1.0 μL of 10 mM Lysine to each sample, and incubating in dark on ice for additional 15 min. The labeled samples were then mixed together. The 2X 2D sample buffer (8 M urea, 4% CHAPS, 20 mg/mL DTT, 2% pharmalytes, and trace amount of bromophenol blue), 100 μL destreak solution, and Rehydration buffer (7 M urea, 2 M thiourea, 4% CHAPS, 20 mg/mL DTT, 1% pharmalytes, and trace amount of bromophenol blue) were added to the labeling mix to make the total volume of 250 μL. They were Mixed well and spined before loading the labeled samples into strip holder.

2.3.3. IEF and SDS-PAGE. After loading the labeled samples, IEF (pH3-10 Linear) was run following the protocol provided by Amersham BioSciences. Upon finishing the IEF, the IPG strips were incubated in the freshly made equilibration buffer 1 (50 mM Tris-HCl, pH 8.8, containing 6 M urea, 30% glycerol, 2% SDS, trace amount of bromophenol blue, and 10 mg/mL DTT) for 15 minutes with gentle shaking. Then the strips were rinsed in the freshly made equilibration

Table 1: Upregulated salivary proteins.

Access no.	Gene ID	%Cov	Name	Ratio	*P* value
P63261	ACTG	65.1	Actin, cytoplasmic 2	1.207	0.030
P07108	ACBP	28.7	Acyl-CoA-binding protein	1.161	0.002
P06733	ENOA	61.3	Alpha-enolase	1.193	0.030
P04083	ANXA1	56.1	Annexin A1	1.457	0.000
P03973	ALK1	36.4	Antileukoproteinase 1 precursor	2.188	0.004
Q8N4F0	BPIL1	27.3	Bactericidal/permeabilityincreasing	1.386	0.000
P35321	SPR1A	70.8	Cornifin-A	1.696	0.003
P22528	SPR1B	61.8	Cornifin-B	1.722	0.000
P01040	CYTA	87.8	Cystatin-A	1.788	0.000
P04080	CYTB	72.4	Cystatin-B	1.514	0.000
P01034	CYTC	62.3	Cystatin-C precursor	1.183	0.030
P35527	K1C9	25.5	Cytokeratin-9	1.512	0.001
Q9UGM3	DMBT1	39.0	Deleted in malignant brain tumors 1	1.191	0.000
Q01469	FABPE	45.2	Fatty acid-binding protein, epidermal	1.191	0.000
P01877	IGHA2	52.6	Ig alpha-2 chain C region	1.125	0.040
P01834	KAC	88.7	Ig kappa chain C region	1.128	0.040
P06309	KV205	31.6	Ig kappa chain V-II region GM607	1.274	0.030
P18510	IL1RA	31.6	Interleukin-1 receptor antagonist protein	2.050	0.000
P22079	PERL	46.5	Lactoperoxidase precursor	1.190	0.000
P31025	LCN1	46.6	Lipocalin-1 precursor	1.853	0.000
P26038	MOES	15.3	Moesin	1.991	0.020
P62937	PPIA	58.2	Peptidyl-prolyl cis-trans-isomerase A	1.553	0.003
P01833	PIGR	58.4	Polymeric-immunoglobulin receptor	1.452	0.000
Q16378	PROL4	58.2	Proline-rich protein 4 precursor	3.092	0.000
P05109	S10A8	58.1	Protein S100-A8	1.318	0.000
P06702	S10A9	57.0	Protein S100-A9	1.833	0.000
Q96DA0	U773	27.5	Protein UNQ773/PRO1567 precursor	1.930	0.000
P29508	SPB3	20.3	Serpin B3	2.910	0.000
Q96DR5	SPLC2	52.2	Short-palate lung and nasal epith. carc.	1.435	0.000
Q9UBC9	SPRR3	81.1	Small proline-rich protein 3	2.035	0.000
P60174	TPIS	42.2	Triosephosphate isomerase	1.257	0.012
P07477	TRY1	35.2	Trypsin-1 precursor	3.135	0.000
P62988	UBIQ	68.4	Ubiquitin	1.142	0.003
Q6P5S2	CF058	31.8	Uncharacterized protein C6orf58	1.603	0.000

buffer 2 (50 mM Tris-HCl, pH 8.8, containing 6 M urea, 30% glycerol, 2% SDS, trace amount of bromophenol blue, and 45 mg/mL DTT) for 10 minutes with gentle shaking. Next, the IPG strips were rinsed in the SDS-gel running buffer before transferring into 13.5% SDS gels. The SDS gels were run at 15°C until the dye front exuded out of the gels.

2.3.4. Image Scan and Data Analysis. Gel images were scanned immediately following the SDS-PAGE using Typhoon TRIO (Amersham BioSciences). The scanned images were then analyzed by Image Quant software (version 6.0, Amersham BioSciences), followed by in-gel analysis using DeCyder software version 6.0 (Amersham BioSciences). The fold change of the protein expression levels was obtained from in-gel DeCyder analysis.

2.4. Top-Down Mass Spectrometry Using iTRAQ Labeling. A thorough explanation for the top-down mass spectrometry using iTRAQ labeling can be found in detail in previous publications [9, 10]. Briefly, the saliva samples were thawed and immediately centrifuged to remove insoluble materials. The supernatant was assayed for protein using the Bio-Rad protein assay (Hercules, CA, USA), and an aliquot containing 100 μg of each specimen was precipitated with six volumes of −20°C acetone. The precipitate was resuspended and treated according to the manufacturer's instructions. Protein digestion and reaction with iTRAQ labels was carried out as previously described and according to the manufacturer's instructions (Applied Biosystems, Foster City, CA). Briefly, the acetone precipitable protein was centrifuged in a tabletop centrifuge at 15,000 ×g for

Table 2: Downregulated salivary proteins.

Access no.	Gene ID	%Cov	Name	Ratio	*P* value
Q01518	CAP1	11.4	Adenylyl cyclase	0.7295	0.0077
P02763	|A1AG1	37.8	Alpha-1-acid glycoprotein	0.7571	0.0070
P04217	A1BG	21.2	Alpha-1B-glycoprotein	0.5602	0.0420
P01023	A2MG	23.3	Alpha-2-macroglobulin	0.4395	0.0000
P02647	APOA1	52.1	Apolipoprotein A-I	0.8928	0.0488
P02812	PRB2	100.0	Salivary prp 2	0.8307	0.0020
P01024	CO3	18.3	Complement C3	0.7227	0.0434
P28325	CYTD	39.4	Cystatin-D	0.8297	0.0027
P09228	CYTT	76.6	Cystatin-SA	0.7736	0.0003
P13646	K1C13	70.3	cytoskeletal 13	0.1058	0.0000
P19013	K2C4	72.3	cytoskeletal 4	0.1269	0.0000
P13647	K2C5	53.7	cytoskeletal 5	0.2291	0.0019
P06396	GELS	34.7	Gelsolin	0.6744	0.0004
P00738	HPT	51.2	Haptoglobin	0.6346	0.0000
P69905	HBA	31.7	Hemoglobin subunit alpha	0.5039	0.0000
P68871	HBB	56.5	Hemoglobin subunit beta	0.6774	0.0000
P16403	H12	18.8	Histone H1.2	0.3436	0.0056
P16104	H2AX	34.3	Histone H2A.x (H2a/x)	0.1531	0.0014
Q16778	|H2B2E	38.1	Histone H2B type 2-E	0.2383	0.0005
Q71DI3	H32	39.0	Histone H3.2	0.1580	0.0000
P62805	H4	50.5	Histone H4	0.1913	0.0000
P01857	IGHG1	46.4	Ig gamma-1 chain C region	0.5308	0.0000
P01859	IGHG2	42.0	Ig gamma-2 chain C region	0.5593	0.0000
P01777	HV316	20.2	Ig heavy chain V-III region TEI	0.6363	0.0408
P01842	LAC	83.8	Ig lambda chain C regions	0.7805	0.0017
P01871	MUC	30.2	Ig mu chain C region	0.7708	0.0009
P02788	TRFL	58.5	Lactotransferrin	0.8219	0.0012
P08246	ELNE	9.7	Leukocyte elastase	0.5594	0.0304
P14780	MMP9	28.0	Matrix metalloproteinase-9	0.5891	0.0002
P05164	PERM	37.0	Myeloperoxidase	0.4892	0.0016
P80303	NUCB2	27.1	Nucleobindin-2	0.8093	0.0370
Q06830	PRDX1	15.1	Peroxiredoxin-1	0.7488	0.0010
P07737	PROF1	65.7	Profilin-1	0.6752	0.0010
P80511	S10AC	40.2	Protein S100-A12	0.7363	0.0121
Q08188	TGM3	20.8	Glutamyltransferase E precursor	0.6357	0.0074
P02787	TRFE	51.6	Serotransferrin precursor	0.5730	0.0000
P37837	TALDO	29.7	Transaldolase	0.6777	0.0119
P08670	VIME	27.5	Vimentin	0.4832	0.0407

20 minutes. The acetone supernatant was removed and the pellet resuspended in 20 ȚL dissolution buffer. The soluble fraction was denatured, and disulfides were reduced by incubation in the presence of 0.1% SDS and 5 mM TCEP (tris-(2-carboxyethyl) phosphine) at 60°C for one hour. Cysteine residues were blocked by incubation at room temperature for 10 minutes with MMTS (methyl methanethiosulfonate). Trypsin was added to the mixture to a protein: trypsin ratio of 10 : 1. The mixture was incubated overnight at 37°C. The protein digests were labeled by mixing with the appropriate iTRAQ reagent and incubating at room temperature for one hour. On completion of the labeling reaction, the four separate iTRAQ reaction mixtures were combined. Since there are a number of components that can interfere with the LCMSMS analysis, the labeled peptides are partially purified by a combination of strong cation exchange followed by reverse-phase chromatography on preparative columns. The combined peptide mixture is diluted 10-fold with loading buffer (10 mM, KH_2PO_4 in 25% acetonitrile at pH 3.0) and applied by syringe to an ICAT Cartridge-Cation Exchange column (Applied Biosystems, Foster City, CA) column that has been equilibrated with the same buffer. The column is washed with 1 mL loading buffer to remove contaminants. To improve the resolution of peptides

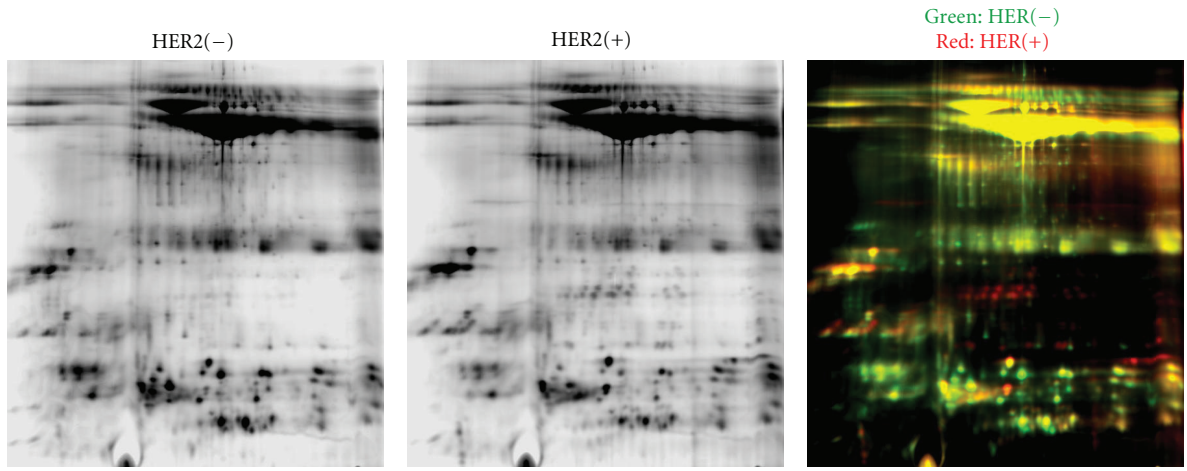

Figure 1: This figure illustrates the protein profiles for HER2/neu-receptor-positive and HER2/neu-receptor-negative samples. As shown in the far right red and green dyed gel comparisons, there are numerous differences between the two profiles.

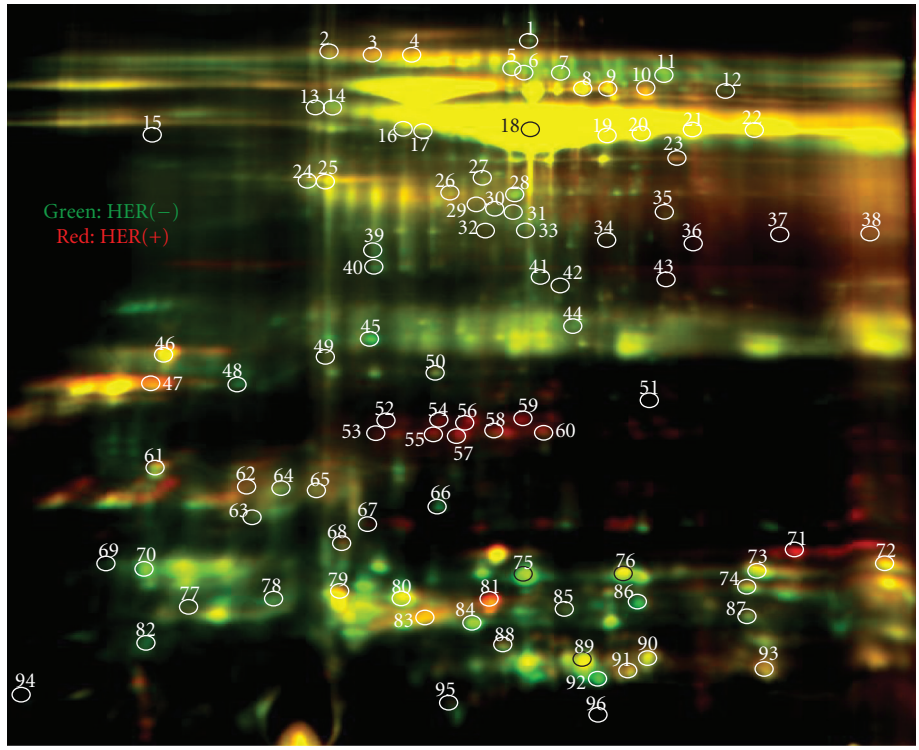

Figure 2: This figure demonstrates the differences in salivary protein profiles between HER2/neu -positive and HER2/neu -negative samples. Please change.

during LCMSMS analysis, the peptide mixture is partially purified by elution from the cation exchange column in three fractions. Stepwise elution from the column is achieved with sequential 0.5 mL aliquots of 10 mM KH_2PO_4 at pH 3.0 in 25% acetonitrile containing 116 mM, 233 mM, and 350 mM KCl, respectively. The fractions are evaporated by Speed Vac to about 30% of their volume to remove the acetonitrile and then slowly applied to an Opti-Lynx Trap C18 100 μL reverse-phase column (Alltech, Deerfield, IL) with a syringe. The column was washed with 1 mL of 2% acetonitrile in 0.1% formic acid and eluted in one fraction with 0.3 mL of 30% acetonitrile in 0.1% formic acid. The fractions were dried by lyophilization and resuspended in 10 μL 0.1% formic acid in 20% acetonitrile solution. Each of the three fractions

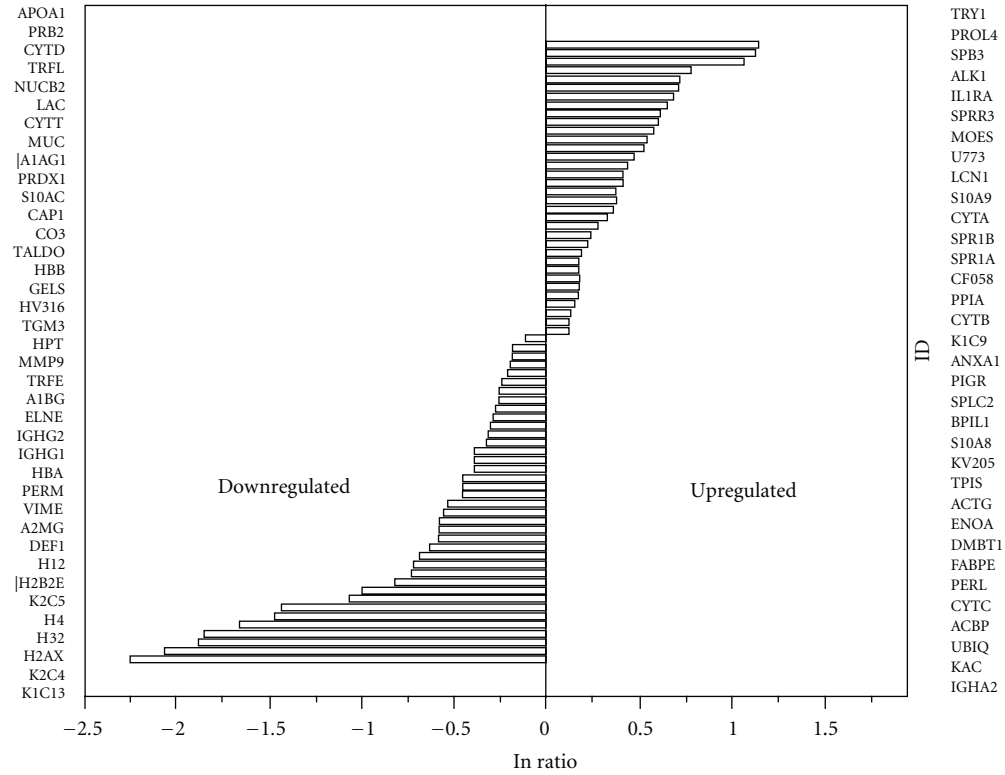

Figure 3: The figure represents the natural logarithm differential expression of salivary proteins. To the right and left of the figure listed in rank order of expression are the up- and downregulated proteins, respectively.

was analyzed by reverse-phase nano-LCMS/MS on an API QSTAR XL mass spectrometer (ABS Sciex Instruments).

2.5. Bioinformatics. The Swiss-Prot database was employed for protein identification, while the PathwayStudio bioinformatics software package was used to determine Venn diagrams that were also constructed using the NIH software program (http://ncrr.pnl.gov/). Graphic comparisons with log conversions and error bars for protein expression were produced using the ProQuant software. Candidates with either protein score C.I. percentage or Ion C.I. percentage greater than 95 were considered significant.

3. Results

3.1. 2D Gel Results. Figures 1 and 2 illustrate the results of the 2D gel analyses. Figure 1 demonstrates the protein comparisons between the pooled HER2/neu-receptor-positive and the HER2/neu-receptor-negative pooled specimens. Figure 2 represents the spots of interest that were selected up by Ettan Spot Picker (Amersham BioSciences) based on the in-gel analysis and spot picking design by DeCyder software. As shown, there are 96 spots of interest illustrated on the 2D gel analysis. This visually indicates the differing salivary protein patterns between HER2/neu-positive and HER2/neu-negative patients.

3.2. LC-MS/MS Mass Spectrometry Results. The results yielded 188 comparative salivary proteins among the HER2/neu-positive and HER2/neu-negative samples. Among the total number of proteins, 71 were significantly differentially expressed between the two specimens. There were 34 upregulated proteins and 37 downregulated proteins. Listed in Table 1 is the 34 upregulated proteins, and in Table 2, the 37 downregulated proteins.

Of the 34 proteins listed in Table 1, the mean percent peptide coverage for the complete panel of proteins was 50.3% (±19.6) with a range of 15.3% to 88.7% coverage. The mean protein ratio was 1.64 (±54.2) and ranged in value with a maximum of 3.13 to a maximum minimum of 1.12. Likewise, the mean alpha level was $P < 0.007(\pm 0.013)$ and ranged in value with a maximum of $P < 0.04$ to a maximum minimum of $P < 0.000001$.

Of the 37 downregulated salivary proteins listed in Table 2, the mean percent peptide coverage for the complete panel of proteins was 40.1% (±20.7) with a range of 9.7% to 100% coverage. The mean protein ratio was 1.64 (±0.561) and ranged in value with a maximum of 0.89 to a maximum minimum of 0.10. Likewise, the mean alpha level was $P < 0.009$ (±0.015) and ranged in value with a maximum of $P < 0.05$ to a maximum minimum of $P < 0.000001$. Figure 3 illustrates the comparison of the log ratio of the relative intensity (HER2+/HER2−) of the total 71 up- and downregulated salivary proteins. Additionally,

Table 3: Altered protein in saliva and in SKBR3 cell lines.

Access no.	Gene ID	Name	Reference
P06733	ENOA	Alpha-enolase	[11]
P04083	ANXA1	Annexin A1	[12]
P01034	CYTC	Cystatin-C precursor	[12]
P35527	K1C9	Cytokeratin-9	[13]
Q01469	FABPE	Fatty acid-binding protein, epidermal	[12]
P26038	MOES	Moesin	[14]
P62937	PPIA	Peptidyl-prolyl cis-trans-isomerase A	[12]
P01833	PIGR	Polymeric-immunoglobulin receptor	[12]
P05109	S10A8	Protein S100-A8	[12]
P06702	S10A9	Protein S100-A9	[12]
P13646	K1C13	cytoskeletal 13	[13]
P13647	K2C5	cytoskeletal 5	[13]
P06396	GELS	Gelsolin	[12]
P00738	HPT	Haptoglobin	[12]
P16104	H2AX	Histone H2A.x (H2a/x)	[13]
Q16778	H2B2E	Histone H2B type 2-E	[13]
Q06830	PRDX1	Peroxiredoxin-1	[12]
P07737	PROF1	Profilin-1	[11]
P05109	S10A8	Protein S100-A8	[12]
P06702	S10A9	Protein S100-A9	[12]

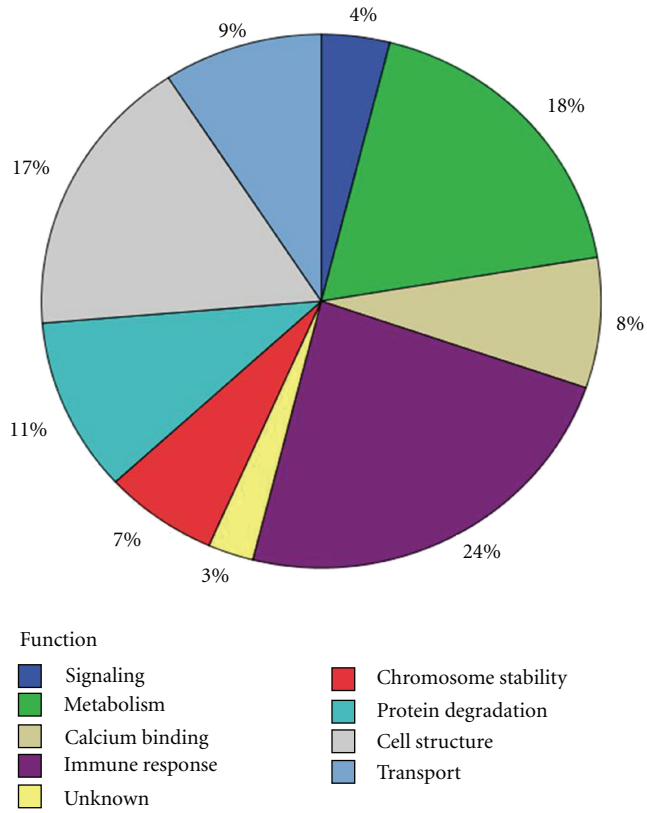

Figure 4: This figure represents the percentage of expressed proteins according to their cellular function.

Figure 4 illustrates the protein function of the panel of 71 proteins. Proteins related to cellular metabolism and immune response comprised nearly 42% of the protein panel. Cellular structure constituted 17% of the protein panel, which is consistent with SKBR3 and other cell line protein analyses [15]. Additionally, there were a considerable number of histones that were present in the functional protein profile.

4. Discussion

To the best of our knowledge, this is the first attempt to determine salivary protein profile alterations related to HER2/neu receptor status. Therefore, we have only a few references by which to compare our data. Additionally, a complete proteomic catalog of the SKBR3 cell line is also not available to compare to the salivary protein profiles, which are altered secondary to HER2 receptor status. Of the articles that were identified through the PubMed Central (United States National Library of Medicine) search engine [11–17], twenty (28%) of the 71 of the salivary proteins were found cited among the manuscripts [11–17] and reported to be altered in the SKBR3 cell lines. These salivary proteins are listed in Table 3 with the references that cited the SKBR3 protein phenotype alterations.

The numerous proteins in the panel need validation; however, the authors selected Profilin-1 as a test case to determine if the results of the proteomic analyses are feasible. As illustrated in Figure 5, Profilin-1 is present in both the SKBR3 and the human salivary gland (HSG) epithelial cell lines. Additionally, Profilin-1 is present in saliva and is downregulated to HER2-receptor-positive status. The pilot evidence supports the proteomic prediction.

It is worth noting that among the list (Table 3) of SKBR3 cell lysates proteins, there is a distinct absence of any proteins related to immune response to inflammatory cancer activity as compared to the salivary proteins listed in both Tables 1 and 2. The findings at this point suggest the strength of this *in vivo* model which could be indicative of response to therapy in the event these proteins are diminished in activity during treatment, thereby, indicating a response to therapy.

Further research is required to support the theories presented in this paper. For example, proteomic analyses of low-abundance proteins in the SKRB3 cell line lysates and saliva are required in order to address gaps in varying molecular pathways. Studies validating the panel of markers are also necessary, and an assessment of salivary protein modulation during trastuzumab therapy is essential.

5. Conclusions

The results of the study suggest salivary protein alterations secondary to HER2 receptor status. This is not surprising considering that the ductal cells of the salivary glands contain

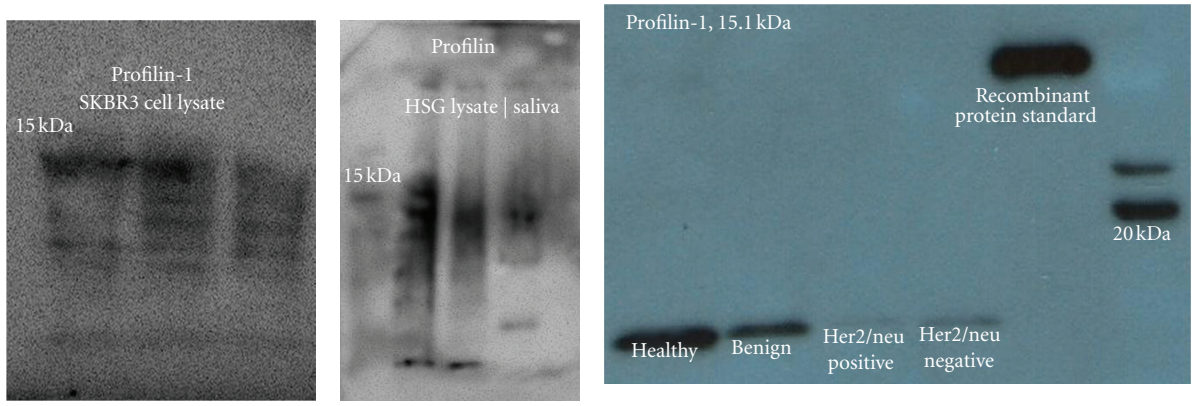

Figure 5: It illustrates the presence of profilin-1 in the SKBR3 and HSG cell lysates and saliva sampled from healthy, benign, and malignant tumor patients. Profilin is a downregulated protein in the presence of malignancy, and it is visualized by the lighter bands associated with malignancy. It is also worth noting that the Her2/neu-receptor-negative band is darker than the Her2/neu-receptor-positive counterpart suggesting further downregulation of the profiling-1 protein.

HER2/neu receptors. More importantly, the study raises the notion that salivary gland protein secretions may be used as a "real-time", *in vivo* model for studying breast cancer progression [9, 10]. Currently, there are three major methods for creating models for studying breast cancer progression [18]. The three methods utilize either breast cancer tumor cell lines xenografts of cell lines, and the third method uses animals—in this case genetically engineered mice [19] for creating various models for studying breast cancer [18]. All three models have generated useful insight into cancer progression; however, despite their utility, no individual model recapitulates all aspects of cancer progression [18, 19].

Hence, an adjunct, *in vivo* model system is needed for breast cancer tumorigenesis and predictive modeling for treatment response [18, 19]. The authors have demonstrated in previous studies that the salivary protein profiles are altered in the presence of ductal carcinoma *in situ* and are further altered in the presence of lymph node involvement [9, 10]. The preliminary findings of this paper coupled with previous studies do imply that this *in vivo* experimental model system, which utilizes one of the most easily obtained body fluids for marker analysis, may fill in the current gaps in our understanding of breast cancer pathogenesis, signaling pathways, the efficacy of varying chemotherapeutics, and identifying novel therapies. Most importantly, this new approach may shed new light on metastatic progression that is the principle cause of patient mortality.

Acknowledgments

The Avon Breast Cancer Foundation (no. 07-2007-071), Komen Foundation (KG080928), Gillson-Longenbaugh Foundation, and the Texas Ignition Fund supported the research presented in this paper. The authors would also like to thank Dr. William Dubinsky for the LC-MS/MS salivary mass spectrometry analyses.

References

[1] A. C. Wolff, M. E. H. Hammond, J. N. Schwartz et al., "American Society of Clinical Oncology/College of American Pathologists guideline recommendations for human epidermal growth factor receptor 2 testing in breast cancer," *Journal of Clinical Oncology*, vol. 25, no. 1, pp. 118–145, 2007.

[2] M. E. Hammond, D. F. Hayes, and A. C. Wolff, "Clinical Notice for American Society of Clinical Oncology-College of American Pathologists guideline recommendations on ER/PgR and HER2 testing in breast cancer," *Journal of Clinical Oncology*, vol. 29, no. 15, p. e458, 2011.

[3] J. S. Ross and J. A. Fletcher, "The HER-2/*neu* oncogene in breast cancer: prognostic factor, predictive factor, and target for therapy," *Stem Cells*, vol. 16, no. 6, pp. 413–428, 1998.

[4] S. Koscielny, P. Terrier, M. Spielmann, and J. C. Delarue, "Prognostic importance of low c-erbB2 expression in breast tumors," *Journal of the National Cancer Institute*, vol. 90, no. 9, p. 712, 1998.

[5] W. Y. Huang, B. Newman, R. C. Millikan et al., "Risk of breast cancer according to the status of HER-2/*neu* oncogene amplification," *Cancer Epidemiology Biomarkers & Prevention*, vol. 9, no. 1, pp. 65–71, 2000.

[6] L. R. Howe and P. H. Brown, "Targeting the HER/EGFR/ErbB family to prevent breast cancer," *Cancer Prevention Research*, vol. 4, no. 8, pp. 1149–1157, 2011.

[7] J. Baselga, "Phase I and II clinical trials of trastuzumab," *Annals of Oncology*, vol. 12, supplement 1, pp. S49–S55, 2001.

[8] S. Ménard, P. Valagussa, S. Pilotti et al., "Response to cyclophosphamide, methotrexate, and fluorouracil in lymph node-positive breast cancer according to HER2 overexpression and other tumor biologic variables," *Journal of Clinical Oncology*, vol. 19, no. 2, pp. 329–335, 2001.

[9] C. F. Streckfus, O. Mayorga-Wark, D. Arreola, C. Edwards, L. Bigler, and W. P. Dubinsky, "Breast cancer related proteins are present in saliva and are modulated secondary to ductal carcinoma *in situ* of the breast," *Cancer Investigation*, vol. 26, no. 2, pp. 159–167, 2008.

[10] C. F. Streckfus, K. A. Storthz, L. Bigler, and W. P. Dubinsky, "A comparison of the proteomic expression in pooled saliva

specimens from individuals diagnosed with ductal carcinoma of the breast with and without lymph node involvement," *Journal of Oncology*, vol. 2009, Article ID 737619, 11 pages, 2009.

[11] Y. M. Kulkarni, V. Suarez, and D. J. Klinke, "Inferring predominant pathways in cellular models of breast cancer using limited sample proteomic profiling," *BMC Cancer*, vol. 10, article 291, 2010.

[12] S. J. Pitteri, K. S. Kelly-Spratt, K. E. Gurley et al., "Tumor microenvironment-derived proteins dominate the plasma proteome response during breast cancer induction and progression," *Cancer Research*, vol. 71, no. 15, pp. 5090–5100, 2011.

[13] S. L. Wu, W. S. Hancock, G. G. Goodrich, and S. T. Kunitake, "An approach to the proteomic analysis of a breast cancer cell line (SKBR-3)," *Proteomics*, vol. 3, no. 6, pp. 1037–1046, 2003.

[14] E. Charafe-Jauffret, C. Ginestier, F. Monville et al., "Gene expression profiling of breast cell lines identifies potential new basal markers," *Oncogene*, vol. 25, no. 15, pp. 2273–2284, 2006.

[15] R. A. Harris, A. Yang, R. C. Stein et al., "Cluster analysis of an extensive human breast cancer cell line protein expression map database," *Proteomics*, vol. 2, no. 2, pp. 212–223, 2002.

[16] D. Zhang, L. K. Tai, L. L. Wong, L. L. Chiu, S. K. Sethi, and E. S. C. Koay, "Proteomic study reveals that proteins involved in metabolic and detoxification pathways are highly expressed in HER-2/*neu*-positive breast cancer," *Molecular & Cellular Proteomics*, vol. 4, no. 11, pp. 1686–1696, 2005.

[17] J. Kao, K. Salari, M. Bocanegra et al., "Molecular profiling of breast cancer cell lines defines relevant tumor models and provides a resource for cancer gene discovery," *PLoS ONE*, vol. 4, no. 7, Article ID e6146, 2009.

[18] T. Vargo-Gogola and J. M. Rosen, "Modelling breast cancer: one size does not fit all," *Nature Reviews Cancer*, vol. 7, no. 9, pp. 659–672, 2007.

[19] L. Hennighausen, "Mouse models for breast cancer," *Breast Cancer Research*, vol. 2, no. 1, pp. 2–7, 2000.

Hindawi Publishing Corporation
Journal of Oncology
Volume 2012, Article ID 796729, 14 pages
doi:10.1155/2012/796729

Research Article

Adamantyl Retinoid-Related Molecules Induce Apoptosis in Pancreatic Cancer Cells by Inhibiting IGF-1R and Wnt/β-Catenin Pathways

Lulu Farhana,[1,2,3] Marcia I. Dawson,[4] Jayanta K. Das,[1,2] Farhan Murshed,[1,5] Zebin Xia,[4] Timothy J. Hadden,[1] James Hatfield,[1] and Joseph A. Fontana[1,2,3]

[1] *John D Dingell VA MC, Wayne State University, Detroit, MI 48201, USA*
[2] *Department of Oncology, Wayne State University, Detroit, MI 48201, USA*
[3] *Karmanos Cancer Institute, Wayne State University, Detroit, MI 48201, USA*
[4] *Sanford-Burnham Medical Research Institute, La Jolla, CA 92037, USA*
[5] *Department of Neurobiology, Harvard University, Cambridge, MA 02138, USA*

Correspondence should be addressed to Joseph A. Fontana, joseph.fontana@va.gov

Received 31 October 2011; Revised 17 January 2012; Accepted 30 January 2012

Academic Editor: Reidar Grenman

Pancreatic carcinoma has a dismal prognosis as it often presents as locally advanced or metastatic. We have found that exposure to adamantyl-substituted retinoid-related (ARR) compounds 3-Cl-AHPC and AHP3 resulted in growth inhibition and apoptosis induction in PANC-1, Capan-2, and MiaPaCa-2 pancreatic cancer cell lines. In addition, AHP3 and 3-Cl-AHPC inhibited growth and induced apoptosis in spheres derived from the $CD44^+/CD24^+$ ($CD133^+/EpCAM^+$) stem-like cell population isolated from the pancreatic cancer cell lines. 3-Cl-AHPC-induced apoptosis was preceded by decreasing expression of IGF-1R, cyclin D1, β-catenin, and activated Notch-1 in the pancreatic cancer cell lines. Decreased IGF-1R expression inhibited PANC-1 proliferation, enhanced 3-Cl-AHPC-mediated apoptosis, and significantly decreased sphere formation. 3-Cl-AHPC inhibited the Wnt/β-catenin pathway as indicated by decreased β-catenin nuclear localization and inhibited Wnt/β-catenin activation of transcription factor TCF/LEF. Knockdown of β-catenin using sh-RNA also induced apoptosis and inhibited growth in pancreatic cancer cells. Thus, 3-Cl-AHPC and AHP3 induce apoptosis in pancreatic cancer cells and cancer stem-like cells and may serve as an important potential therapeutic agent in the treatment of pancreatic cancer.

1. Introduction

Pancreatic cancer is the fourth leading cause of cancer associated mortality. Approximately 50% of the patients present with locally advanced unresectable disease and 35% with metastatic disease [1]. In those patients who undergo resection, 75% develop a recurrence and succumb to metastatic pancreatic cancer [1]. The dismal prognosis of pancreatic cancer is further accentuated by its poor response to chemotherapy and to radiation therapy. Although treatment with gemcitabine has resulted in some improvement in the overall well-being of some of the patients, no chemotherapeutic regimen has had a significant impact on the survival of patient with metastatic disease with median survivals in the 4 to 6 month range. Thus the discovery of new therapeutic agents and approaches to patients with pancreatic cancer is of paramount importance.

Examination of tumors has resulted in the observation that a subpopulation of the tumor cells possess the properties of stem cells, that is, cells that are capable of undergoing self-renewal and as well as generating the heterogeneous lineages of cancer cells that comprise the majority of the tumor [2]. Pancreatic cancer stem cells have been identified in both pancreatic carcinoma cell lines as well as pancreatic cancer tissue obtained from patients [1, 3, 4]. A major emphasis has now been placed on detecting the specific pathways that are required for the proliferation and maintenance of these stem cells in the hope of developing specific targeted therapies resulting in the death of these cells.

We and others have shown that a unique class of compounds termed the adamantyl-substituted retinoid-related molecules (ARRs) (*E*)-4-[3-(1-adamantyl)-4-hydroxyphenyl]-3-chlorocinnamic acid (3-Cl-AHPC) and (*E*)-3-{2-[3-(1-adamantyl)-4-hydroxyphenyl]-5-pyrimidinyl}-2-propenoic acid (AHP3 or BI-2005) inhibits proliferation and induces apoptosis *in vitro* and *in vivo* of a number of malignant cell types [5–9]. In this paper, we demonstrate that the ARRs are not only capable of inhibiting the growth of pancreatic cancer cells *in vitro* but also inhibit the growth and induce apoptosis in the pancreatic stem-like cell population. Exposure to the ARR compounds AHP3 and 3-Cl-AHPC resulted in the inhibition of stem cell sphere formation as well as apoptosis induction in the stem-like cells. Apoptosis induction was preceded by marked inhibition of IGF-1R, cyclin D1, β-catenin, and Notch-1 expression in pancreatic cells, but only IGF-1R, cyclin D1, and β-catenin in the cancer stem-like cells. Decreased IGF-1R expression enhanced ARR apoptosis induction and inhibited pancreatic carcinoma growth and sphere formation. β-catenin knockdown inhibited TCF/LEF transcriptional activity and downregulated Wnt/β-catenin target genes. The subsequent enhanced apoptosis and inhibition of growth in pancreatic cells suggests that the inhibition of Wnt/β-catenin signaling pathway is important for 3-Cl-AHPC-mediated apoptosis.

2. Materials and Methods

2.1. Reagents. 3-Cl-AHPC was synthesized as described [5, 6]. DMEM-F12 medium, fetal bovine serum (FBS), lipofectamine 2000, and Prolong antifade kit were purchased from Invitrogen (Carlsbad, CA). Antibodies and their sources were as follows: antibodies for flow cytometry, CD44-PE, CD24-FITC, anti-EpCAM-PerCP-Cy5.5, and anti-c-Myc antibody from BD Biosciences (San Jose, CA) and CD44-APC-Cy7 and CD24-APC from Biolegend (San Diego, CA). Anti-CD44, anti-IGF-1Rβ, anti-β-catenin, anti-caspase 3, anti-cleaved caspase-3, and activated anti-cleaved Notch-1 (Val 1744) were from Cell Signaling Technology (Boston, MA); anti-CD24 and anti-cyclin D1 antibodies from Santa Cruz Biotechnology (Santa Cruz, CA); CD133-PE and CD326-FITC (EpCAM) from Miltenyi Biotec Inc. (Auburn, CA), and anti-α-tubulin antibody from Oncogene Research Products (Boston, MA). Anti-mouse IgG-TRITC conjugate for CD44, anti-rabbit IgG-FITC conjugate for CD24 and 3-(4,5-dimethylthiazol-2yl)-2, 5-diphenyltetrazolium bromide (MTT), 4′,6-Diamidino-2-phenylindole dihydrochloride (DAPI), and puromycin were purchased from Sigma-Aldrich (St. Louise, MO).

2.2. Cell Culture. Human pancreatic carcinoma cell lines, PANC-1, Capan-2, AsPc-1, MiaCaPa-2, and COLO357 were obtained from the American Type Culture Collection (ATCC, Rockville, MD) and maintained in DMEM-F12 medium containing 10% FBS and 100 μg/mL gentamycin.

2.3. Apoptosis and Growth Inhibition. Pancreatic cancer cell lines were treated with 1 μM 3-Cl-AHPC and AHP3 for various indicated time. Apoptosis in cells was analyzed by flow cytometry using Annexin V-FITC binding together with propidium iodide (PI) staining (Annexin V-FITC apoptosis Detection Kit 1, BD Biosciences, San Diego, CA). Data acquisition was done on a FACS Calibur flow cytometer (BD) and analyzed with CellQuest software (BD Biosciences). 3-Cl-AHPC- and AHP3-mediated inhibition of cell growth were determined by 3-(4,5-dimethylthiazol-2yl)-2,5-diphenyltetrazolium bromide (MTT) assay. The cells were seeded on 96-well plates at a density of 4×10^4 cells/well in a volume of 200 μL culture medium. 1 μM AHP3 and 3-Cl-AHPC in DMSO (final concentration 0.1%) were added to the cells for various times. 25 μL/well of MTT (5 mg/mL) was added to the medium and incubated for 4 h. After discarding the medium, MTT precipitates were solubilized with 200 μL DMSO and the plates read on a BioTeK Synergy HT (BioTeK Instrument Inc., Vermont) at an absorbance 570 nm. All experiments were performed in quadruplicate to determine means and standard deviations. Cell apoptosis was assessed using acridine orange/ethidium bromide staining as described [10]. The spheres were stained with acridine orange/ethidium bromide staining and immediately visualized and photographed with fluorescence microscope (OLYMPUS CKX41). For DAPI staining, the spheres were incubated with DAPI stain for 30 minutes at 37°C. Then spheres were visualized and photographed with a fluorescence microscope.

3. Fluorescence-Activated Cell Sorting (FACS) of $CD44^+/CD24^+$ Cells and Sphere Formation

3.1. Isolation of $CD44^+/CD24^+$ Cells. Cells were grown to 70–80% confluence and then trypsinised and washed with sorting buffer (1 × PBS, 5% FCS). The cells were resuspended with 100 μL sorting buffer and incubated with 15–20 μL anti-CD133-PE, anti-EpCAM-PerCP-Cy5.5, anti-CD24-FITC, and anti-CD44-PE primary antibodies for 30 min at ice. The cells were washed and resuspended in 500 μL of sorting buffer and sorted using flow cytometry FACSAria system (BD Immunocytochemistry Systems, Franklin lakes, NJ).

3.2. Sphere Formation. The sorted $CD133^+$, $CD44^+/CD24^+$ $EpCAM^+$, and $CD44^+/CD24^+$ cells using flow cytometry were suspended in serum-free stem cell medium containing DMEM/F12 (1 : 1) supplemented with B27 (Life Technologies, Gaithersburg, MD), 20 ng/mL EGF (Biomol International, Plymouth, PA), 20 ng/mL fibroblast growth factor (Biomol International, Plymouth, PA), and 100 μg/mL gentamycin. Approximately 150–200 cells per well were seeded in an ultralow-attachment 96-well plate (Corning Inc, Lowell, MA). 3-Cl-AHPC and AHP3 were added the day after cells were plated or after 7 days of sphere formation. Spheres were photographed and measured utilizing an Olympus microscope (OLYMPUS CKX41) and Olympus microscope digital camera with DP2-BSW software (Olympus soft imaging solutions GmbH, Germany).

3.3. Western Blots. Cells were extracted with lysis buffer containing 25 mM Tris-Cl buffer (pH 8.0), 150 mM NaCl, 0.2% nondiet P-40, 10% glycerol 10 mM NaF, 8 mM β-glycerophosphate, 0.2 mM Na_3VO_4, 1 mM DTT, and 10 μL/mL protease inhibitor cocktail (Sigma Aldrich, St. Louise, MO), and Western blots were performed as we previously described [11].

3.4. Immunofluorescence. Approximately 150 spheres were fixed with 4% paraformaldehyde in 1% Triton X-100, washed in PBS, dehydrated in methanol (25%, 50%, 75% 95%, and 100%), and then rehydrated in descending percentage of methanol and washed in PBS. Spheroids were incubated in 3% normal goat serum (Vector Lab, Burlingame, CA) at 4°C for 24 h and washed in phosphate-buffered saline with 0.5% Tween 20 (PBST). Then spheres were incubated with primary antibodies anti-CD44 and anti-CD24 for 48 h at 4°C, washed in PBST, and incubated with anti-mouse IgG-TRITC conjugate for CD44 and CD133 and anti-rabbit IgG-FITC conjugate for CD24 and CD326 (EpCAM) for 24 h. Spheres were mounted in 8 chambered slides and fluorescence staining analyzed. Spheres grown in 96-well ultralow-attachment plates were incubated with DAPI at 37°C for 30 minutes to assess DAPI staining. For β-catenin immunostaining, PANC-1cells were grown in eight chambered slide and then treated with 3-Cl-AHPC for 24 h. Cells were blocked with 3% normal goat serum at 4°C for 1 h and then incubated with anti-β-catenin antibody for overnight at 4°C. After washing with 1XPBS, cells were incubated with anti-rabbit IgG-FITC conjugate antibody for 2 h. Cells were washed with PBS and then placed on cover slips with prolong gold antifade reagent (Cell Signaling Technology, Boston, MA).

3.5. Sphere Block Preparation and In Situ Sphere Cell Death Detection. DMSO (vehicle) and 3-Cl-AHPC-treated spheres were centrifuged at 1000 rpm for 5 minutes, washed in PBS, 22% bovine serum albumin added to the spheres pellet, 95% ethanol placed on the spheres pellet, and the pellet allowed to harden for 30 minutes. Neutral buffered formalin (10%) was added to fix the cell pellet for at least 2 h and the spheres were then placed in a labeled plastic tissue embedding cassette containing 10% neutral buffered formalin overnight. The spheres were processed in a Sakura Tissue-Tek Processor for overnight dehydration in graded ethanol, clearing in xylene and infiltration with paraffin. The spheres were placed in a 4 μm embedding mold for final paraffin embedding.

The TUNEL assay was performed using the *In Situ* Cell Death Detection kit, POD (Roche-Applied-Science, Mannheim, Germany), according to the manufacturer's instructions. The paraffin embedding spheres were deparaffinized and rehydrated; then tissues sections were incubated with proteinase K solution (10–20 μg/mL) for 30 min. Tissues were then rinsed twice in PBS and reacted with 50 μL of the TUNEL reaction mixture at room temperature for 60 min in a dark, humidified chamber. Sections were again rinsed in PBS and incubated for 30 min with 50 μL of the Converter-POD (Roche-Applied-Science) and followed by 3-amino-9-ethylcarbazole (AEC). Sections were then counterstained with hematoxylin. As negative controls, corresponding sections were treated in the same way without terminal deoxynucleotidyl transferase.

3.6. shRNA Plasmids. Human GIPZ lentiviral shRNAmir expression vector GFP-tagged-pGIPZ-shRNA-IGF-1R was purchased from Open Biosystems (Thermo Scientific, Huntsville, AL). shRNA-IGF-1R expression vectors were stably transfected into PANC-1 cell lines using lipofectamine 2000. Stable cell lines were selected with puromycin. The scrambled sequence shRNA-vector was used as a control. pGIPZ-shRNA expression vector clone ID V2LSH-20147, V2LSH-131072, V3LSH-377850, V3LSH-377852, and V3LSH-377849 inhibited IGF-1R expression more effectively in PANC-1 cells than other clones from a set of eight tested clones.

sh-RNA-β-catenin-pSIREN-RetroQ expression vectors were constructed according to the manufacturer's instructions (Clontech, CA). The gene silencing target sequences were from the coding sequence of the PubMed Accession number NM_001904.3, and sh-RNA sequences 5′-CCATgg-AACCAgACAgAAA-3′ (catenin-KD-1) and 5′-ggATgTggA-TACCTCCCAAg-3′ (catenin-KD2) were synthesized from Integrated DNA technology Inc. (Coralville, IA). sh-β-catenin sequences were used for directional cloning 5′-*Bam*H I and 3 *EcoR* I overhang nucleotide in pSIREN-RetroQ vector. shRNA regions in plasmid backbone were confirmed by sequencing. sh-β-catenin plasmids were used to transfect the cell lines utilizing the lipofectamine method. The stable cell lines were selected with puromycin, and sh-β-catenin knockdown cell lines were grown in presence of puromycin. Scramble sequence sh-vector was used as a control.

3.7. TCF/LEF-Luciferase Assay. In order to determine the activation of Wnt/β-catenin signaling, the transcription factor T-cell-factor/lymphoid-enhancing-factor- (TCF/LEF)-Luc reporter plasmid was used in PANC-1 cells. Cells were transduced with Cignal TCF/LEF-Luc reporter lentiviral plasmid (SA Biosciences, Frederick, MD) in presence of polybrene (8 μg/mL) for 48 h and the cells were selected with puromycin (1 μg/mL). TCF/LEF cells were treated with 3-Cl-AHPC for 24 h. Cells were harvested and analyzed for TCF/LEF activity using a luciferase assay kit (Promega-Biosciences, San Luis Obispo, CA) as followed by the instructions of manufacturer and the activity was measured on a BioTeK Synergy HT.

3.8. Statistical Analysis. All statistics were performed using VassarStats web statistical software (Richard Lowry, Poughkeepsie, NY, USA). One-way analysis of variance (ANOVA) was performed to detect any differences between groups of sphere control, 3-Cl-AHPC-treated spheres and AHP3-treated spheres. If the result of the ANOVA is significant ($P < 0.01$ versus control), pairwise comparisons between the groups were made by a post hoc test (Tukey's HSD procedure). The significance level was set at $P < 0.01$ versus control and $P < 0.05$ versus control. Square brackets were

used in the figures to indicate treatments that are significantly different from the control.

4. Results

4.1. AHP3 and 3-Cl-AHPC Induction of Apoptosis in COLO357, PANC-1, AsPc-1, Capan-2, and MiaPaCa-2 Cells. AHP3 and 3-Cl-AHPC inhibited growth and induced apoptosis in Ras wild type COLO357 and Ras mutant PANC-1, AsPc-1, Capan-2, and MiaPaCA-2 pancreatic carcinoma cells. 1 μM AHP3 or 3-Cl-AHPC resulted in the inhibition of proliferation (Figure 1(a)). There was an 80% inhibition COLO357 growth, 50 to 60% inhibition of PANC-1 growth, 70% inhibition of Capan-2 growth, and 60 to 70% inhibition of MiaPaCa-2 cells at 72 h by both 3-Cl-AHPC and AHP3. AsPc-1 cells demonstrated increased resistance to both 3-Cl-AHPC and AHP3 with only 47% and 25% growth inhibition by 3-Cl-AHPC and AHP3, respectively, at 72 h (Figure 1(a)).

Exposure of COLO357 cells to 1 μM concentrations of 3-Cl-AHPC or AHP3 resulted in apoptosis induction of 80% of the cells at 48 h. Ras mutant cell lines displayed enhanced resistance to AHP3 and 3-Cl-AHPC-mediated apoptosis when compared to Ras wild type cell line COLO357 (Figure 1(b)). 3-Cl-AHPC and AHP3 exposure resulted in 22% apoptosis at 24 h and 50% and 48% apoptosis, respectively, at 48 h in PANC 1 cells (Figure 1(b)). Similar results were noted with Capan-2 cells with 40 and 50% apoptosis at 24 h and 48 h, respectively (Figure 1(b)). 3-Cl-AHPC and AHP3 exposure resulted in 35% and 40% apoptosis of AsPC-1 cells at 48 h, respectively (Figure 1(b)). Control MiaPaCa-2 cells showed 60% Annexin V-FITC positivity; however, these cells were not apoptotic by any other criteria and grew normally in culture. Therefore, acridine orange/ethidium bromide staining was utilized as we have previously described to assess DNA fragmentation and apoptosis [6]. Exposure to 3-Cl-AHPC and AHP3 resulted in 30% apoptosis at 48 h and 60% induction of apoptosis at 72 h and 96 h.

Numerous studies have supported the concept that the stem cell population is responsible for the persistent resistance of cancer cells to chemotherapy as well as their metastatic behavior [12–15]. Previous studies have shown that pancreatic cancers and pancreatic cancer cell lines contain a small segment of cell population characterized by expression of CD133 or CD44/CD24/EpCAM positivity and which can be utilized to identify this cancer stem cell population [16–19]. While there appears to be significant overlap between CD133 positive and $CD44^+/CD24^+$ cells, this overlap appears to vary between different tumor samples with only 10 to 40% of the $CD44^+/CD24^+$ cells expressing CD133 [4]. The intriguing observation that both CD133 positive and $CD44^+/CD24^+$ cells have been found to be tumor initiating cells and possess many of the characteristics of cancer stem cells suggests that heterogeneity exists in the pancreatic cancer stem cell population.

Pancreatic cancer stem cells have been characterized by stem cell markers $CD133^+$ and $CD44^+/CD24^+/EpCAM^+$ (epithelial adhesion molecule)/ESA (epithelial specific antigen) [3, 4, 20]. To investigate the efficiency of ARR in inhibiting the growth of cancer stem cells, we examined the inhibition of sphere formation in $CD44^+/CD24^+/EpCAM^+$ and $CD133^+$ cancer stem cells. PANC-1 cells were sorted by flow cytometry to obtain $CD133^+$ and $CD44^+/CD24^+/EpCAM^+$ expressing cells and cells were allowed to form spheres in the DMEM/F12-B27 medium for 7 days. 3-Cl-AHPC and AHP3 exposure completely inhibited sphere formation as well as addition of 3-Cl-AHPC or AHP3 on day 7 after sphere formation resulted in significant inhibition of sphere growth of $CD133^+$ and $CD44^+/CD24^+/EpCAM^+$ PANC-1 stem cells (Figures 2(a)–2(d)). Sphere formation in nonadherent conditions is a unique property of cancer stem cells in general [16]. Studies have demonstrated resistance of pancreatic stem cells to chemotherapy agents including gemcitabine [3, 12, 15]. We assessed the ability of ARRs to inhibit sphere formation from the sorted $CD44^+/CD24^+$ stem-like cells in B27 medium. 3-Cl-AHPC or AHP3 addition at the time of PANC-1 seeding in B27 medium completely inhibited sphere formation by the cells at day 7 and day 14 (Figure 2(e) and see Figure S1A in Supplementary Material available online at doi: 10.1155/2012/796729.), while addition of 3-Cl-AHPC or AHP3 on day 7 after sphere formation resulted in a 70% inhibition of sphere formation as well as degradation of the sphere cells at day 14 (Figure 2(f) and Supplementary Figure S1B). In order to determine the expression of CD44, CD24, EpCAM, and CD133 in $CD44^+/CD24^+$ sphere cells, we stained the spheres with fluorescent antibody for TRITC-conjugate-CD44 and CD133, and FITC-conjugate-CD24 and EpCAM. Utilizing confocal microscopy overlay, we confirmed that the PANC-1 spheres consisted of $CD44^+/CD24^+$ cells (Supplementary Figure S2A). These cells expressed not only $CD44^+/CD24^+$ but also CD133 as well as EpCAM (Supplementary Figure S2B).

3-Cl-AHPC or AHP3 addition to the $CD44^+/CD24^+$ MiaPaCa-2 and Capan-2 cells at the time of seeding in the B27 medium also totally inhibited spheres formation (Figures 3(a) and 3(c)). Similarly, 3-Cl-AHPC or AHP3 exposure at day 7 after sphere formation taken place resulted in a 70% and 50% inhibition of sphere size in the MiaPaCa-2 and Capan-2 cells, respectively (Figures 3(b) and 3(d)).

The 3-Cl-AHPC dose required to inhibit sphere formation by the PANC-1 cells was determined. The addition of 0.25, 0.5, or 1 μM 3-Cl-AHPC to PANC-1 cells at the time of seeding in B27 medium resulted in more than a 50% inhibition of sphere formation (Figure 4(a)); 0.1 μM did not inhibit sphere formation (Figure 4(a)). 3-Cl-AHPC concentrations of 0.5 and 1 μM were required to reduce PANC-1 sphere size greater than 80% when added at day 7 after sphere formation (Figure 4(b)), resulting in disaggregation of the sphere and apoptosis induction of the cells, as documented by DNA fragmentation demonstrated by acridine orange/ethidium bromide, DAPI staining, and positive TUNEL staining of the spheres (Figures 4(c), 4(d), and 4(e)).

Further evidence of AHP3 and 3-Cl-AHPC-mediated apoptosis of $CD44^+/CD24^+$ PANC-1 cells was demonstrated by Annexin V-FITC and PI staining. 3-Cl-AHPC and AHP3 exposure of PANC-1 cells resulted in 80% apoptosis after 96 h treatment (Figure 5(a) and Supplementary Figure S2C).

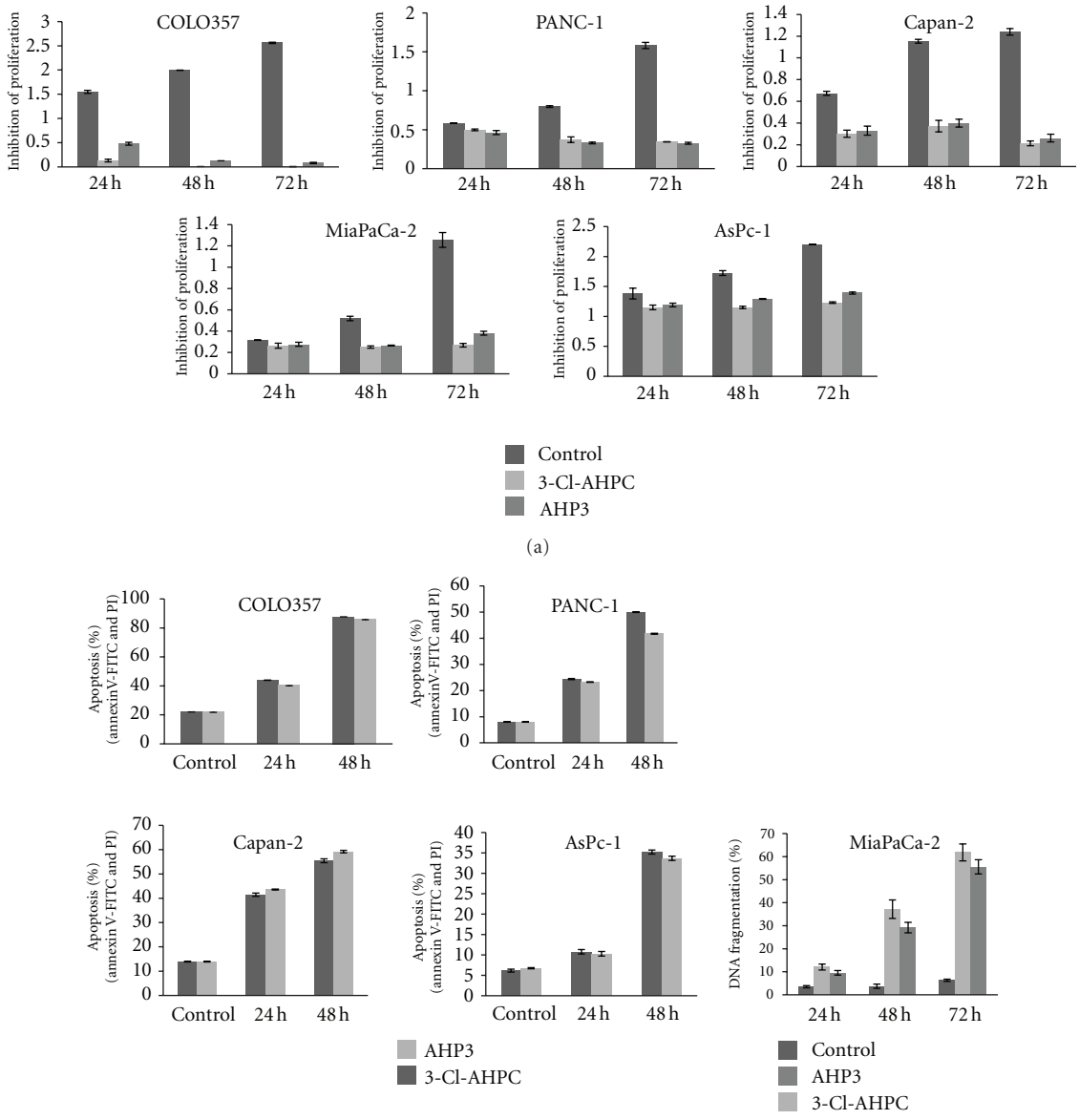

Figure 1: 3-Cl-AHPC- and AHP3-mediated proliferation inhibition and apoptosis induction in pancreatic cancer cell lines. The cells were exposed to 1 μM 3-Cl-AHPC or AHP3 for various times. (a) Proliferation inhibition was evaluated by MTT assay as described Section 2 and expressed as absorbance (OD) measured at 570 nm. The error bars represent the mean of three separate determinations ± the standard deviation (SD). (b) Induction of apoptosis in pancreatic cancer cells by 3-Cl-AHPC and AHP3. Cells were seeded at 1×10^4 cells/mL and grown for 24 h and then exposed to 1 μM AHP3 or 3-Cl-AHPC for indicated times. Induction of apoptosis and cell death was assessed using Annexin V-FITC labeling with propidium iodide (PI) staining in COLO357, PANC-1, Capan-2 AsPc-1, or acridine orange/ethidium bromide staining in MiaPaCa-2. The error bars represent the mean of three separate determinations ± the standard deviation (SD). All treated samples are significantly different from vehicle control.

We sorted the 3-Cl-AHPC- and AHP3-treated PANC-1 cells for $CD44^+/CD24^+$cells and assessed the percentage of these cells that were apoptotic by determining Annexin V-FITC positive staining. Flow cytometry analysis showed that $CD44^+/CD24^+$-gated early apoptotic (Annexin V-FITC + and PI−) cells were 36% and 40% for the 3-Cl-AHPC- and AHP3-treated cells, respectively (Figure 5(b) and Supplementary Figure S2D, upper panel). Late apoptotic cells (Annexin V-FITC + and PI +) were 51% and 57% for the 3-Cl-AHPC- and AHP3-treated cells, respectively (Figure 5(b)

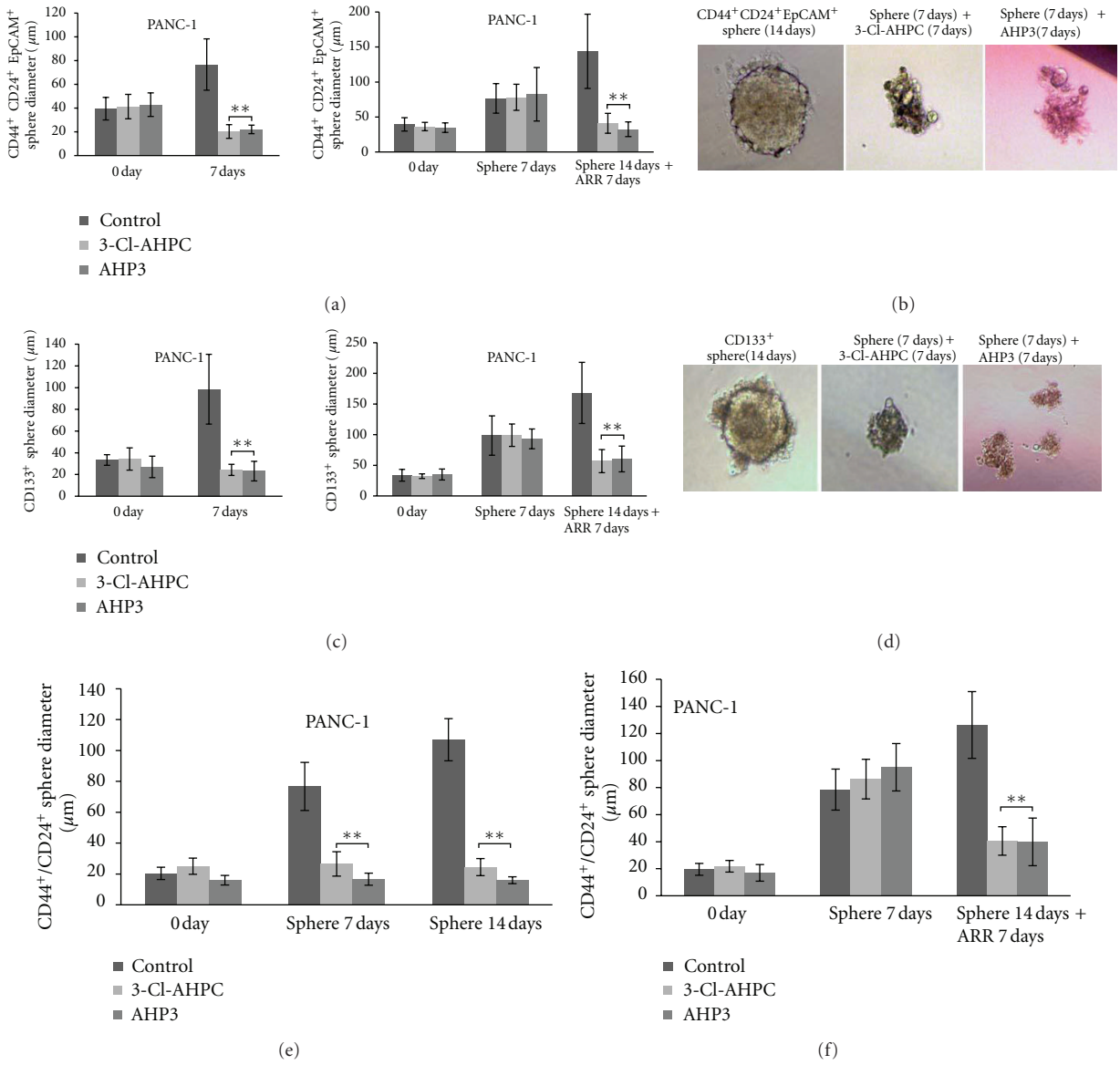

Figure 2: 3-Cl-AHPC-mediated inhibition and degradation of pancreatic cancer stem cells spheres of $CD133^+$, $CD44^+/CD24^+/EpCAM^+$, and stem-like spheres of $CD44^+/CD24^+$ PANC-1 cells. ((a), (b) and (c), (d)) 3-Cl-AHPC and AHP3 exposure resulted in inhibition of $CD44^+/CD24^+/EpCAM^+$ and $CD133^+$cells growth and sphere formation and degradation of the derived spheres. ((e), (f)) AHP3 and 3-Cl-AHPC inhibited sphere formation and inhibition of growth and degradation of the $CD44^+/CD24^+$-derived spheres. For sphere formation, the $CD44^+/CD24^+/EpCAM^+$, $CD133^+$, and $CD44^+/CD24^+$ cells were sorted by flow cytometry and approximately 200–300 cells were seeded with B27 containing DMEM/F12 medium in 96-well low attachment plates and 1 μM 3-Cl-AHPC or AHP3 added either the day after seeding or 7 days following sphere formation. The sizes of spheres were photographed and measured on a 100 μm scale and magnification 400X using Olympus fluorescence microscope digital camera software and DP2-BSW software. The error bars represent the mean of 15 sphere determinations ± the standard deviation. ** was significantly different in comparison to control spheres. Data were analyzed by ANOVA, Tukey HSD test for multiple comparisons. $^{**}P < 0.01$ versus control.

and Supplementary Figure S2D, bottom panel). Thus, a total of 80% of the $CD44^+/CD24^+$ PANC-1 cell population were apoptotic after 96 h exposure to either 3-Cl-AHPC or AHP3 (Figure 5(c) and Supplementary Figure S2E).

The ability of AHP3 and 3-Cl-AHPC to induce apoptosis in $CD44^-/CD24^-$, $CD44^+/CD24^-$, $CD44^-/CD24^+$, and $CD44^+/CD24^+$ cells was also examined. These cell populations were isolated from PANC-1 cells and treated with 3-Cl-AHPC. The addition of 1 μM 3-Cl-AHPC to the various cell populations resulted in the growth inhibition and the induction of apoptosis as indicated by DNA fragmentation (Supplementary Figures S3 and S4).

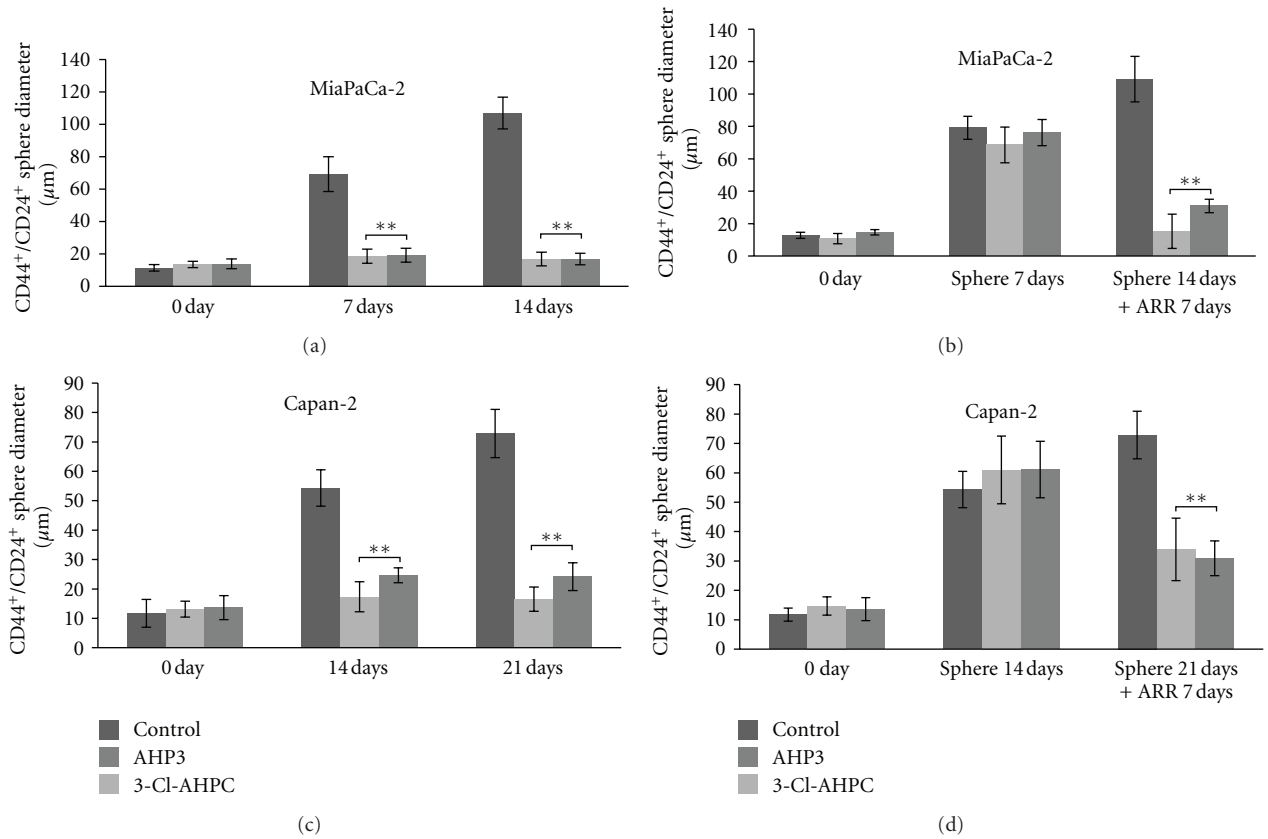

Figure 3: 3-Cl-AHPC- (1 μM) and AHP3- (1 μM) mediated inhibition of CD44$^+$/CD24$^+$ stem-like cell sphere formation and degradation of spheres derived from MiaPaCa-2 and Capan-2 cell lines. 3-Cl-AHPC and AHP3 were added at the time cells were seeded ((a), (c)) or 7 days after cells sphere formation ((b), (d)). The ARR affect on sphere growth was assessed at days 7 and 14 (a), days 7 and 14 (b), days 14 and 21 (c), and days 14 and 21 (d), respectively. The error bars represent the mean of 15 sphere determinations ± the standard deviation. ** Was significantly different in comparison to control spheres. Data were analyzed by ANOVA, Tukey HSD test for multiple comparisons. **$P < 0.01$ versus control.

4.2. 3-Cl-AHPC Decreases Expression of IGF-1R, Cyclin D1, and β-Catenin in Pancreatic Cancer Cells. 3-Cl-AHPC and AHP3 exposure on the expression of cyclin D1, β-catenin, and IGF-1R in the pancreatic cancer cells was assessed. Cyclin D1 is an important regulatory protein required in cell cycle progression, and overexpression has been associated with a poor prognosis in patients with pancreatic cancer [21]. Inhibition of cyclin D1 expression has been found to inhibit pancreatic cancer growth [21]. Abnormal expression of β-catenin was found to be associated with the development of metastatic pancreatic cancer as well as the upregulation of cyclin D1, c-Myc, and matrix-metalloproteinase-7 [22, 23]. IGF-1R and IGF-1 are overexpressed in human pancreatic tumors. IGF-1R signaling regulates proliferation, invasion, and angiogenic growth factor expression by pancreatic cancer cells [24–26].

3-Cl-AHPC exposure on pancreatic cancer cells decreased expression of IGF-1R, cyclin D1, and β-catenin prior to the inhibition of proliferation and the induction of apoptosis (Figures 5(d) and 5(e)). There was a 82%, 90%, 68%, and 31% inhibition of IGF-1R expression in the PANC-1, Capan-2, MiaPaCa-2, and AsPc-1cells, respectively, at 48 h following 3-Cl-AHPC exposure. 3-Cl-AHPC-mediated inhibition of cyclin D1 expression was 80%, 85%, 52%, and 69% in PANC-1, Capan-2, MiaPaCa-2, and AsPc-1cells, respectively, at 48 h (Figures 5(d) and 5(e)), and Supplementary Figure S5A). The addition of 3-Cl-AHPC to the PANC-1, Capan-2, MiaPaCa-2, and AsPc-1 cells resulted in a decrease of 65%, 66%, 22%, and 43%, respectively, in β-catenin expression (Figures 5(a) and 5(e) and Supplementary Figure S5A). Similarly, 3-Cl-AHPC exposure in COLO357 cells decreased IGF-1R (43%), cyclin D1 (93%), and β-catenin (85%), respectively, at 24 h following 3-Cl-AHPC exposure (Figure 5(e) and Supplementary Figure S5A). AHP3 exposure in PANC-1 cells also decreased IGF-1R, cyclin D1, and β-catenin (Supplementary Figure S5B). These results suggest that decrease of IGF-1R, cyclin D1, and β-catenin reflects a phenomenon general to ARR-mediated apoptosis induction in pancreatic cancer cells.

A 58%, 95%, and 50% decrease in IGF-1R, cyclin D, and β-catenin expression was noted in the PANC-1 CD44$^+$/CD24$^+$spheres following exposure to 3-Cl-AHPC, respectively, followed by apoptosis (Figure 6(a) and Supplementary Figure S5C). Sphere apoptosis was supported by the observation of cleavage of caspase 3 following 3-Cl-AHPC exposure on PANC-1 sphere cells (Figure 6(a)).

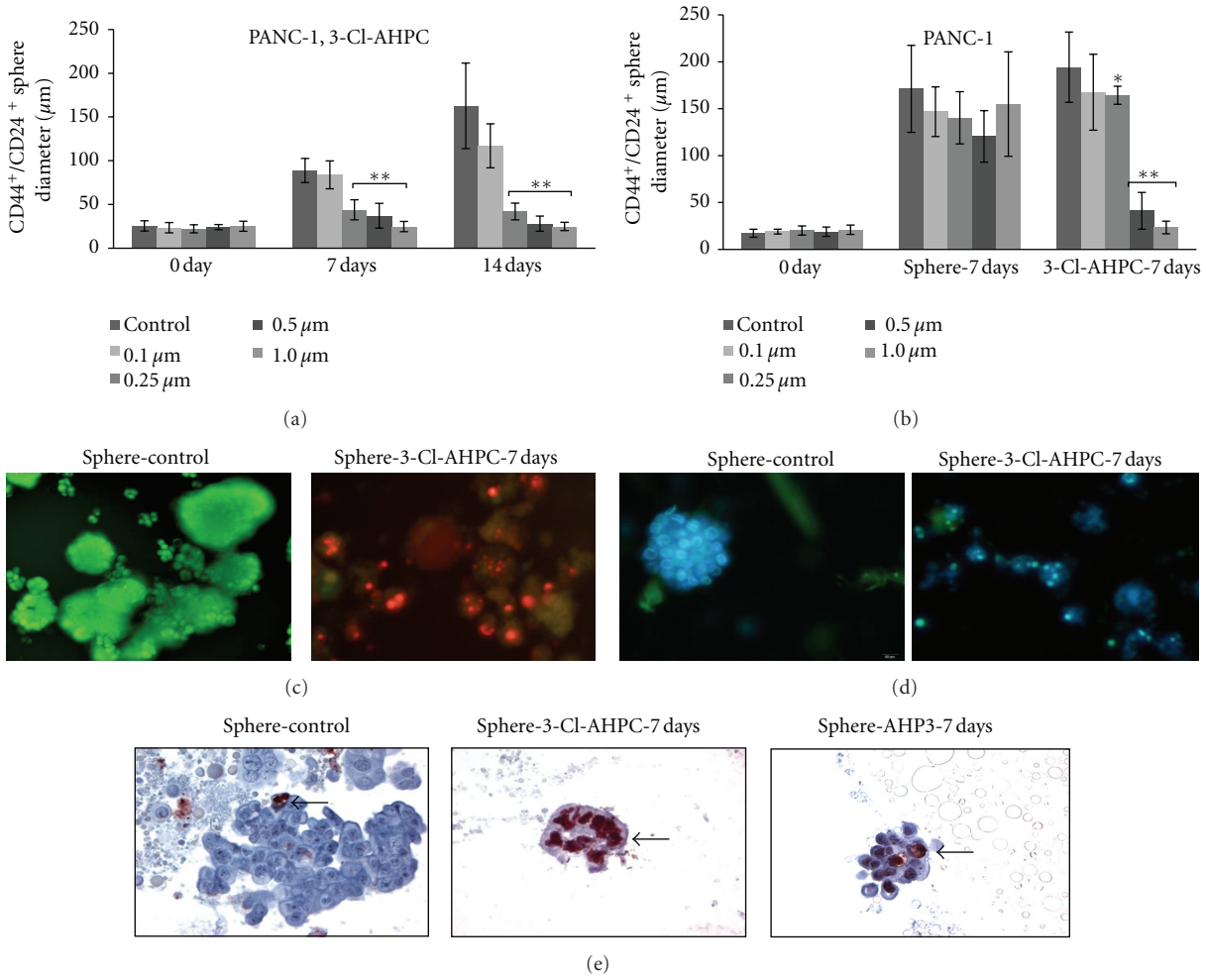

Figure 4: Dose-response effect of 3-Cl-AHPC on $CD44^+/CD24^+$ cells sphere formation and apoptosis in PANC-1 sphere cells. (a) Addition of 0.25, 0.5, and 1.0 μM 3-Cl-AHPC added at time of cell seeding inhibited sphere formation at 7 and 14 days. (b) 0.5 and 1.0 μM 3-Cl-AHPC inhibited sphere formation when added 7 days following sphere formation. (c) 1.0 μM 3-Cl-AHPC induced apoptosis in $CD44^+/CD24^+$ sphere cells as indicated by nuclear fragmentation detected by acridine orange/ethidium bromide and (d) DAPI staining. Spheres were visualized and photographed utilizing a fluorescence microscope. (e) Apoptosis of sphere cells as demonstrated by TUNEL assay. $CD44^+/CD24^+$ spheres were treated with 1.0 μM ARRs for 7 days (7D) after sphere formation. Details of slides preparation, visualization, antibodies utilized, and TUNNEL assay methodologies were as described in Section 2.

Self-renewal of CSCs has been shown to be regulated by the Wnt/β catenin, Hedgehog, and Notch signaling pathways [27, 28]. Lee et al. [4] found that expression of sonic hedgehog transcripts was increased by 46-fold in the CD44/CD24/EpCAM positive cells derived from pancreatic cancer cells while there was only a 4-fold increase in the CD44/CD24/EpCAM negative population. 3-Cl-AHPC downregulated the GLI1, GLI2, and Ptch1 mRNA expression in the hedgehog pathway (Figure 6(b)) and decreased the basal activated cleaved Notch-1 (Val 1744) expression in PANC-1 cells but not in $CD44^+/CD24^+$spheres (Figure 6(a)).

In order to examine the biological relevance of decreased IGF-1R expression, IGF-1R expression was inhibited in PANC-1 cells utilizing pGIPZ-lentiviral-shRNA-IGF-1R expression vector (Figure 6(d)). Decreased IGF-1R expression inhibited the growth of the PANC-1 pancreatic cancer cells and increased the 3-Cl-AHPC-mediated inhibition of $CD44^+/CD24^+$sphere size (Figure 6(c) and Supplementary Figure S6A). Decreased IGF-1R expression in IGF1R-KD1 and IGF1R-KD2 cells significantly inhibited sphere formation by the PANC-1 $CD44^+/CD24^+$ cells and enhanced ARR induction of apoptosis in the IGF-1R knockdown PANC-1 cells (Figures 6(c) and 6(d)).

Wnt/β-catenin signaling pathway leads to dephosphorylation, stabilization, and nuclear translocation of β-catenin. Nuclear β-catenin forms a complex with TCF/LEF family transcription factors and acts as a coactivator to express target genes in canonical Wnt signaling pathway such as CCND1 and MYC [27, 29]. We found that exposure to the 3-Cl-AHPC resulted in a decrease in nuclear β-catenin (Figures 7(a) and 7(b)) and also significantly decreased the TCF/LEF- transcriptional activity in wild-type cells as well as $CD44^+/CD24^+$ stably transfected TCF/LEF-sorted cells (Figure 7(c)). 3-Cl-AHPC decreased the expression

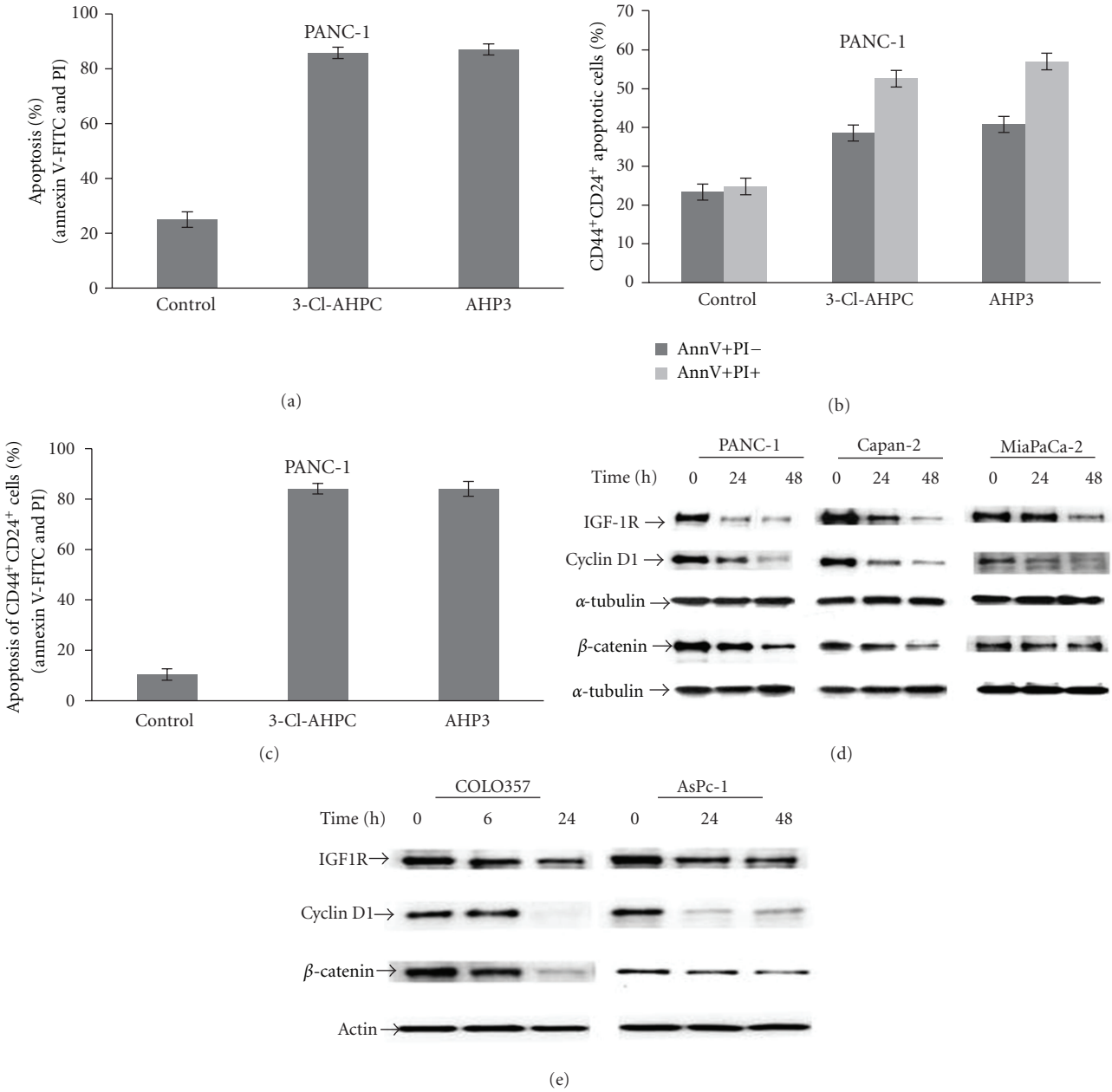

Figure 5: 3-Cl-AHPC and AHP induced apoptosis in PANC-1 $CD44^+/CD24^+$ cells and 3-Cl-AHPC decreased expression of IGF-1R, cyclin D1, and β-catenin in pancreatic cancer cells. (a) Percentage of total apoptotic cells. (b) Percentage of $CD44^+/CD24^+$ cells in the early (Annexin V-FITC positive and PI negative) or late (Annexin V-FITC positive and PI positive) apoptotic cell populations. (c) Percentage of total $CD44^+/CD24^+$ apoptotic cells (Annexin V-FITC positive and PI positive). Cells were treated with 1.0 μM 3-Cl-AHPC and AHP3 for 96 h. Antibody-conjugated markers CD44-APC-Cy7, CD24-APC, Annexin V-FITC, and PI were used to detect apoptotic and $CD44^+/CD24^+$ cells from the same samples. The error bars represent the mean of three separate determinations ± the standard deviation. ((d), (e)) IGF-1R, cyclin D1, and β-catenin expression decreased following 3-Cl-AHPC exposure in pancreatic cancer cells.

of Wnt/β-catenin pathway responsive cyclin D1 and c-Myc in the PANC-1 cells within 24 h (Figures 5(d) and 7(d)). Inhibition of β-catenin expression using sh-RNA β-catenin significantly inhibited cell growth and enhanced 3-Cl-AHPC-mediated induction of apoptosis (Figures 7(e) and 7(f) and Supplementary Figure S6C). Thus, β-catenin expression and its general antiapoptotic effect mediated through a number of the β-catenin target genes inhibit ARR apoptosis induction.

5. Discussion

ARRs at physiologically achievable concentrations induce apoptosis of a number of pancreatic cancer cell lines as well as inhibit sphere formation by the $CD44^+/CD24^+$ stem-like cell population derived from the pancreatic cancer cell lines. Although ARRs were initially synthesized to demonstrate selectivity in the activation of retinoid nuclear receptor (RAR) subtypes, they have been shown to inhibit growth and

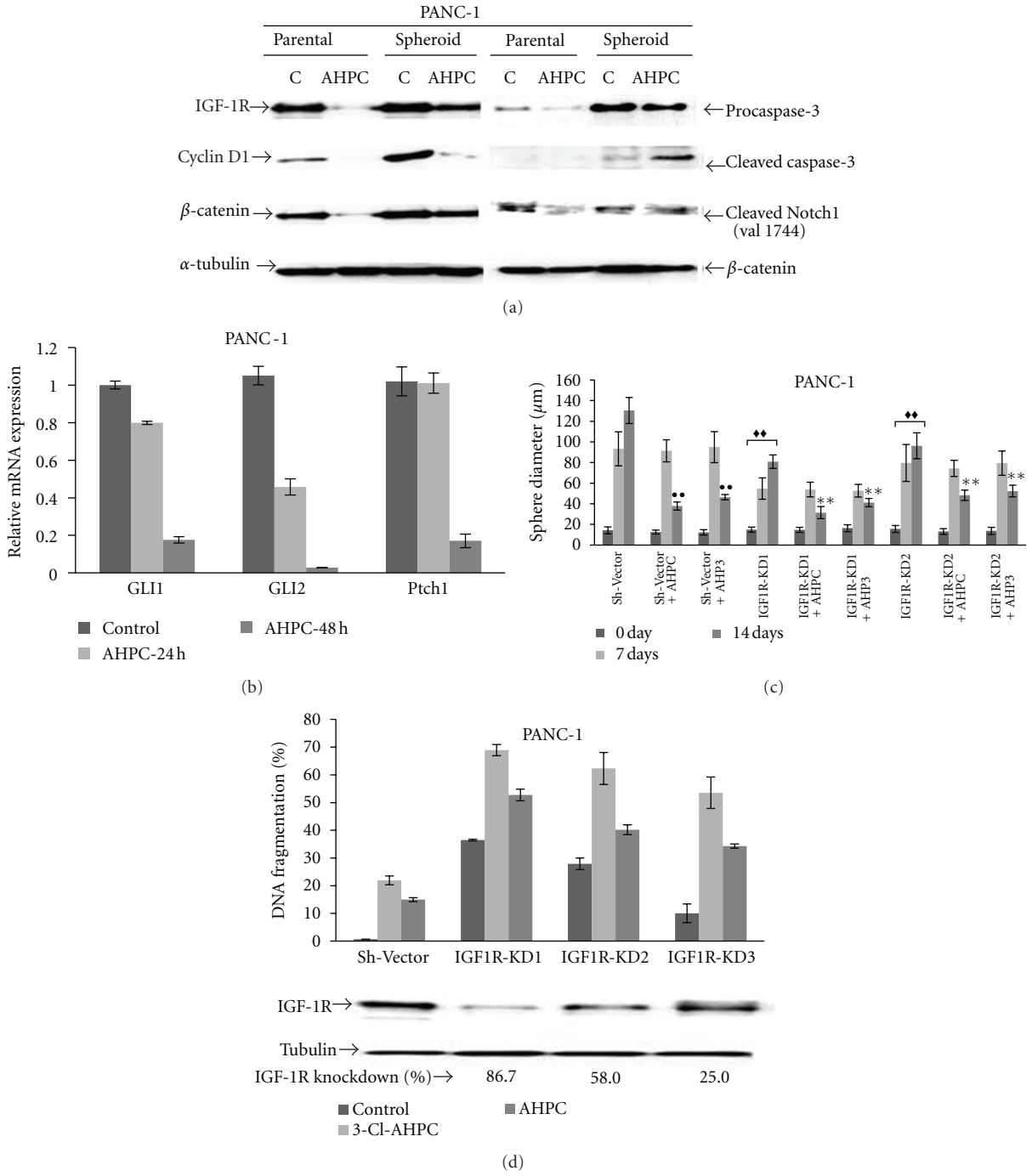

Figure 6: 3-Cl-AHPC decreased expression of IGF-1R, cyclin D1, β-catenin, and cleaved Notch-1 and increased levels of cleaved-caspase-3 in $CD44^+/CD24^+$spheres. (a) IGF-1R, cyclin D1, and β-catenin expression decreased cleaved-caspase-3 increased with no change in Notch-1 protein levels in spheres following exposure to 3-Cl-AHPC. Pancreatic cancer cells and PANC-1 spheres were exposed to 1.0 μM 3-Cl-AHPC for 7 days. Western blots were prepared as described in Materials and Methods. (b) mRNA expression of GLI1, GLI2, and Ptch1 in PANC-1 cells. Cells were grown in the presence of 1 μM 3-Cl-AHPC or vehicle alone (control). (c) Knockdown of IGF-1R expression by sh-IGF-1R inhibited sphere formation and enhanced ARR inhibition of sphere formation. The error bars represent the mean of three separate determinations +/− the standard deviation. •• was significantly different between spheres comprised of sh-vector cells treated with vehicle and 3-Cl-AHPC or AHP3. ♦♦ was significantly different between spheres comprised of sh-vector and IGF-1R-KD1 or IGF-1R-KD 2 at 7 and 14 days, respectively. ** was significantly different in comparison between IGF-1R-KDl/IGF-1R-KD2 spheres (vehicle treated) and IGF-1R-KD1/IGF-1R-KD2 spheres treated with 3-Cl-AHPC or AHP3. Data were analyzed by ANOVA, Tukey HSD test for multiple comparisons, ♦♦, ••, and $^{**}P < 0.01$. (d) Knockdown (KD) of IGF-1R enhanced AHP3- and 3-Cl-AHPC-mediated apoptosis in the PANC-1 cells and IGF-IR protein expression in IGF-1R knockdown cells. Apoptosis was assessed using acridine orange/ethidium bromide staining as described in Section 2.

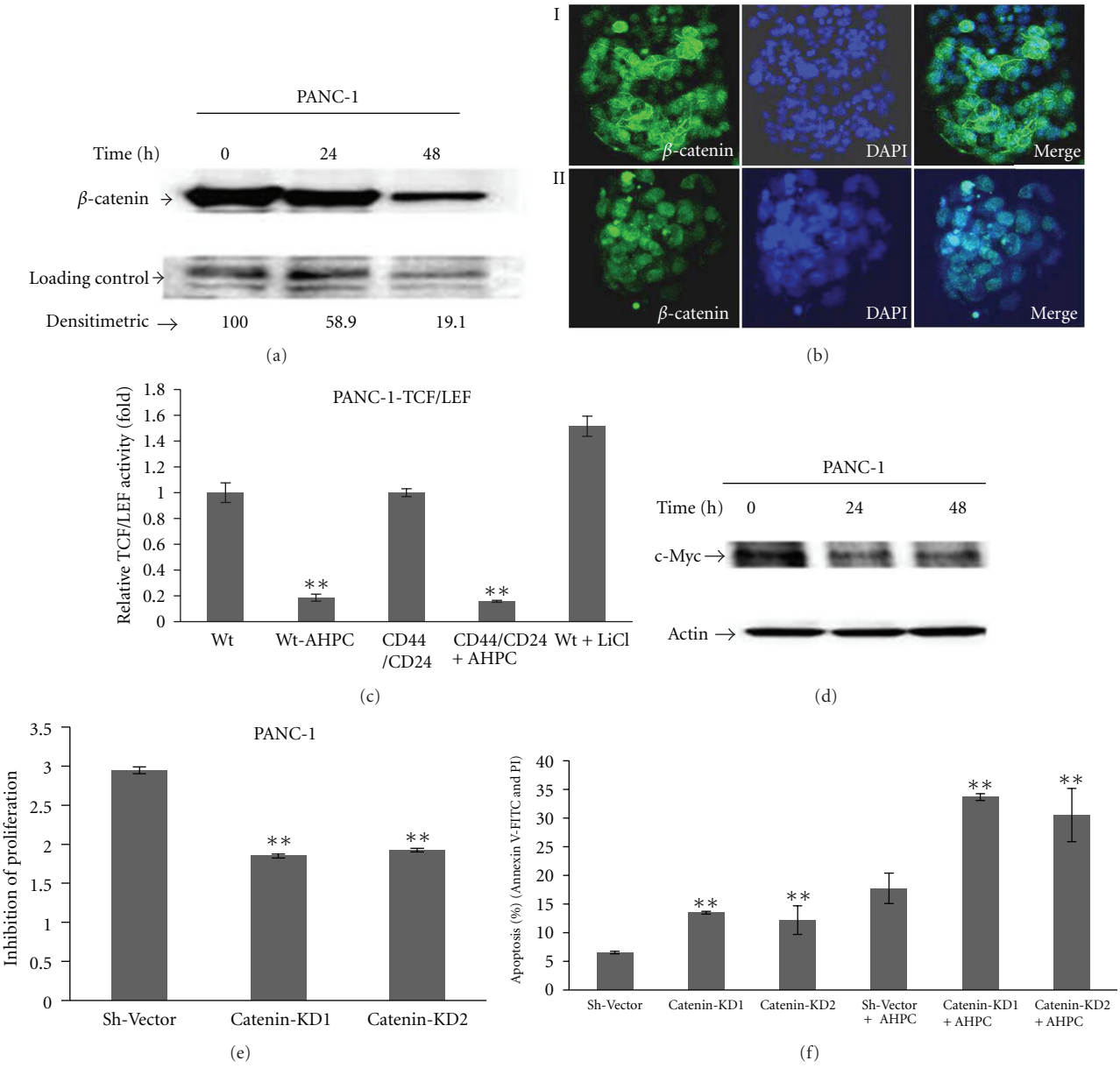

Figure 7: 3-Cl-AHPC mediated inhibition of the activation of TCF/LEF in Wnt/β-catenin pathway and decreased of β-catenin nuclear localization. (a) 3-Cl-AHPC decreased nuclear β-catenin as indicated by Western blot using nuclear extracts and densitometric quantification. (b) Nuclear β-catenin in control- (i) and 3-Cl-AHPC- (ii) treated PANC-1 cells using confocal fluorescent microscope (magnification 40X). Cells were grown in eight chambered slides and then treated with 3-Cl-AHPC for 24 h. Slide was prepared as described in Section 2. DAPI was used for nuclear staining for 1 min and mounted the slide with prolong gold antifade kit. (c) 3-Cl-AHPC inhibited TCF/LEF activity in Wnt/β-catenin signaling in stably transfected Cignal TCF/LEF-Luc reporter PANC-1 cell lines and 50 mM LiCl was used as a positive control. For CD44/CD24 cells, TCF/LEF stably transfected cells were sorted by flow cytometry and followed the procedure same as wild type (Wt) stable cell line. Luciferase promoter activity values are expressed as fold using a total protein concentration for internal normalization. The error bars represent the mean of three separate determinations ± the standard deviation (SD). (d) 3-Cl-AHPC decreased Wnt/β-catenin signaling responsive c-Myc protein. ((e) and (f)) Knock down of β-catenin inhibited cell proliferations and enhanced more apoptosis in sh-β-catenin knockdown (KD) PANC-1 cell lines. Proliferation inhibition was evaluated after 72 h of seeding the cells by MTT assay and expressed as absorbance measured at 570 nm. The error bars represent the mean of three separate determinations ± the standard deviation (SD). ** (<0.01) was significantly different in comparison between sh-vector and Catenin-KDl/Catenin-KD2 and also between sh-vector and catenin-KD1/Catenin-KD2 treated with 3-Cl-AHPC, respectively.

induce apoptosis in different malignant cell types independent of RAR and retinoid x receptor (RXR) activation and function [30–34]. We found that Ras wild type and mutant pancreatic cancer cell lines COLO357, PANC-1, Capan-2, AsPc-1 cells, and MiaPaCa-2 display significant sensitivity to AHP3- and 3-Cl-AHPC-mediated growth inhibition and apoptosis induction.

Numerous mechanisms have been suggested through which ARR induces apoptosis in these cells [29–33]. The ability of the ARRs to enhance or inhibit the expression of a number of genes and proteins has been demonstrated [30–35]. We have found that both 3-Cl-AHPC and AHP3 significantly decreased IGF-1R and β-catenin expression and that the decreased expression of IGF-1R and β-catenin inhibited the growth and enhanced apoptosis of the pancreatic cancer cells suggesting that decreased IGF-1R and β-catenin expression potentiates ARR-mediated apoptosis.

Recent studies have demonstrated that malignant tumors are heterogeneous in composition with the stem cell population representing those cells that display resistance to chemotherapy and have greater metastatic potential [3, 29, 36]. Huang et al. utilized CD44/CD24/EpCAM positivity to identify the stem cell population in the PANC-1 pancreatic cell line [37]. They found that this stem cell population—which represented 2.1–3.5% of the total cell population—displayed a slower growth rate than CD44/CD24 negative cells and when injected rapidly formed large tumors in nude mice at week 4 while CD44/CD24 negative cells did not form tumors. Simeone similarly used CD24/CD44/EpCAM to identify a pancreatic CSC population that displayed the ability to form tumor cell spheres as well as enhanced tumor formation in nude mice [38]. In contrast, Hermann and colleagues utilized CD133 positivity to select a pancreatic cancer stem cell population from freshly isolated patient-derived tumors [3]. These CD133 positive cancer stem cells represented a heterogeneous population of tumor-initiating cells and only 500 of these cells were required to form orthotropic tumors in athymic mice [3]. Thus, markers purportedly in cancer stem cells appear not to detect all cancer stem cells in a particular tumor. We found however that spheres generated from $CD44^+/CD24^+$expressing pancreatic cancer cells also expressed CD133 as well as EpCAM. More recently, other markers, such as Aldehyde dehydrogenase (ALDH), have been found to be associated with the pancreatic cancer stem cell population [39].

IGF-1 and its receptor IGF-1R play a major role in proliferation, invasive potential, and metastatic behavior of pancreatic cancer cells [24–26]. IGF-1 exposure decreased phosphorylation and inactivation of PTEN and activation of PI3K, AKT, and the NF-κB pathway in a number of pancreatic cancer cell lines resulting in their enhanced proliferation and invasiveness [24]. Other investigators have demonstrated that IGF-1R regulated hypoxia-inducible factor-1α, vascular endothelial growth factor, and angiogenesis through an autocrine loop in pancreatic cancer cells [25]. Further studies have documented that IGF-1/IGF-1R-mediated enhanced pancreatic carcinoma proliferation and invasiveness requires an interaction between IGF-1R and the hepatocyte growth receptor c-Met [26]. Dallas et al. have recently demonstrated enhanced IGF1R expression as well cancer stem cell markers in colon cancer cells displaying chemotherapy resistance [40]. In addition, these cells displayed greater sensitivity in terms of inhibition of growth following exposure to IGF-1R inhibitory antibody [40]. The addition of either ARR to the PANC-1, Capan-2, or MiaPaCa-2 cells downregulated expression of IGF-1R, cyclin D1, and β-catenin; decreased expression of these important proteins in the adherent cells, and the $CD44^+/CD24^+$ stem-like cells occurred prior to the onset of inhibition of cellular proliferation and the induction of apoptosis. We found that IGF-1R was significantly expressed in the pancreatic cancer sphere cells and its expression was markedly inhibited by exposure to 3-Cl-AHPC. The importance of IGF-1R in the proliferation of the pancreatic cancer cells, as well as their resistance to apoptosis, was documented by the observation that IGF-1R knockdown inhibited proliferation, enhanced 3-Cl-AHPC-mediated apoptosis, and inhibited sphere formation in PANC-1 cells.

Several investigators have demonstrated that β-catenin is essential for normal pancreatic development through the canonical Wnt signaling pathway but this pathway is downregulated in adult pancreas [41, 42]. Mutations in β-catenin or abnormal canonical Wnt signaling activity have been documented in pancreatic cancer [43–45]. Heiser et al. [45] have demonstrated that enhanced Wnt/β-catenin signaling in itself can induce pancreatic tumorgenesis and that activation of other oncogenes in the presence of enhanced Wnt/β-catenin signaling induces distinct pancreatic tumor formation. Addition of 3-Cl-AHPC downregulated β-catenin expression in pancreatic cancer cells and inhibited Wnt/β-catenin activation of transcription factor TCF/LEF and also downregulated Wnt/β-catenin pathway responsive genes cyclin D1 and c-Myc in PANC-1 cells. We found that β-catenin was significantly expressed in the pancreatic cancer sphere cells and that 3-Cl-AHPC inhibited this expression. 3-Cl-AHPC also downregulated GLI1, GLI2, and Ptch1 mRNA expression in the hedgehog pathway. ARR-mediated inhibitory effect on the self-renewal pathways, hedgehog and Wnt/β-catenin, may contribute to the inhibition of pancreatic cancer stem-like cell spheres. AHP3 and 3-Cl-AHPC may have a potential therapeutic role in the treatment of pancreatic cancer and further studies will delineate underlying mechanisms of inhibition for cancer stem cell self-renewal pathways.

6. Conclusions

Pancreatic cancer is resistant to chemotherapy and is a leading cause of cancer death. The adamantyl-substituted retinoid-related compounds 3-Cl-AHPC and AHP3 inhibit both pancreatic cancer and pancreatic stem-like cancer cells growth at physiologically achievable concentration. Inhibition of IGF-1R and β-catenin potentiates ARR-mediated growth inhibition and induction of apoptosis. 3-Cl-AHPC and AHP3 apoptosis induction in pancreatic cancer and pancreatic stem-like cancer cells suggested a potential therapeutic agent for pancreatic cancer.

Conflict of Interests

The authors declare that they have no conflict of interests.

Acknowledgments

The authors thank Dr. Edi Levi, John D. Dingell VA Medical Center, Detroit, for the microphotograph of immunofluorescence slides and Dr. Eric Van Buren, Karmanos Cancer Institute, for the flow cytometry. This work was supported by Veterans Affairs Merit Review Grant and NCI grants (J. A. Fontana and M. I. Dawson).

References

[1] F. Bednar and D. M. Simeone, "Pancreatic cancer stem cells and relevance to cancer treatments," *Journal of Cellular Biochemistry*, vol. 107, no. 1, pp. 40–45, 2009.

[2] M. F. Clarke, J. E. Dick, P. B. Dirks et al., "Cancer stem cells—perspectives on current status and future directions: AACR workshop on cancer stem cells," *Cancer Research*, vol. 66, no. 19, pp. 9339–9344, 2006.

[3] P. C. Hermann, S. L. Huber, T. Herrler et al., "Distinct populations of cancer stem cells determine tumor growth and metastatic activity in human pancreatic cancer," *Cell Stem Cell*, vol. 1, no. 3, pp. 313–323, 2007.

[4] C. J. Lee, J. Dosch, and D. M. Simeone, "Pancreatic cancer stem cells," *Journal of Clinical Oncology*, vol. 26, no. 17, pp. 2806–2812, 2008.

[5] L. Farhana, M. I. Dawson, Z. Xia et al., "Adamantyl-substituted retinoid-related molecules induce apoptosis in human acute myelogenous leukemia cells," *Molecular Cancer Therapeutics*, vol. 9, no. 11, pp. 2903–2913, 2010.

[6] Y. Zhang, M. I. Dawson, R. Mohammad et al., "Induction of apoptosis of human B-CLL and ALL cells by a novel retinoid and its nonretinoidal analog," *Blood*, vol. 100, no. 8, pp. 2917–2925, 2002.

[7] L. Farhana, M. I. Dawson, F. Murshed, and J. A. Fontana, "Maximal adamantyl-substituted retinoid-related molecule-induced apoptosis requires NF-B noncanonical and canonical pathway activation," *Cell Death and Differentiation*, vol. 18, no. 1, pp. 164–173, 2011.

[8] Y. Zhang, J. Soto, K. Park et al., "Nuclear receptor SHP, a death receptor that targets mitochondria, induces apoptosis and inhibits tumor growth," *Molecular and Cellular Biology*, vol. 30, no. 6, pp. 1341–1356, 2010.

[9] Y. H. Han, X. Cao, B. Lin et al., "Regulation of Nur77 nuclear export by c-Jun N-terminal kinase and Akt," *Oncogene*, vol. 25, no. 21, pp. 2974–2986, 2006.

[10] D. L. Spector, R. D. Goldman, and L. A. Leinwand, *Cells-A Laboratory Manual: Culture and Biochemical Analysis of Cells*, vol. 1, Goldspring Harbor Laboratory Press, Cold Spring Harbor, NY, USA, 1998.

[11] L. Farhana, M. I. Dawson, M. Leid et al., "Adamantyl-substituted retinoid-related molecules bind small heterodimer partner and modulate the Sin3A repressor," *Cancer Research*, vol. 67, no. 1, pp. 318–325, 2007.

[12] A. N. Shah, J. M. Summy, J. Zhang, S. I. Park, N. U. Parikh, and G. E. Gallick, "Development and characterization of gemcitabine-resistant pancreatic tumor cells," *Annals of Surgical Oncology*, vol. 14, no. 12, pp. 3629–3637, 2007.

[13] J. Zhou, C. Y. Wang, T. Liu et al., "Persistence of side population cells with high drug efflux capacity in pancreatic cancer," *World Journal of Gastroenterology*, vol. 14, no. 6, pp. 925–930, 2008.

[14] A. Jimeno, G. Feldmann, A. Suárez-Gauthier et al., "A direct pancreatic cancer xenograft model as a platform for cancer stem cell therapeutic development," *Molecular Cancer Therapeutics*, vol. 8, no. 2, pp. 310–314, 2009.

[15] P. H. Sung, J. Wen, S. Bang, S. Park, and Y. S. Si, "CD44-positive cells are responsible for gemcitabine resistance in pancreatic cancer cells," *International Journal of Cancer*, vol. 125, no. 10, pp. 2323–2331, 2009.

[16] C. Li, D. G. Heidt, P. Dalerba et al., "Identification of pancreatic cancer stem cells," *Cancer Research*, vol. 67, no. 3, pp. 1030–1037, 2007.

[17] J. L. Dembinski and S. Krauss, "Characterization and functional analysis of a slow cycling stem cell-like subpopulation in pancreas adenocarcinoma," *Clinical and Experimental Metastasis*, vol. 26, no. 7, pp. 611–623, 2009.

[18] M. T. Mueller, P. C. Hermann, J. Witthauer et al., "Combined targeted treatment to eliminate tumorigenic cancer stem cells in human pancreatic cancer," *Gastroenterology*, vol. 137, no. 3, pp. 1102–1113, 2009.

[19] M. Quante and T. C. Wang, "Stem cells in gastroenterology and hepatology," *Nature Reviews Gastroenterology and Hepatology*, vol. 6, no. 12, pp. 724–737, 2009.

[20] O. Gires, C. A. Klein, and P. A. Baeuerle, "On the abundance of EpCAM on cancer stem cells," *Nature Reviews Cancer*, vol. 9, no. 2, p. 143, 2009.

[21] M. T. Yip-Schneider, H. Wu, M. Ralstin et al., "Suppression of pancreatic tumor growth by combination chemotherapy with sulindac and LC-1 is associated with cyclin D1 inhibition in vivo," *Molecular Cancer Therapeutics*, vol. 6, no. 6, pp. 1736–1744, 2007.

[22] Y. J. Li, Z. M. Wei, Y. X. Y. X. Meng, and X. R. Ji, "β-catenin up-regulates the expression of cyclinD1, c-myc and MMP-7 in human pancreatic cancer: relationships with carcinogenesis and metastasis," *World Journal of Gastroenterology*, vol. 11, no. 14, pp. 2117–2123, 2005.

[23] Z. Wang and Q. Ma, "β-Catenin is a promising key factor in the SDF-1/CXCR4 axis on metastasis of pancreatic cancer," *Medical Hypotheses*, vol. 69, no. 4, pp. 816–820, 2007.

[24] J. Ma, H. Sawai, Y. Matsuo et al., "IGF-1 Mediates PTEN suppression and enhances cell invasion and proliferation via activation of the IGF-1/PI3K/AKT signaling pathway in pancreatic cancer cells," *Journal of Surgical Research*, vol. 160, no. 1, pp. 90–101, 2010.

[25] O. Stoeltzing, W. Liu, N. Reinmuth et al., "Regulation of hypoxia-inducible factor-1α, vascular endothelial growth factor, and angiogenesis by an insulin-like growth factor-I receptor autocrine loop in human pancreatic cancer," *American Journal of Pathology*, vol. 163, no. 3, pp. 1001–1011, 2003.

[26] T. W. Bauer, R. J. Somcio, F. Fan et al., "Regulatory role of c-Met in insulin-like growth factor-I receptor—mediated migration and invasion of human pancreatic carcinoma cells," *Molecular Cancer Therapeutics*, vol. 5, no. 7, pp. 1676–1682, 2006.

[27] M. Katoh and M. Katoh, "WNT signaling pathway and stem cell signaling network," *Clinical Cancer Research*, vol. 13, no. 14, pp. 4042–4045, 2007.

[28] Y. Li, M. S. Wicha, S. J. Schwartz, and D. Sun, "Implications of cancer stem cell theory for cancer chemoprevention by natural dietary compounds," *Journal of Nutritional Biochemistry*, vol. 22, no. 9, pp. 799–806, 2011.

[29] C. Y. Logan and R. Nusse, "The Wnt signaling pathway in development and disease," *Annual Review of Cell and Developmental Biology*, vol. 20, pp. 781–810, 2004.

[30] L. Farhana, M. I. Dawson, L. Xu, and J. A. Fontana, "SHP and Sin3A expression are essential for adamantyl-substituted retinoid-related molecule-mediated nuclear factor-κB activation, c-Fos/c-Jun expression, and cellular apoptosis," *Molecular Cancer Therapeutics*, vol. 8, no. 6, pp. 1625–1635, 2009.

[31] S. Y. Sun, P. Yue, L. Mao et al., "Identification of receptor-selective retinoids that are potent inhibitors of the growth of human head and neck squamous cell carcinoma cells," *Clinical Cancer Research*, vol. 6, no. 4, pp. 1563–1573, 2000.

[32] L. Mologni, I. Ponzanelli, F. Bresciani et al., "The novel synthetic retinoid 6-[3-adamantyl-4-hydroxyphenyl]-2- naphthalene carboxylic acid (CD437) causes apoptosis in acute promyelocytic leukemia cells through rapid activation of caspases," *Blood*, vol. 93, no. 3, pp. 1045–1061, 1999.

[33] S. Y. Sun, P. Yue, R. A. S. Chandraratna, Y. Tesfaigzi, W. K. Hong, and R. Lotan, "Dual mechanisms of action of the retinoid CD437: nuclear retinoic acid receptor-mediated suppression of squamous differentiation and receptor-independent induction of apoptosis in UMSCC22B human head and neck squamous cell carcinoma cells," *Molecular Pharmacology*, vol. 58, no. 3, pp. 508–514, 2000.

[34] X. P. Lu, A. Fanjul, N. Picard et al., "Novel retinoid-related molecules as apoptosis inducers and effective inhibitors of human lung cancer cells in vivo," *Nature Medicine*, vol. 3, no. 6, pp. 686–690, 1997.

[35] J. Miao, S.-E. Choi, S. M. Seok et al., "Ligand-dependent regulation of the activity of the orphan nuclear receptor, small heterodimer partner (SHP), in the repression of bile acid biosynthetic CYP7A1 and CYP8B1 genes," *Molecular Endocrinology*, vol. 25, no. 7, pp. 1159–1169, 2011.

[36] P. C. Hermann, S. Bhaskar, M. Cioffi, and C. Heeschen, "Cancer stem cells in solid tumors," *Seminars in Cancer Biology*, vol. 20, no. 2, pp. 77–84, 2010.

[37] P. Huang, C. Y. Wang, S. M. Gou, H. S. Wu, T. Liu, and J. X. Xiong, "Isolation and biological analysis of tumor stem cells from pancreatic adenocarcinoma," *World Journal of Gastroenterology*, vol. 14, no. 24, pp. 3903–3907, 2008.

[38] D. M. Simeone, "Pancreatic cancer stem cells: implications for the treatment of pancreatic cancer," *Clinical Cancer Research*, vol. 14, no. 18, pp. 5646–5648, 2008.

[39] M. P. Kim, J. B. Fleming, H. Wang et al., "ALDH activity selectively defines an enhanced tumor-initiating cell population relative to CD133 expression in human pancreatic adenocarcinoma," *PLoS ONE*, vol. 6, no. 6, 2011.

[40] N. A. Dallas, L. Xia, F. Fan et al., "Chemoresistant colorectal cancer cells, the cancer stem cell phenotype, and increased sensitivity to insulin-like growth factor-I receptor inhibition," *Cancer Research*, vol. 69, no. 5, pp. 1951–1957, 2009.

[41] L. C. Murtaugh, A. C. Law, Y. Dor, and D. A. Melton, "β-Catenin is essential for pancreatic acinar but not islet development," *Development*, vol. 132, no. 21, pp. 4663–4674, 2005.

[42] S. Papadopoulou and H. Edlund, "Attenuated Wnt signaling perturbs pancreatic growth but not pancreatic function," *Diabetes*, vol. 54, no. 10, pp. 2844–2851, 2005.

[43] A. M. Lowy, C. Fenoglio-Preiser, O. J. Kim et al., "Dysregulation of β-catenin expression correlates with tumor differentiation in pancreatic duct adenocarcinoma," *Annals of Surgical Oncology*, vol. 10, no. 3, pp. 284–290, 2003.

[44] G. Zeng, M. Germinaro, A. Micsenyi et al., "Aberrant Wnt/β-catenin signaling in pancreatic adenocarcinoma," *Neoplasia*, vol. 8, no. 4, pp. 279–289, 2006.

[45] P. W. Heiser, D. A. Cano, L. Landsman et al., "Stabilization of β-catenin induces pancreas tumor formation," *Gastroenterology*, vol. 135, no. 4, pp. 1288–1300, 2008.

Hindawi Publishing Corporation
Journal of Oncology
Volume 2012, Article ID 853797, 13 pages
doi:10.1155/2012/853797

Review Article

Dual Roles of *METCAM* in the Progression of Different Cancers

Guang-Jer Wu[1,2]

[1] *Department of Microbiology and Immunology, Emory University, School of Medicine, Atlanta, GA 30322, USA*
[2] *Department of Bioscience Technology, Chung Yuan Christian University, Chung-Li 32023, Taiwan*

Correspondence should be addressed to Guang-Jer Wu, gwu@emory.edu

Received 16 October 2011; Revised 31 December 2011; Accepted 12 January 2012

Academic Editor: Omer Faruk Hatipoglu

METCAM, an integral membrane cell adhesion molecule (*CAM*) in the *Ig*-like gene superfamily, is capable of performing typical functions of *CAM*s, such as mediating cell-cell and cell-extracellular interactions, crosstalk with intracellular signaling pathways, and modulating social behaviors of cells. *METCAM* is expressed in about nine normal cells/tissues. Aberrant expression of *METCAM* has been associated with the progression of several epithelial tumors. Further *in vitro* and *in vivo* studies show that *METCAM* plays a dual role in the progression of different tumors. It can promote the malignant progression of several tumors. On the other hand, it can suppress the malignant progression of other tumors. We suggest that the role of *METCAM* in the progression of different cancer types may be modulated by different intrinsic factors present in different cancer cells and also in different stromal microenvironment. Many possible mechanisms mediated by this *CAM* during early tumor development and metastasis are suggested.

1. Introduction

Human *METCAM* (*huMETCAM*), a *CAM* in the immunoglobulin-like gene superfamily, is an integral membrane glycoprotein. Alternative names for *METCAM* are *MUC18* [1], *CD146* [2], *MCAM* [3], *MelCAM* [4], *A32* [5], and *S-endo 1* [6]. To avoid confusion with mucins and to reflect its biological functions, we have renamed *MUC18* as *METCAM* (*met*astasis *CAM*), which means an immunoglobulin-like *CAM* that affects or regulates metastasis, [7]. The *huMETCAM* has 646 aminoacids that include a N-terminal extracellular domain of 558 aminoacids, which has 28 aminoacids characteristics of a signal peptide sequence at its N-terminus, a transmembrane domain of 24 aminoacids (amino acid number 559–583), and a cytoplasmic domain of 64 aminoacids at the C-terminus. *HuMETCAM* has eight putative N-glycosylation sites (*Asn-X-Ser/Thr*), of which six are conserved, and are heavily glycosylated and sialylated resulting in an apparent molecular weight of 113,000–150,000. The extracellular domain of the protein comprises five immunoglobulin-like domains (V-V-C2-C2-C2) [1, 7] and an X domain [7]. The cytoplasmic tail contains peptide sequences that will potentially be phosphorylated by protein kinase A (*PKA*), protein kinase C (*PKC*), and casein kinase 2 (*CK 2*) [1, 7, 8]. My lab has also cloned and sequenced the mouse *METCAM* (*moMETCAM*) cDNA, which contains 648 aminoacids with a 76.2% identity with *huMETCAM*, suggesting that *moMETCAM* is likely to have biochemical properties and biological functions similar to the human counterpart [9]. The structure of the *huMETCAM* protein is depicted in Figure 1, suggesting that *METCAM*, similar to most *CAMs,* plays an active role in mediating cell-cell and cell-extracellular interactions, crosstalk with many intracellular signaling pathways, and modulating the social behaviors of cells [7].

HuMETCAM is expressed in a limited number of normal tissues, such as hair follicular cells, smooth muscle cells, endothelial cells, cerebellum, normal mammary epithelial cells, basal cells of the lung, activated T cells, intermediate trophoblast [10], and normal nasopharyngeal epithelial cells [11]. The protein is overly expressed in most (67%) malignant melanoma cells [1], and in most (more than 80%) premalignant prostate epithelial cells (PIN), high-grade prostatic carcinoma cells, and metastatic lesions [12, 13]. *HuMETCAM* is also expressed in other cancers, such as gestational trophoblastic tumors, leiomyosarcoma, angiosarcoma, haemangioma, Kaposi's sarcoma, schwannoma, some lung squamous and small cell carcinomas, some breast

cancer, some neuroblastoma [10], and also nasopharyngeal carcinoma [11] and ovarian cancer [14].

It is now well documented that in addition to tissue-specific signatures in different cancer types, cancers from different tissues also express some common genes [15–17]. One group of them is cell adhesion molecules (*CAMs*). *CAMs* do not merely act as a molecular glue to hold together homotypic cells in a specific tissue or to facilitate interactions of heterotypic cells; *CAMs* also actively govern the social behaviors of cells by affecting the adhesion status of cells and modulating cell signaling [18]. They control cell motility and invasiveness by mediating the remodeling of cytoskeleton [18]. They also actively mediate the cell-to-cell and cell-to-extracellular matrix interactions to allow cells to constantly respond to physiological fluctuations and to alter/remodel the surrounding microenvironment for survival [19]. They do so by crosstalk with cellular surface growth factor receptors, which interact with growth factors that may be secreted from stromal cells or released from circulation and embedded in the extracellular matrix [18, 19]. Thus, an altered expression of *CAMs* affects the motility and invasiveness of many tumor cells *in vitro* and metastasis *in vivo* [18, 19]. *CAMs* also play an important role in the favorable soil that provides a proper microenvironment at a suitable period to awaken the dormant metastatic tumor cells to enter into an aggressive growth phase. Actually, the metastatic potential of a tumor cell, as documented in many carcinomas, is the consequence of a complex participation of many over- and under-expressed *CAMs* [18, 19]. Based on the above information, aberrant expression of *huMETCAM* may also affect the motility and invasiveness of many tumor cells *in vitro* and metastasis *in vivo*. It is logical to hypothesize that *HuMETCAM/MUC18* should play an important role in promoting the malignant progression of many cancer types [7, 18]. However, recently we observed an unexpected opposite function of *METCAM/MUC18* in the malignant progression of a mouse melanoma subline and ovarian cancer cells, in which it functioned as a tumor and metastasis suppressor (Wu, unpublished results). In this paper, we will review its dual roles in the tumorigenesis and metastasis in different cancer types.

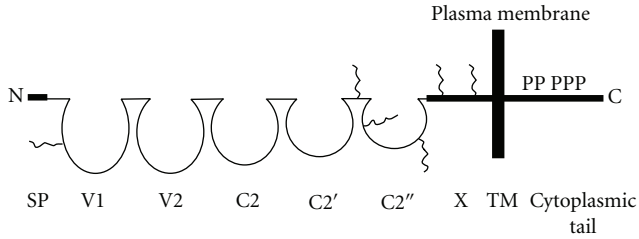

Figure 1: *HuMETCAM* protein structure. SP stands for signal peptide sequence: V1, V2, C2, C2′, and C2″ for five Ig-like domains (each held by a disulfide bond) and X for one domain (without any disulfide bond) in the extracellular region, and TM for transmembrane domain. P stands for five potential phosphorylation sites (one for *PKA*, three for *PKC*, and one for *CK2*) in the cytoplasmic tail. The six conserved N-glycosylation sites are shown as wiggled lines in the extracellular domains of V1, the region between C2′ and C2″, C2″, and X.

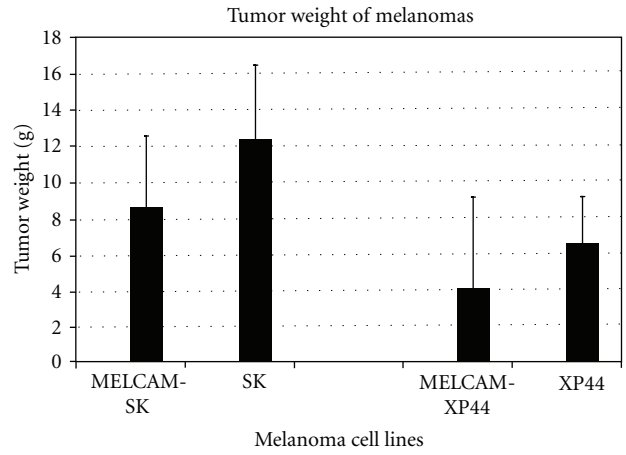

Figure 2: Effect of overexpression of *huMETCAM* on tumor formation of two human melanoma cell lines, *SK* and *XP-44* [20]. *MELCAM-SK* and *MELCAM-XP-44* were two clones of human melanoma cell lines, *SK* and *XP-44*, respectively, which were transfected with *huMETCAM* and expressed a high level of *huMETCAM*. Statistical analysis was not possible because detailed data was not provided.

2. *METCAM* and Tumorigenesis

METCAM-induced tumorigenesis has been studied in melanoma, prostate cancer, breast cancer, and ovarian cancer. Overexpression of *METCAM* may have no effect, a negative effect, or a positive effect on tumorigenesis, dependent upon the cell lines used, as shown in the following.

2.1. METCAM and Melanoma Tumorigenesis. Overexpression of *METCAM* had a slight tumor suppression effect on tumorigenesis of human melanoma cells in xenograft mice [20], as shown in Figure 2, but it had no effect on tumorigenesis of two sublines, number 3 and number 10, of the mouse melanoma cell line K1735 in syngeneic mice [21]. Figure 3 shows only the effect of *moMETCAM* on the tumorigenesis of K1735-3.

Only one group showed that overexpression of *METCAM* increased tumorigenesis of a human melanoma cell line in xenograft mice [3]; however, the results were questionable because only the tumorigenicity of one mouse injected with *METCAM*-expressing clone and one mouse with control cells was determined, and thus no standard deviations were indicated and no statistical analysis was done, as shown in Figure 4.

The most compelling evidence for its tumor suppressor effect is in the subline number 9 of the mouse melanoma cell line *K1735* (*K9*) in syngeneic *C3H* mice. Overexpression of *moMETCAM* in the *K9* cells decreased subcutaneous tumorigenesis in immunocompetent syngeneic *C3H* mice [22, 23, and unpublished results], as shown in Figure 5.

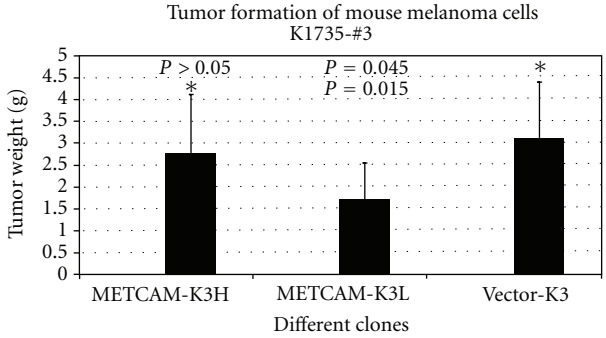

Figure 3: Effect of overexpression of *moMETCAM* on tumor formation of a mouse melanoma cell line *K1735* subline number 3 [21]. METCAM-K3H and METCAM-K3L were two K3 clones transfected with *moMETCAM* cDNA; expressed a high and a low level of *moMETCAM*, respectively. Vector-K3, as a negative control, was one clone transfected with an empty vector and did not express any *moMETCAM*. Asterisk was the reference for the *P* value calculation. The *P* values should be compared with the reference (asterisk) on the same row.

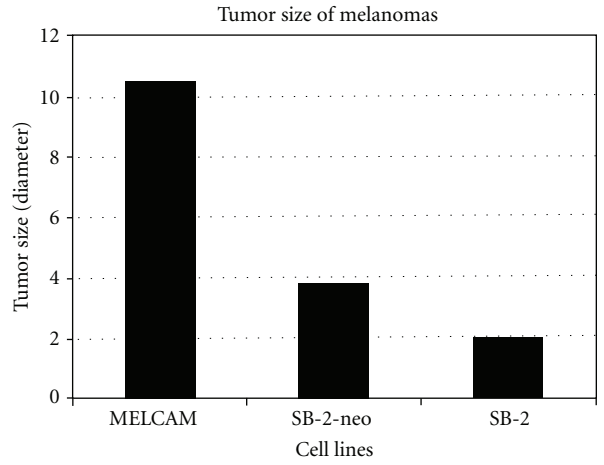

Figure 4: Effect of overexpression of *huMETCAM* on tumor formation of a human melanoma cell line *SB-2* [3]. *SB-2* is a human melanoma cell line, which did not express any *huMETCAM*. SB-2-neo is the SB-2 cells transected with the empty vector, as a negative control. *MELCAM* is a clone of the SB-2 cells which were transfected with *huMETCAM* cDNA and expressed a high level of *huMETCAM*. Since tumor formation was only shown in one nude mouse for each clone, statistical analysis was not possible.

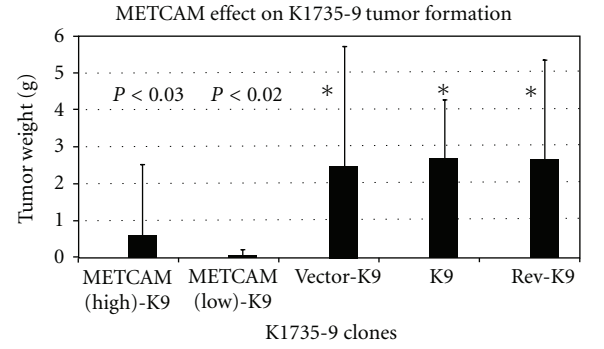

Figure 5: Effect of overexpression of *moMETCAM* on tumor formation of a mouse melanoma *K1735* subline number 9 (*K9*) in immune competent syngeneic *C3H* mice. METCAM-K9H and METCAM-K9L were two transfected clones, which expressed a high and a low level of *moMETCAM*, respectively. Vector-K9 was one clone transfected with the empty vector, as a negative control. K9 was parental K1735 subline number 9 cells, also as a negative control. Rev-K9, in which the *moMETCAM* cDNA was inserted into the expression vector in antisense orientation, is also as a control clone. Vector-K9, K9, and Rev-K9 did not express any *moMETCAM*.

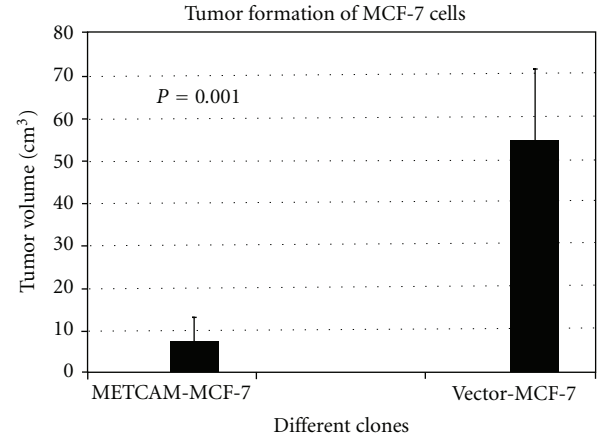

Figure 6: Effect of overexpression of *huMETCAM* on tumor formation of a human breast cancer cell line *MCF-7* [24]. METCAM-MCF-7 was a clone, which expressed a high level of *huMETCAM/MUC18* after transfection with the cDNA. Vector MCF-7 was a clone, which did not express any *huMETCAM* after transfection with an empty vector. Cells were injected subcutaneously into female *SCID* mice [24].

2.2. METCAM and Breast Cancer Tumorigenesis. Shih et al. showed that *METCAM* was not expressed in *MCF-7* cell line [24], and they showed that the overexpression of *huMETCAM* in *MCF-7* cells suppressed tumor formation of the cells in *SCID* mice, as shown in Figure 6, suggesting that *METCAM* is a possible tumor suppressor in breast cancer [24].

We have confirmed from their Western blot and immunohistochemistry results that *METCAM* is not expressed in *MCF-7* cells (0%), very weakly expressed in *SK-BR-3* cells (5%), and weakly expressed, though slightly higher levels than the above two cells lines, in the human mammary cancer cell lines, *MDA-MB-231* (a low metastatic cell line) (16%), and *MDA-MB-468* (a high metastatic cell line) (22%), as shown in Figure 7.

Recently gene expression profiles of breast cancer cell lines have indicated that the gene expression profiles of *MCF-7* and *SK-BR3* are more closely related to the luminal subtype of the breast cancers, whereas those of *MDA-MB-231* and *MDA-MB-468* are more closely related to the basal-like subtype [25, 26]. It appeared that *METCAM* is not or weakly expressed in cell lines established from luminal subtypes, but it is moderately expressed in cell lines established from

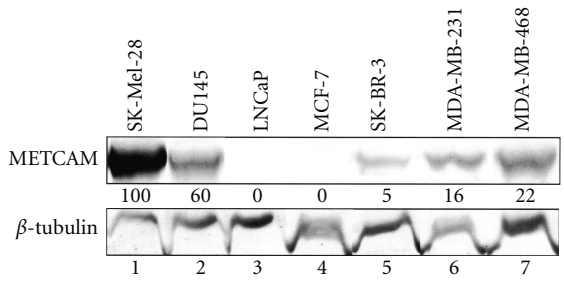

Figure 7: Expression of *huMETCAM* in four human breast cancer cell lines, *MCF-7*, *SK-BR-3*, *MDA-MB-231*, and *MDA-MB-468*. *SK-Mel-28*, a human melanoma cell line, which expressed a very high level of *huMETCAM*, was used as a positive control (100%). Two human prostate cancer cell lines, *DU145* and *LNCaP*, which expressed different levels of *huMETCAM* (60% and 0%, resp.) were used as positive and negative controls.

basal-like subtypes, *MDA-MB-231* and *MDA-MB-468*. Recently Ouhtit et al. [27] found that overexpression of *METCAM* inhibited the *in vitro* invasiveness of *MDA-MB-231* cells, supporting the notion of Shih et al. On the contrary, Garcia et al. [28] and Zabouo et al. [29] supported the opposite role of *METCAM* in the progression of human breast cancer cells in that it plays a role of tumor promoter. However, all three groups did not substantiate their claim with studies in animal models. To resolve this controversy, we recently reinvestigated the role of *METCAM* in the tumorigenesis of human breast cancer cells in animal models and found that overexpression of *METCAM* promoted the tumorigenesis of four human breast cancer cell lines, *MCF7*, *SK-BR-3*, *MDA-MB-231*, and *MDA-MB-468* [30, 31]. Tumorigenesis of *MCF-7* in female *SCID* mice [30] is shown in Figure 8, and that of *SK-BR-3* in female nude mice [31] in Figure 9.

Thus, the tumor suppression role of *METCAM* in tumorigenesis of human breast cancer cells is not supported by the above evidence. On the contrary, it suggests the alternative notion that *METCAM* increased tumorigenesis and perhaps also the metastasis of human breast cancer cells.

2.3. METCAM and Ovarian Cancer Tumorigenesis. Recently, both our group and another group found that *METCAM* was upregulated in human ovarian cancer specimens, suggesting that *METCAM* may be a marker for the poor prognosis of ovarian cancer patients [14, 32], and that *METCAM* may play a positive role in the development of ovarian cancer [14, 32]. However, preliminary animal tests (injection of *BG-1* cells in nonorthotopic, subcutaneous sites of female nude mice) show that overexpression of *METCAM* did not have any significant effect on the tumor formation of a human ovarian cancer cell line, *BG-1* (data not shown). To rule out the possibility that this effect might be an artifact because the tests were carried out in the nonorthotopic, subcutaneous sites, which did not provide a proper microenvironment for tumorigenesis, we carried out further tests of the effect of overexpression of *METCAM* on tumorigenesis of *BG-1* cells by injecting the clones in an orthotopic site, the intraperitoneal cavity of female *SCID* mice. We found that tumorigenesis of BG-1 clones was also very poor, suggesting that estrogen supplement by subcutaneous implantation may enhance the tumorigenesis of *BG-1* cells in both immunodeficient mice. Nevertheless, the test of the effect of overexpression of *METCAM* on tumorigenesis of *BG-1* cells in orthotopic sites had a somewhat suppressive effect, as shown in Figure 10 [33].

We also carried out animal studies by using another human ovarian cancer cell line, *SK-OV-3* and found that overexpression of *METCAM* suppressed tumorigenesis of *SK-OV-3* cells at both nonorthotopic, subcutaneous sites, as well as an orthotopic site (the intraperitoneal cavity) [34], as shown in Figure 11.

2.4. METCAM and Prostate Cancer Tumorigenesis. Overexpression of *METCAM* significantly increases the tumor-take and promote tumorigenicity and tumorigenesis of a human prostate cancer cell line, *LNCaP,* as shown in Figure 12 [35, 36].

2.5. METCAM Tumorigenesis of Other Cancer Cell Lines. We found that *moMETCAM* was expressed at a higher level in a mouse angiosarcoma clone, *SVR*, which was transfected with *H-Ras*, than in the immortalized normal endothelial cell line control, *MS-1* (Figure 13). The higher level of *moMETCAM* expression appeared to correlate with the higher tumorigenicity of the *SVR* cell line [7, 37], suggesting a positive role for *METCAM* in promoting angiosarcoma [7].

There is a negative correlation of *METCAM* expression with the human nasopharyngeal carcinoma specimens, suggesting that *METCAM* may also play a tumor suppressor role in the tumorigenesis of nasopharyngeal carcinoma [11]. A tumor suppressor role of *METCAM* may also be implicated in haemangiomas, since *METCAM* expression was decreased during the progression of haemangiomas [38].

3. *METCAM* and Metastasis

METCAM-induced metastasis has been studied in melanoma, prostate cancer, osteosarcoma, and ovarian cancer lines. Overexpression of *METCAM* in melanoma cells mostly have a positive effect on the metastasis of human melanoma cell lines in immunodeficient mice (both athymic nude and *SCID* mice) [3, 20], mouse melanoma cell lines in syngeneic mice [7, 21], and a human prostate cancer cell line, *LNCaP*, in nude mice [7, 13, 36]. Overexpression of *METCAM* also has a positive effect on the metastasis of osteosarcoma cell lines [39]. Surprisingly, we have recently found that overexpression of *METCAM* has a negative effect on the metastasis of one subline, number 9, of mouse melanoma cell K1735 [22, 23, and our unpublished results] and ovarian cancer cell lines [30–32]. Details are described in the following.

3.1. METCAM and Melanoma Metastasis. HuMETCAM was originally found to be abundantly expressed on the cellular surface of most malignant human melanomas; since then, it has been postulated to play a role in the progression of

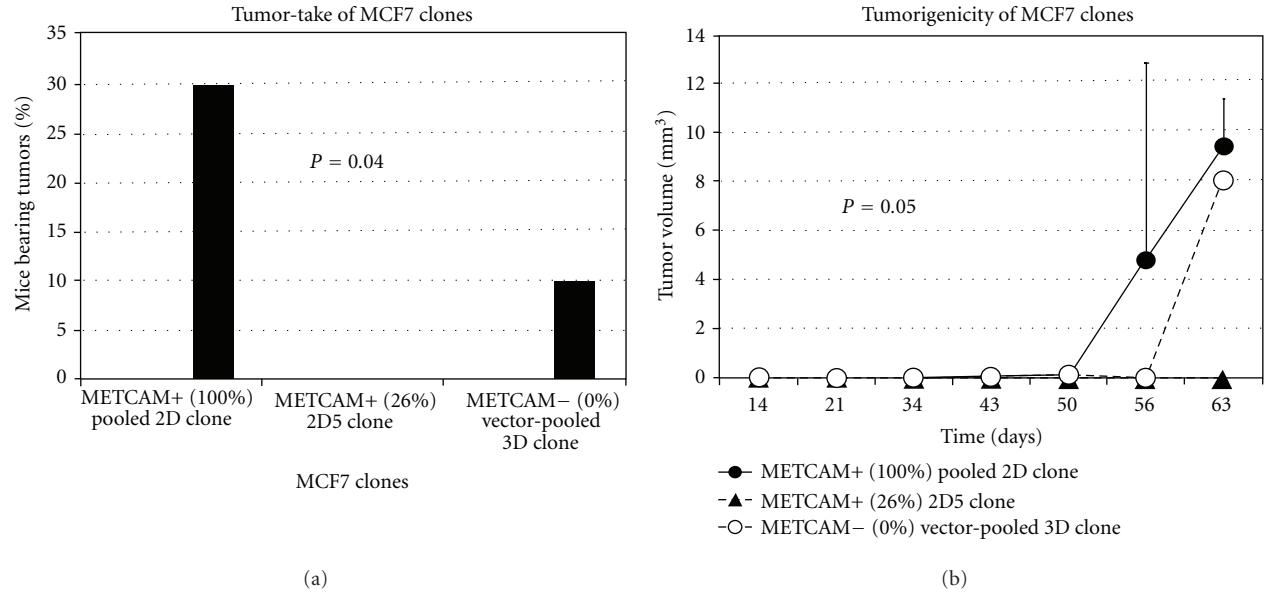

Figure 8: Effect of overexpression of *huMETCAM* on tumor-take (a) and tumorigenicity (b) of a human breast cancer cell line *MCF7 in female SCID mice*. METCAM+ clone 2D pooled was a pooled clone, which expressed 100% of *huMETCAM*, and METCAM+ clone 2D5, which expressed 26% of *huMETCAM*, after transfection with the *huMETCAM* cDNA. Vector clone 3D pooled was a pooled clone, which did not express any *huMETCAM*, after transfection with an empty vector. Cells were injected subcutaneously into female SCID mice [30].

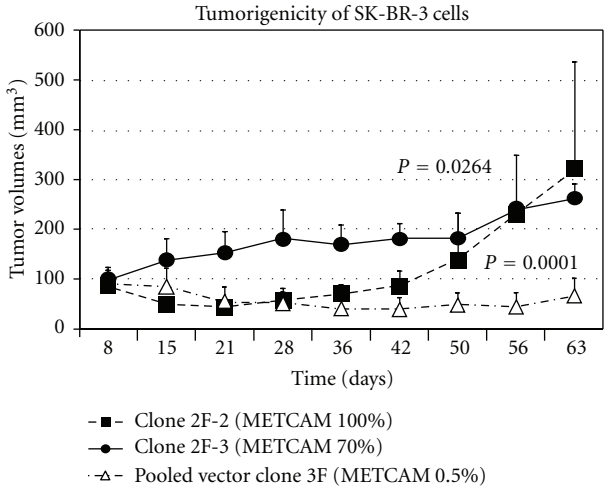

Figure 9: Effect of overexpression of *huMETCAM* on tumor formation of a human breast cancer cell line *SK-BR-3* in female nude mice [31]. Clone 2F-2 and clone 2F-3 expressed 100% and 70% of *METCAM*, respectively. Pooled vector clone 3F expressed only about 0.5% of *METCAM*, as a vector control.

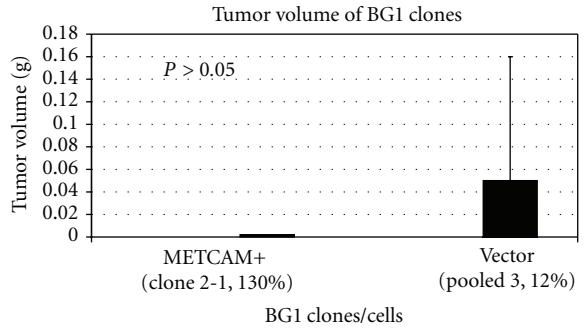

Figure 10: Effect of overexpression of *huMETCAM* on tumorigenicity of a human ovarian cancer cell line BG-1 in an orthotopic site (the intraperitoneal cavity) in female SCID mice. Clone 2-1 expressed 130% of *METCAM*. The vector control, pooled clone 3, expressed 12% of *METCAM*.

human melanoma [1]. This notion is also supported by the positive correlation of *moMETCAM* expression with the metastatic ability of several mouse melanoma cells lines [9]. Definitive proof comes from the results that the stably ectopic expression of the *huMETCAM* cDNA gene in three nonmetastatic human cutaneous melanoma cell lines increases the metastatic abilities of these cell lines in immune-deficient mouse models [3, 20]. Furthermore, the stable, ectopic expression of *moMETCAM* cDNA in two low-metastatic mouse melanoma cell lines increases the metastatic abilities of these cell lines in immune-competent syngeneic mice [21]. However, *METCAM* enables melanoma cells to establish pulmonary metastasis only when the cells are injected into the tail vein (experimental metastasis assay) [3, 20, 21], thus bypassing the initial stages of metastasis. No metastasis was found when *METCAM*-expressing melanoma cells were injected subcutaneously (spontaneous metastasis assay) either in immune-deficient mouse models [3, 20] or in immune-competent syngeneic mouse models [21]. Taken together, *METCAM* definitely promotes the metastasis of melanoma cells, but at later stages [7]; thus overexpression

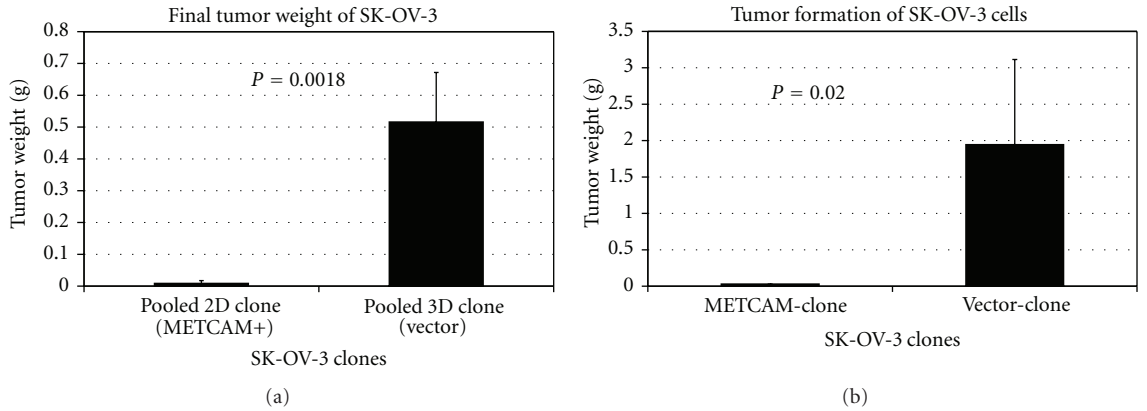

Figure 11: Effect of overexpression of *huMETCAM* on the final tumor weight at *S.C.* sites (a) and orthotopic sites (the intraperitoneal cavity) (b) of a human ovarian cancer cell line *SK-OV-3*. Both Pooled 2D clone and METCAM-clone expressed 100% of *METCAM*. Both pooled 3D clone (vector) and vector clone expressed 0.5% of *METCAM*.

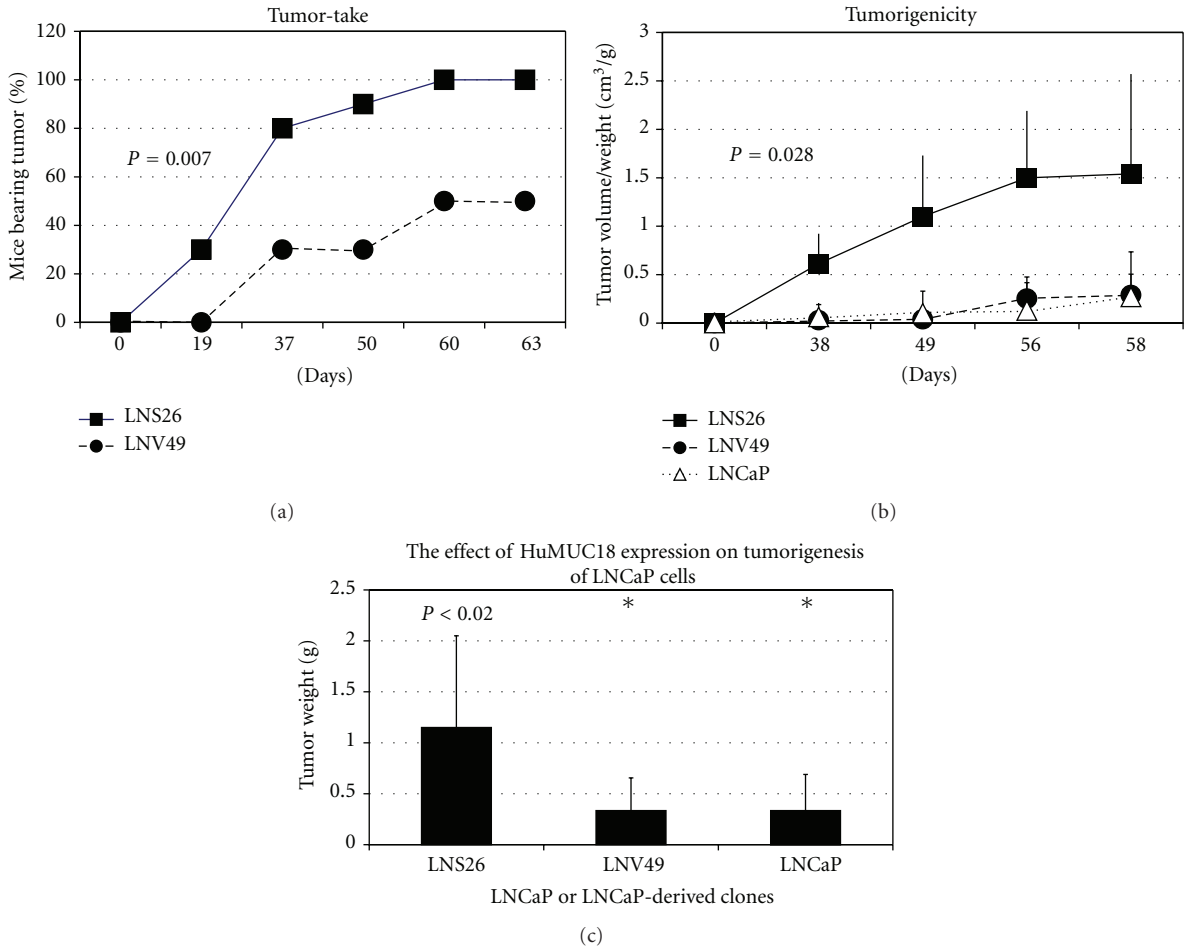

Figure 12: Enforced expression of *huMETCAM* in *LNCaP* cells resulted in an increased tumor-take (a), tumorigenicity (b), and final tumor weight (c) [35]. Clone LNS26 expressed *METCAM*. Both the vector control clone, LNV49, and the parental *LNCaP* cells did not express any *METCAM*.

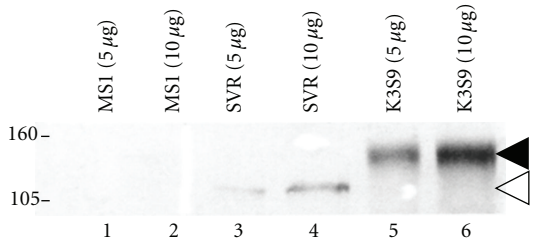

Figure 13: Expression of *moMETCAM* in mouse angiosarcoma cell lines [7]. *MS1* is an immortalized mouse endothelial cell line, which expressed a barely detectable (low) level of *moMETCAM* and was nontumorigenic. *SVR* is a mouse angiosarcoma cell line, which had been transfected with *H-Ras* gene, also expressed *moMETCAM*, and was tumorigenic. K3S9, a clone derived from mouse melanoma *K1735* subline number 3 which had been transfected with a *moMETCAM* cDNA gene, expressed a high level of *moMETCAM* and formed tumor efficiently in syngeneic mice (C3H). Western blot was carried out and detected by our chicken anti-*moMETCAM* antibody [9]. The smaller molecular weight of the *moMETCAM* (about 115 kDa) in angiosarcoma cell lines was probably due to less glycosylation than that in the mouse melanoma cell lines or in most human cancer cell lines (about 150 kDa).

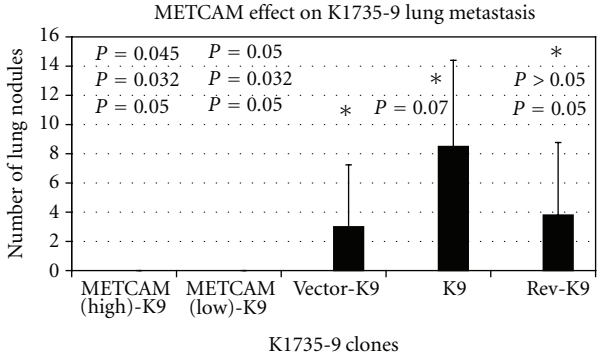

Figure 14: Enforced expression of *moMETCAM* suppressed lung nodule formation of mouse melanoma *K9* cells in syngeneic *C3H* mice. Clones METCAM (high)-K9 and METCAM (low)-K9 clones expressed high and low levels of *moMETCAM*, respectively. Vector-K9, K9 parental cells, and Rev-K9, in which the *moMETCAM* cDNA was inserted into the expression vector in antisense orientation, were the control clones that did not express any *moMETCAM*.

of *METCAM* did not initiate the metastasis of melanoma cells. This result is consistent with the recent observation that fibroblast growth factor 2, but neither *huMETCAM* nor integrin actually initiates the malignant progression of subcutaneous melanocyte into melanoma [40].

In contrast to these results, overexpression of *moMETCAM* in one mouse melanoma cell line *K1735* subline number 9 (*K9*) decreased pulmonary lung nodule formation when cells were injected into tail veins (experimental metastasis test) [22, 23, and unpublished results], as shown in Figure 14.

3.2. METCAM and Prostate Cancer Metastasis. Overexpression of *METCAM* is not limited to melanoma as previously thought [7, 10]. Our group has pioneered the successful determination of *huMETCAM* expression in prostate cancer cells and tissues using our chicken polyclonal *anti-huMETCAM* and carried out extensive studies of *huMETCAM*-mediated prostate cancer metastasis [8]. We have used molecular biological and immunological methods to study the expression of *huMETCAM* in three established prostate cancer cell lines and human prostate cancer tissues, and in immunohistochemical studies of paraffin-embedded human prostate cancer tissue sections [7, 8, 12, 13]. From the results, we have suggested that *huMETCAM* may be a new diagnostic marker for the metastatic potential of human prostate cancer. This is further corroborated by results of a positive correlation of *moMETCAM* expression with the progression of mouse prostate adenocarcinoma in a transgenic mouse model, *TRAMP* [41]. From these results, we have also suggested that *huMETCAM* may be a key determinant in promoting tumorigenesis and metastasis of human prostate cancer cells [7]. To test this hypothesis, we determined the effect of ectopic expression of *huMETCAM* on the ability of human prostate *LNCaP* cells to form tumor in the prostate gland and to initiate metastasis in nude mice. We found that overexpression of *METCAM* had a positive effect on the metastasis of the human prostate cancer cell, *LNCaP*, when the cells were injected at the orthotopic site (the dorsolateral lobes of the nude mice) [36]. The metastatic lesions were found in multiple organs, such as seminal vesicles, ureter, kidney, and periaortic lymph nodes [36]. Different mice had metastatic lesions in one or two organs, but all of them had metastatic lesions in the lymph nodes. The parental *LNCaP* cells, which do not express any *METCAM,* can form tumors in the prostate, but these tumors did not manifest any metastasis. The metastatic lesions in the bones were not examined. But our recent preliminary results appear to show that overexpression of *METCAM* may be able to enhance establishment of the growth of a bone-homing *C42B* clone of *LNCaP* cells in nude mice. Further tests are in process [Wu et al., unpublished results].

Taken together, *METCAM* can actually initiate the metastasis of *LNCaP* cells, thus affecting the progression of prostate cancer cells at the early stage of metastasis [7, 36].

3.3. METCAM and Osteosarcoma Metastasis. Recently, one group has shown that *METCAM* is overly expressed in two of the six human osteosarcoma cell lines. Overexpression of *METCAM* increased the spontaneous lung metastasis of an osteosarcoma cell line *KRIB*. The metastasis can be blocked by a humanized antibody against *METCAM,* suggesting *METCAM* plays a positive role in the progression of osteosarcomas [39].

3.4. METCAM and Ovarian Cancer Metastasis. Recently we found that overexpression of METCAM/MUC18 suppressed metastasis and ascites formation of *SK-OV-3* cells in the intraperitoneal cavity [34], as shown in Figure 15.

3.5. METCAM and Metastasis of Other Cancer Cell Lines. Decreased expression of *METCAM* has been correlated with

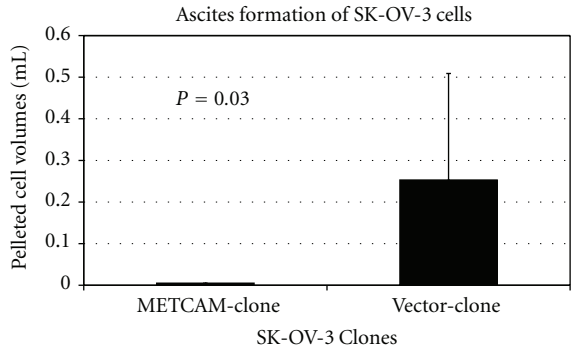

Figure 15: Enforced expression of *huMETCAM* in human ovarian *SK-OV-3* cells suppressed solid tumor formation and ascites formation in the intraperitoneal cavity. METCAM-clone expressed 100% of *METCAM*. Vector-clone expressed 0.5% of *METCAM*.

the progression of haemangioma, suggesting the possible negative effect of *METCAM* on progression of haemangioma [38]. Though *METCAM* was downregulated in nasopharyngeal carcinoma, interestingly it was upregulated again in metastatic lesions in nasopharyngeal patients, suggesting that *METCAM* may play a positive role in the malignant progression of nasopharyngeal carcinoma after a transient suppression of tumorigenesis [11].

Taken together, we suggest that the possible tumor and metastasis suppressor role of *METCAM* may not be limited to melanoma and ovarian cancers, and that this may be a new function of *METCAM* yet to be explored.

Summary. Table 1 summarizes the possible role of *METCAM* in the tumorigenesis and metastasis of various tumors/cancers.

Taken together, *huMETCAM* is a tumor promoter for prostate and breast cancers, and a metastatic gene for most melanoma cell lines, prostate cancer, osteosarcoma, and perhaps, breast cancer and nasopharyngeal carcinoma. It is a tumor suppressor for a mouse melanoma subline and ovarian cancers, and perhaps, haemangioma and nasopharyngeal carcinoma; it is a metastasis suppressor for a mouse melanoma subline, ovarian cancer, and perhaps, haemangioma.

4. Mechanisms of *METCAM*-Mediated Tumorignesis and Metastasis

How does *METCAM* mediate or regulate tumorigenesis and metastasis of cancer cells? By deducing knowledge learned from the tumorigenesis of other tumors [15–19, 42] and the *huMETCAM*-mediated progression of melanoma [43–45] and angiogenesis [2, 46–51], we may be able to find some common clues to begin understanding its mechanisms.

First, the transcriptional expression of *METCAM* gene may be regulated by *PKA/CREB* (cAMP-responsive element binding protein), *AP-2α* [44, 45], and other transcription factors, such as *SP-1*, *c-Myb*, *N-Oct2*, *ETs*, *CArG*, *Egr-1,* and transcription factors binding to insulin-response elements, as shown in Figure 16 [7].

Among these potential regulators, it is well documented that the *AP-2α* transcription factor plays a crucial tumor suppressor role in the progression of melanoma, prostate, and breast cancer [45]. It has been shown that *PKA/CREB* plays a positive role in the progression of melanoma, and perhaps also applicable to breast cancer and prostate cancer, by inhibiting the expression of AP-*2α* and increasing the expression of *METCAM* [45]. However, the expression level of *AP-2α* in other cancers has not been explored. The roles of other transcription regulators, tissue-specific enhancers and repressors, epigenetic control, and control at the level of chromatin remodeling of the gene have still yet to be investigated [7].

Second, since the cytoplasmic tail of *METCAM* contains consensus sequences potentially to be phosphorylated by *PKA*, *PKC*, and *CK2*, it may manifest its functions by crosstalk with various signaling pathways mediated by these protein kinases [7]. For example, *METCAM* expression in melanoma cells is reciprocally regulated by *AKT*, in which *AKT* up-regulates the level *METCAM* and overexpression of *METCAM* activates endogenous *AKT*, which in turn inhibits apoptosis and increases survival ability [43]. However, it is not clear if a similar mechanism is also used in breast, prostate, and other cancers. Also, the detailed mechanism of how *AKT* up-regulates the expression of *METCAM* has not been worked out. *PKA*, *PKC*, and *CK2* may phosphorylate the cytoplasmic tail of *METCAM*, which then facilitates its interaction with *FAK,* thus promoting cytoskeleton remodeling. Alternatively, after phosphorylation of its cytoplasmic tail by these protein kinases, *METCAM* may interact with the downstream effectors of *Ras*, activating *ERK* and *JNK,* which in turn may transcriptionally activate the expression of *AKT* or other genes that promote the proliferation and angiogenesis of tumor cells. Though *METCAM* has not been shown to be a substrate of *CK2,* which has been shown to phosphorylate other *CAMs*, such as *CD44*, *E-cadherin*, *L1-CAM*, and *vitronectin*, it is also likely that *CK2* may be able to phosphorylate *METCAM* [46] and link it to *AKT* to affect the proliferation, survival, and other tumorigenesis-related functions of tumor cells [47].

Third, after the engagement of *METCAM* with the ligand(s) or extracellular matrix, it may transmit the outside-in signals into tumor cells by activating *FAK* and the downstream-signaling components, promoting cytoskeleton remodeling and increasing tumor cell motility and invasiveness [2, 7].

Fourth, from what we know about the roles of other *CAM*s in the progression of other tumors [15–19, 42], it is logical to postulate that *METCAM* may affect cancer cell progression by crosstalk with signaling pathways that affect apoptosis, survival and proliferation, and angiogenesis of tumor cells [7, 18, 42]. Thus, *METCAM* may affect tumorigenesis and metastasis by altering the expression of various indexes in apoptosis, survival signaling, proliferation signaling, and angiogenesis. To support this notion, we have found that *METCAM* promotes the progression of prostate cancer cells by rendering the cells with increased proliferative ability by elevating levels of *Ki67* and *PCNA*, with increased survival ability by elevating the level of phosphorylated *AKT*,

Table 1: The role of *METCAM* in the tumorigenesis and metastasis of various cancer cells.

Cancer cells	Tumorigenesis	Metastasis	References
Clinical prostate cancer and human prostate cancer cell lines	Increasing	Increasing (effect is in the early stage of initiation)	[7, 8, 12, 13, 35, 36]
Mouse prostate carcinomas in TRAMP mice	Increasing	Increasing	[41]
Clinical melanoma and human melanoma cell lines	No effect	Increasing (effect is in the late stages)	[3, 20]
Mouse melanoma cell line of K1735 subline number 3 and 10s	No effect or slight suppression	Increasing (effect is in the late stages)	[9, 21]
Mouse melanoma cell line K1735 subline number 9	Suppression	Suppression	[22, 23] and Wu et al. unpublished results
Angiosarcoma	Increasing	Not determined	[7, 37] and Wu et al. unpublished results
Human ovarian cancer cell lines BG-1 and SK-OV-3	Suppression	suppression	[33, 34]
Human osteosarcoma cell lines	Not determined	Increasing	[39]
Human breast cancer cell line MCF-7	Suppression	Not determined	[24]
Human breast cancer cell lines MCF-7 and SK-BR-3	Increasing	Not determined	[30, 31]
Haemangiomas	Suppression?	Not determined	[38]
Nasopharyngeal carcinoma	Suppression?	Not determined	[7, 11]

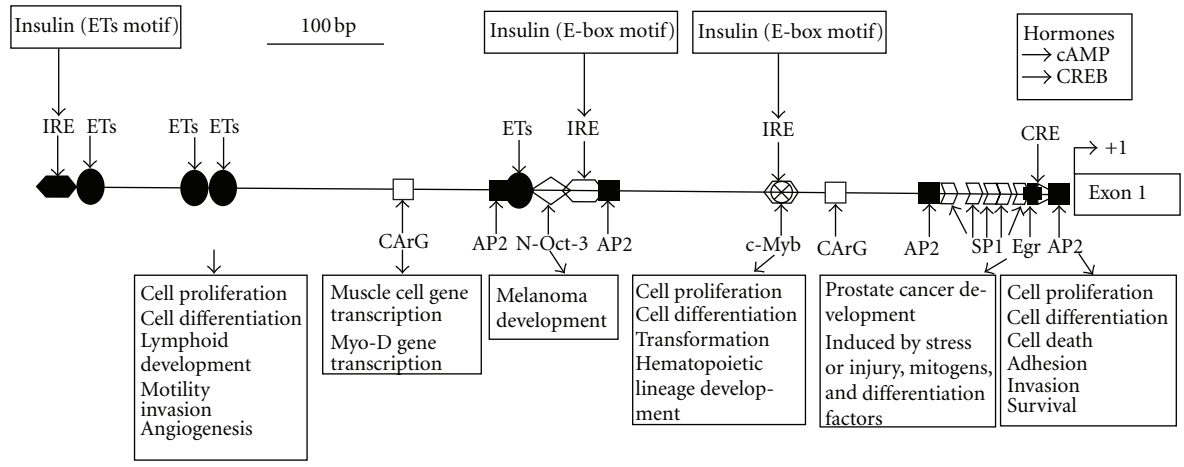

Figure 16: The promoter of the *huMETCAM* gene. The locations of various transcriptionally regulatory elements are shown in the 900 bp promoter region of the *huMETCAM* gene. The possible function of each element is also indicated. The promoter contains four AP-2 (activator protein-2, GCCNNNGGC), one CRE (cAMP response element, TGACGTCA), one Egr (early growth response element, CCCTG), five SP-1 (CCGCCC), two CArG (CC(A/t)6GG), three IRE (two insulin responsive elements with E-box motif, CANNTG, and one with Ets motif, ACGGAT), one c-Myb (coincided with one IRE with E-box motif, CACCTG), one N-Oct-3 (or brn-2, GCCTGAAT), and four Ets elements (GGAA).

and with increased angiogenic ability by elevating levels of *VEGF*, *VEGFR2,* and *CD31* [35]; but it has no effect on the process of apoptosis. In contrast to this, *METCAM* promotes the progression of melanoma cells differently by preventing the apoptosis of melanoma cells [47] and reciprocally affecting the expression of a survival index, phospho-*AKT* [43]. Further systematic studies by using specific RNAis to knockdown the downstream effectors one-by-one in the *METCAM*-expressing clones may be necessary to further understand this aspect of mechanism.

Fifth, *METCAM* may mediate hematogenous spreading of melanoma cells, which had been implicated by its expression in endothelial cells, as well as in malignant melanoma cells [48], further shown to be present in the junctions of endothelial cells [49, 50] and essential for tumor angiogenesis in at least three tumor cell lines [51] and human prostate

cancer *LNCaP* cells [52]. It is highly likely that *METCAM* expression may promote hematogenous spreading of prostate cancer cells, similar to melanoma cells [49]. Similar mechanisms may also be used for the *METCAM*-mediated hematogenous spreading of breast cancer and osteosarcoma cells. However, it is not known if *METCAM* also plays a role in the lymphatic spread of cancer cells. Recent results from one group showed that *METCAM* is one of the lymphatic metastasis-associated genes, which is upregulated in malignant mouse hepatocarcinoma [53]; suggesting that *METCAM* may also play a role in promoting lymphatic metastasis of cancer cells. However, the details of how *METCAM* mediates hematogenous or lymphatic spreading of cancer cells have still yet to be investigated. Labeling the cells with viable dyes and following the process in real time by using a newly developed nonintruding, but highly photopenetrating imaging method of photoacoustic tomography (PAT) [54, 55] may be useful for monitoring each step in the *METCAM*-mediated progression. For the *METCAM*-mediated dynamic spreading of melanoma cells *in vivo*, the PAT imaging method coupled with using hairless syngeneic mouse animal models [56] should reveal more clearly the process in real time.

Sixth, *METCAM* has been shown to express in normal mesenchymal cells (smooth muscle, endothelium, and Schwann cells) in the tissue stroma and be a marker for the mesenchymal stem cells [57], *METCAM* may play an important role in regulating tumor dormancy or awakening, driving or preventing cancer cells to premetastatic niche, and formatting a microenvironment for favorable or unfavorable tumor growth in secondary sites.

Seventh, *METCAM* may affect the progression of cancer cells by interactions with the host immune system, which, however, has been shown to have a paradoxical role in tumor progression [58]. Recently, one group has shown that a subset of host B lymphocytes may control melanoma metastasis through METCAM-dependent interaction [59]. On the other hand, it is highly likely that the tumor suppression effect of *METCAM* expression in melanoma *K1735-9* subline may be due to the interaction of *METCAM*-expressing cells with the host immune defense system in the immunocompetent syngeneic *C3H* brown mouse, since the intrinsic motility and invasiveness of mouse melanoma *K1735-9* was increased by the *METCAM* expression [22, 23]. For example, the surface *METCAM* expressed in this particular melanoma cell line may have a homophilic interaction with the *NK* cells, which also express *METCAM* and enhance cytotoxic functions of *NK* cells [60]. This hypothesis should be testable by studying the METCAM-mediated metastasis of METCAM-expressing K1735-9 cells in various genetically altered mice with a knockout of *CD4+ T* cells, *CD8+ T* cells, or *NK* cells, or mice with a combined knockout of these immune cells.

Eighth, malignant progression of cancer cells has been shown to associate with an abnormal glycosylation, resulting in expression of altered carbohydrate determinants [61]. Thus, the glycosylated status of *METCAM* in different cancer types may be different from normal cells, thus manifesting positive or negative effect on the progression of different cancer types. This aspect of the METCAM-mediated cancer progression has not been well studied, but is especially intriguing since METCAM possesses six conserved N-glycosylation sites in the extracellular domain [7, 8].

We should always keep in mind that mechanisms of *METCAM*-mediated cancer progression may be slightly different in different cancer cells due to their different intrinsic properties, which provides different cofactors and/or different ligand(s) that either positively or negatively regulate the *METCAM*-mediated tumorigenesis and metastasis. To further understand the role of *METCAM* in these processes, it is essential to diligently identify the cofactors and the *METCAM*-cognate heterophilic ligand(s), which modulate the biological functions of *METCAM*. The endeavor in this direction appears to be promising from our preliminary attempts that we may have successfully found a possible candidate of METCAM's heterophilic ligand in *METCAM*-expressing human prostate cancer cells [7].

Mechanisms of *METCAM*-mediated negative role in the progression of some cancer cells have not been studied at all. Does *METCAM* in some cancers behave like E-cadherin, which always plays a negative role in the tumorigenesis and metastasis of most epithelial cancer cells [18]? But even *E-cadherin* may function differently in different cancer cells. For example, its expression is temporally different and correlates with different stages during the progression of ovarian cancer [62]: *E-cadherin* is not expressed in the ovarian surface epithelial cells, expressed in premalignant lesions and in well-differentiated tumors, and finally not expressed in late-stage invasive tumors [62]. Likewise, *METCAM* may express and function normally in the normal nasopharyngeal epithelium, transiently reduce its expression and lose its function during the development of nasopharyngeal carcinoma, resume its expression, and function in the invasion stage of the cancer. Alternatively, METCAM may behave differently from *E-cadherin* by being modulated by different cofactors or ligands, which are expressed at different stages of the cancer. The tumor suppressor role of *METCAM* in ovarian cancer cells may not be due to the altered intrinsic properties of the cancer cells, since the intrinsic motility and invasiveness of human ovarian cancer BG-1 and *SK-OV-3* cells was not affected by the *METCAM* expression [34, 35]. Our preliminary results appear to suggest a special mechanism that a soluble form of *METCAM*, which is produced by *MMP*s in the METCAM-expressing cells, may mediate the suppressive effect in ovarian cancer cells, similar to the production of a soluble form of *P-cadherin* by the induced MMPs in breast cancer cells, which then dictates, instead of suppresses, the aggressive behavior of the breast cancer cells [63].

5. Conclusions and Clinical Applications

METCAM may have a key positive function in the progression of angiosarcoma, breast cancer, osteosarcoma, prostate cancer, and most melanoma cell lines. On the other hand, it may also have a key function in suppressing the progression of a few melanoma cell lines, ovarian cancer, haemangioma, and other cancers. To further understand its mechanisms in

these processes, it is crucial to define its functional domains, identify its cognate ligand(s) and cofactor regulators, and study its crosstalk with members of various signaling pathways [7]. These model systems may be useful for real-time observation of the dynamic process of cancer progression by using a nonintrusive and high photo-penetrating imaging system, such as the newly developed photoacoustic tomography (*PAT*), to further understanding the process in mouse models [54, 55]. The knowledge gained would also be useful for designing effective means to decrease, or even to block the metastatic potential of these cancers. Along these lines, a preclinical trial of using *doxazosin*, an α1-adrenergic antagonist that has been used to treat the *BPH* patients, has been shown to be able to suppress prostate cancer metastasis in the *TRAMP* mouse model [64]. Furthermore, preclinical trials using a fully humanized anti-*METCAM* antibody against melanoma growth and metastasis [65, 66] and using a mouse anti-*METCAM* monoclonal antibody against angiogenesis and tumor growth of hepatocarcinoma, leiomyosarcoma, and pancreatic cancer [51] have been successfully demonstrated. Alternatively, small soluble peptides derived from *METCAM* may also be useful for blocking the tumor formation and tumor angiogenesis [52, 67, 68]. The attachment of these reagents to nanoparticles may be another alternative for therapeutic use [69].

Acknowledgment

The author thanks Mr. Jonathan C.-Y. Wu for critical reading of the paper and proof reading of the English Language.

References

[1] J. M. Lehmann, G. Riethmuller, and J. P. Johnson, "MUC18, a marker of tumor progression in human melanoma, shows sequence similarity to the neural cell adhesion molecules of the immunoglobulin superfamily," *Proceedings of the National Academy of Sciences of the United States of America*, vol. 86, no. 24, pp. 9891–9895, 1989.

[2] F. Anfosso, N. Bardin, E. Vivier, F. Sabatier, J. Sampol, and F. Dignat-George, "Outside-in signaling pathway linked to CD146 engagement in human endothelial cells," *Journal of Biological Chemistry*, vol. 276, no. 2, pp. 1564–1569, 2001.

[3] S. Xie, M. Luca, S. Huang et al., "Expression of MCAM/MUC18 by human melanoma cells leads to increased tumor growth and metastasis," *Cancer Research*, vol. 57, no. 11, pp. 2295–2303, 1997.

[4] I. M. Shih, D. E. Elder, M. Y. Hsu, and M. Herlyn, "Regulation of Mel-CAM/MUC18 expression on melanocytes of different stages of tumor progression by normal keratinocytes," *American Journal of Pathology*, vol. 145, no. 4, pp. 837–845, 1994.

[5] I. M. Shih, D. E. Elder, D. Speicher, J. P. Johnson, and M. Herlyn, "Isolation and functional characterization of the A32 melanoma-associated antigen," *Cancer Research*, vol. 54, no. 9, pp. 2514–2520, 1994.

[6] N. Bardin, F. George, M. Mutin et al., "S-Endo 1, a pan-endothelial monoclonal antibody recognizing a novel human endothelial antigen," *Tissue Antigens*, vol. 48, no. 5, pp. 531–539, 1996.

[7] G. J. Wu, "*METCAM*/MUC18 expression and cancer metastasis," *Current Genomics*, vol. 6, no. 5, pp. 333–349, 2005.

[8] G. J. Wu, M. W. H. Wu, S. W. Wang et al., "Isolation and characterization of the major form of human MUC18 cDNA gene and correlation of MUC18 over-expression in prostate cancer cell lines and tissues with malignant progression," *Gene*, vol. 279, no. 1, pp. 17–31, 2001.

[9] H. Yang, M. W. H. Wu, S. W. Wang et al., "Isolation and characterization of mouse MUC18 cDNA gene, and correlation of MUC18 expression in mouse melanoma cell lines with metastatic ability," *Gene*, vol. 265, no. 1-2, pp. 133–145, 2001.

[10] I. M. Shih, "The role of CD146 (Mel-CAM) in biology and pathology," *Journal of Pathology*, vol. 189, no. 1, pp. 4–11, 1999.

[11] J. C. Lin, C. F. Chiang, S. W. Wang et al., "Decreased expression of *METCAM*/MUC18 correlates with the appearance of, but its increased expression with metastasis of nasopharyngealcarcinoma," In press.

[12] G. J. Wu, V. A. Varma, M. W. H. Wu et al., "Expression of a human cell adhesion molecule, MUC18, in prostate cancer cell lines and tissues," *Prostate*, vol. 48, no. 4, pp. 305–315, 2001.

[13] G. J. Wu, "The role of MUC18 in prostate carcinoma," in *Immunohistochemistry and in Situ Hybridization of Human Carcinoma. Vol 1. Molecular Pathology, Lung Carcinoma, Breast Carcinoma, and Prostate Carcinoma*, M. A. Hayat, Ed., chapter 7, pp. 347–358, Elsevier Science/Academic Press, 2004.

[14] G. J. Wu, E. S. Son, E. B. Dickerson et al., "*METCAM*/MUC18 over-expression in human ovarian cancer tissues and metastatic lesions is associated with clinical progression," In press.

[15] B. Vogelstein and K. W. Kinzler, "Cancer genes and the pathways they control," *Nature Medicine*, vol. 10, no. 8, pp. 789–799, 2004.

[16] G. Christofori, "New signals from the invasive front," *Nature*, vol. 441, no. 7092, pp. 444–450, 2006.

[17] G. P. Gupta and J. Massague, "Cancer metastasis: building a framework," *Cell*, vol. 127, no. 4, pp. 679–695, 2006.

[18] U. Cavallaro and G. Christofori, "Cell adhesion and signalling by cadherins and Ig-CAMs in cancer," *Nature Reviews Cancer*, vol. 4, no. 2, pp. 118–132, 2004.

[19] A. Chambers, A. C. Groom, and I. C. MacDonald, "Dissemination and growth of cancer cells in metastatic sites," *Nature Reviews Cancer*, vol. 2, no. 8, pp. 563–572, 2002.

[20] H. Schlagbauer-Wadl, B. Jansen, M. Muller et al., "Influence of MUC18/MCAM/CD146 expression on human melanoma growth and metastasis in SCID mice," *International Journal of Cancer*, vol. 81, no. 6, pp. 951–955, 1999.

[21] G. J. Wu, P. Fu, S. W. Wang, and M. W. H. Wu, "Enforced expression of MCAM/MUC18 increases *in vitro* motility and invasiveness and *in vivo* metastasis of two mouse melanoma K1735 sublines in a syngeneic mouse model," *Molecular Cancer Research*, vol. 6, no. 11, pp. 1666–1677, 2008.

[22] G. J. Wu, Q. Peng, S. W. Wang, H. Yang, and M. W. H. Wu, "Effect of MUC18 expression on the *in vitro* invasiveness and *in vivo* tumorigenesis and metastasis of mouse melanoma cell lines in a syngeneic mouse model," in *Proceedings of the 92nd Annual Meeting of American Association for the Cancer Research*, vol. 42, abstract no. 2776, p. 516, 2001.

[23] G. J. Wu and M. W. H. Wu, "Ectopic expression of MCAM/MUC18 increases *in vivo* motility and invasiveness, but decreases tumorigenesis and metastasis of a mouse melanoma K1735-9 subline in a syngeneic mouse model," In press.

[24] I. M. Shih, M. Y. Hsu, J. P. Palazzo, and M. Herlyn, "The cell-cell adhesion receptor Mel-CAM acts as a tumor suppressor in breast carcinoma," *American Journal of Pathology*, vol. 151, no. 3, pp. 745–751, 1997.

[25] E. Charafe-Jauffret, C. Ginestier, F. Monville et al., "Gene expression profiling of breast cell lines identifies potential new basal markers," *Oncogene*, vol. 25, no. 15, pp. 2273–2284, 2006.

[26] R. M. Neve, K. Chin, J. Fridlyand et al., "A collection of breast cancer cell lines for the study of functionally distinct cancer subtypes," *Cancer Cell*, vol. 10, no. 6, pp. 515–527, 2006.

[27] A. Ouhtit, R. L. Gaur, Z. Y. Abd Elmageed et al., "Towards understanding the mode of action of the multifaceted cell adhesion receptor CD146," *Biochimica et Biophysica Acta*, vol. 1795, no. 2, pp. 130–136, 2009.

[28] S. Garcia, J. P. Dales, E. Charafe-Jauffret et al., "Poor prognosis in breast carcinomas correlates with increased expression of targetable CD146 and c-Met and with proteomic basal-like phenotype," *Human Pathology*, vol. 38, no. 6, pp. 830–841, 2007.

[29] G. Zabouo, A. M. Imbert, J. Jacquemier et al., "CD146 expression is associated with a poor prognosis in human breast tumors and with enhanced motility in breast cancer cell lines," *Breast Cancer Research*, vol. 11, no. 1, article no. R1, 2009.

[30] G. Zeng, S. Cai, and G. J. Wu, "Up-regulation of *METCAM*/MUC18 promotes motility, invasiveness and tumorigenesis of human breast cancer cells," *BMC Cancer*, vol. 11, p. 113, 2011.

[31] G. Zeng, S. Cai, Y. Liu, and G. J. Wu, "*METCAM*/MUC18 augments promotes migration, invasion and tumorigenicity of human breast cancer SK-BR-3 cells," *Gene*, vol. 492, pp. 229–238, 2012.

[32] D. Aldovini, F. Demichelis, C. Doglioni et al., "M-cam expression as marker of poor prognosis in epithelial ovarian cancer," *International Journal of Cancer*, vol. 119, no. 8, pp. 1920–1926, 2006.

[33] G. J. Wu, G. Zeng, and E. L. Son, "*METCAM*/MUC18 overexpression suppresses *in vitro* motility and invasiveness and *in vivo* progression of human ovarian cancer BG-1 cells," In press.

[34] G. Zeng and G. J. Wu, "*METCAM*/MUC18 over-expression suppresses *in vitro* motility and invasiveness and *in vivo* tumor formation of human ovarian cancer SKOV3 cells," In press.

[35] G. J. Wu, M. W. H. Wu, and Y. Liu, "Enforced expression of human *METCAM*/MUC18 increases the tumorigenesis of human prostate cancer cells in nude mice," *Journal of Urology*, vol. 185, pp. 1504–1512, 2011.

[36] G. J. Wu, Q. Peng, P. Fu et al., "Ectopical expression of human MUC18 increases metastasis of human prostate cancer cells," *Gene*, vol. 327, no. 2, pp. 201–213, 2004.

[37] K. R. LaMontagne Jr., M. A. Moses, D. Wiederschain et al., "Inhibition of MAP kinase kinase causes morphological reversion and dissociation between soft agar growth and *in vivo* tumorigenesis in angiosarcoma cells," *American Journal of Pathology*, vol. 157, no. 6, pp. 1937–1945, 2000.

[38] Q. Li, Y. Yu, J. Bischoff, J. B. Mulliken, and B. R. Olsen, "Differential expression of CD146 in tissues and endothelial cells derived from infantile haemangioma and normal human skin," *Journal of Pathology*, vol. 201, no. 2, pp. 296–302, 2003.

[39] E. C. McGary, A. Heimberger, L. Mills et al., "A fully human antimelanoma cellular adhesion molecule/muc18 antibody inhibits spontaneous pulmonary metastasis of osteosarcoma cells *in vivo*," *Clinical Cancer Research*, vol. 9, no. 17, pp. 6560–6566, 2003.

[40] F. Meier, U. Caroli, K. Satyamoorthy et al., "Fibroblast growth factor-2 but not Mel-CAM and/or β3 integrin promotes progression of melanocyte to melanoma," *Experimental Dermatology*, vol. 12, no. 3, pp. 296–306, 2003.

[41] G. J. Wu, C. F. Chiang, P. Fu, W. Huss, N. Greenberg, and M. W. H. Wu, "Increased expression of MUC18 correlates with the metastatic progression of mouse prostate adenocarcinoma in the (TRAMP) model," *Journal of Urology*, vol. 173, no. 5, pp. 1778–1783, 2005.

[42] D. Hanahan and R. A. Weinberg, "The hallmarks of cancer," *Cell*, vol. 100, no. 1, pp. 57–70, 2000.

[43] G. Li, J. Kalabis, X. Xu et al., "Reciprocal regulation of MelCAM and AKT in human melanoma," *Oncogene*, vol. 22, no. 44, pp. 6891–6899, 2003.

[44] V. O. Melnikova, K. Balasubramanian, G. J. Villares et al., "Crosstalk between protease-activated receptor 1 and platelet-activating factor receptor regulates melanoma cell adhesion molecule (MCAM/MUC18) expression and melanoma metastasis," *Journal of Biological Chemistry*, vol. 284, no. 42, pp. 28845–28855, 2009.

[45] V. O. Melnikova, A. S. Dobroff, M. Zigler et al., "CREB inhibits AP-2αexpression to regulate the malignant phenotype of melanoma," *PLoS One*, vol. 5, no. 8, Article ID e12452, 2010.

[46] F. Meggio and L. A. Pinna, "One-thousand-and-one substrates of protein kinase CK2?" *FASEB Journal*, vol. 17, no. 3, pp. 349–368, 2003.

[47] S. R. Datta, A. Brunet, and M. E. Greenberg, "Cellular survival: a play in three AKTs," *Genes and Development*, vol. 13, no. 22, pp. 2905–2927, 1999.

[48] C. Sers, G. Riethmuller, and J. P. Johnson, "MUC18, a melanoma-progression associated molecule, and its potential role in tumor vascularization and hematogenous spread," *Cancer Research*, vol. 54, no. 21, pp. 5689–5694, 1994.

[49] N. Bardin, F. Anfosso, J. Masse et al., "Identification of CD146 as a component of the endothelial junction involved in the control of cell-cell adhesion," *Blood*, vol. 98, pp. 3677–3684, 2001.

[50] Y. Kang, F. Wang, J. Feng, D. Yang, X. Yang, and X. Yan, "Knockdown of CD146 reduces the migration and proliferation of human endothelial cells," *Cell Research*, vol. 16, no. 3, pp. 313–318, 2006.

[51] X. Yan, Y. Lin, D. Tang et al., "A novel anti-CD146 monoclonal antibody, AA98, inhibits angiogenesis and tumor growth," *Blood*, vol. 102, no. 1, pp. 184–191, 2003.

[52] G. J. Wu and E. L. Son, "Soluble *METCAM*/MUC18 blocks angiogenesis during tumor formation of human prostate cancer cells," in *Proceedings of the 97th Annual Meeting of American Association for the Cancer Research*, vol. 47, p. 252, 2006.

[53] B. Song, J. W. Tang, B. Wang, X. N. Cui, C. H. Zhou, and L. Hou, "Screening for lymphatic metastasis-associated genes in mouse hepatocarcinoma cell lines Hca-F and Hca-P using gene chip," *Chinese Journal of Cancer*, vol. 24, no. 7, pp. 774–780, 2005.

[54] Q. Zhang, Z. Liu, P. R. Carney et al., "Non-invasive imaging of epileptic seizures *in vivo* using photoacoustic tomography," *Physics in Medicine and Biology*, vol. 53, no. 7, pp. 1921–1931, 2008.

[55] L. V. Wang, "Prospects of photoacoustic tomography," *Medical Physics*, vol. 35, no. 12, pp. 5758–5767, 2008.

[56] B. S. Schaffer, M. H. Grayson, J. M. Wortham et al., "Immune competency of a Hairless mouse strain for improved preclinical studies in genetically engineered mice," *Molecular Cancer Therapeutics*, vol. 9, no. 8, pp. 2354–2364, 2010.

[57] A. Sorrentino, M. Ferracin, G. Castelli et al., "Isolation and characterization of $CD146^+$ multipotent mesenchymal stromal cells," *Experimental Hematology*, vol. 36, no. 8, pp. 1035–1046, 2008.

[58] K. E. de Visser, A. Eichten, and L. M. Coussens, "Paradoxical roles of the immune system during cancer development," *Nature Reviews Cancer*, vol. 6, no. 1, pp. 24–37, 2006.

[59] F. Staquicini, A. Tandle, S. K. Libutti et al., "A subset of host B lymphocytes controls melanoma metastasis through a melanoma cell adhesion molecule/MUC18-dependent interaction: evidence from mice and humans," *Cancer Research*, vol. 68, no. 20, pp. 8419–8428, 2008.

[60] N. Despoix, T. Walzer, N. Jouve et al., "Mouse CD146/MCAM is a marker of natural killer cell maturation," *European Journal of Immunology*, vol. 38, no. 10, pp. 2855–2864, 2008.

[61] R. Kannagi, M. Izawa, T. Koike, K. Miyazaki, and N. Kimura, "Carbohydrate-mediated cell adhesion in cancer metastasis and angiogenesis," *Cancer Science*, vol. 95, no. 5, pp. 377–384, 2004.

[62] C. Wu, J. Cipollone, S. Maines-Bandiera et al., "The morphogenic function of E-cadherin-mediated adherens junctions in epithelial ovarian carcinoma formation and progression," *Differentiation*, vol. 76, no. 2, pp. 193–205, 2008.

[63] A. S. Ribeiro, A. Albergaria, B. Sousa et al., "Extracellular cleavage and shedding of P-cadherin: a mechanism underlying the invasive behaviour of breast cancer cells," *Oncogene*, vol. 29, no. 3, pp. 392–402, 2010.

[64] C. F. Chiang, E. L. Son, and G. J. Wu, "Oral treatment of the TRAMP mice with doxazosin suppresses prostate tumor growth and metastasis," *Prostate*, vol. 64, no. 4, pp. 408–418, 2005.

[65] L. Mills, C. Ellez, S. Huang et al., "Fully human antibodies to MCAM/MUC18 inhibit tumor growth and metastasis of human melanoma," *Cancer Research*, vol. 62, no. 17, pp. 5106–5114, 2002.

[66] M. C. Leslie, Y. J. Zhao, L. B. Lachman, P. Hwu, G. J. Wu, and M. Bar-Eli, "Immunization against MUC18/MCAM, a novel antigen that drives melanoma invasion and metastasis ," *Gene Therapy*, vol. 14, no. 4, pp. 316–323, 2007.

[67] K. Satyamoorthy, J. Muyrers, F. Meier, D. Patel, and M. Herlyn, "Mel-CAM-specific genetic suppressor elements inhibit melanoma growth and invasion through loss of gap junctional communication," *Oncogene*, vol. 20, no. 34, pp. 4676–4684, 2001.

[68] C. Hafner, U. Samwald, S. Wagner et al., "Selection of mimotopes of the cell surface adhesion molecule Mel-CAM from a random pVIII-28aa phage peptide library," *Journal of Investigative Dermatology*, vol. 119, no. 4, pp. 865–869, 2002.

[69] S. Nie, "Nanotechnology for personalized and predictive medicine," *Nanomedicine*, vol. 4, no. 1, p. 305, 2006.

Hindawi Publishing Corporation
Journal of Oncology
Volume 2012, Article ID 651507, 6 pages
doi:10.1155/2012/651507

Research Article

Angiogenesis in Paget's Disease of the Vulva and the Breast: Correlation with Microvessel Density

Patricia E. Ellis,[1,2] Allan B. MacLean,[1] L. F. Wong Te Fong,[1] Julie C. Crow,[3] and Christopher W. Perrett[1]

[1] *Department of Obstetrics and Gynaecology, Royal Free and University College Medical School (Hampstead Campus), Royal Free Hospital, Rowland Hill Street, London NW3 2PF, UK*
[2] *Department of Obstetrics and Gynaecology, Royal Surrey County Hospital, Guildford, Surrey GU2 7XX, UK*
[3] *Department of Histopathology, Royal Free and University College Medical School (Hampstead Campus), Royal Free Hospital, Rowland Hill Street, London NW3 2PF, UK*

Correspondence should be addressed to Patricia E. Ellis, peellis@hotmail.com

Received 30 October 2011; Accepted 22 January 2012

Academic Editor: Mehmet Gunduz

Our understanding of the pathogenesis of Paget's disease of the vulva and the breast remains limited. Current evidence supports the fact that angiogenesis plays an important role in the pathogenesis of several diseases. Therefore, we sought to define its role, as correlated with microvessel density, in Paget's disease of the vulva and the breast. Microvessels were analysed using anti-von Willebrand factor antibody in 105 cases of Paget's disease of the vulva and the breast comprising 71 cases of Paget's disease of the vulva, including 8 cases with invasive disease, and 34 cases of Paget's disease of the breast. The latter included 12 cases with DCIS, 5 cases with both DCIS and invasive carcinoma, and 6 with carcinoma alone. Eleven cases had no underlying tumour identified. Increased microvessel density was demonstrated in Paget's disease of the breast with DCIS and with carcinoma alone compared to Paget's disease of the breast alone, $P < 0.08$ and $P < 0.013$, respectively. There were no significant differences in microvessel density in the vulval cases. Neovascularisation is an important process in the development of Paget's disease of the breast. Other biological and molecular processes are more involved in the pathogenesis of Paget's disease of the vulva.

1. Introduction

The pathogenesis of Paget's disease of the vulva (PDV) and Paget's disease of the breast (PDB) continues to be an enigma. Despite many theories that have been put forward on their origins and disease progression, the pathogenesis of these two diseases still remains unclear. PDV is an intraepithelial in situ carcinoma which accounts for approximately 1% of all vulval neoplasms [1]. PDB accounts for 0.5–4% of all breast cancers. They are both characterised by the presence of large, pale neoplastic (Paget) cells which are seen within the epidermis of the vulva and the nipple epithelium, respectively. In 10–30% of PDV cases, an invasive adenocarcinoma is present. This is in contrast to PDB where the general consensus is that almost all cases are associated with an in situ or invasive ductal carcinoma. This is based on the epidermotropic theory; Paget cells are ductal carcinoma cells that have migrated up from the underlying carcinoma to the nipple [2]. This theory, however, does not account for the cases of PDB that have no underlying carcinoma [3]. Toker cells have been described as precursor cells of both mammary and extramammary Paget's disease. These cells are found in the basal layer of the epidermis and are adjacent to the lactiferous ducts in the nipple [4]. They also occur as a normal constituent of genital skin in association with mammary like glands of the vulva [5]. The idea that Toker cells are precursors of mammary and extramammary Paget's disease is disputed by differences in immunoprofile and morphological appearance compared to Paget cells [6, 7]. The concept that Paget cells are in fact malignant keratinocytes, which has been transformed in situ, has been put forward as the transformation theory [8]. The transformation theory is favoured for the histogenesis for PDV and for those cases in PDB without an underlying carcinoma.

Angiogenesis is the formation of new capillary blood vessels from preexisting vasculature. It proceeds and sustains

tissue growth and as such is an important component in tumour growth and metastasis. The exact timing of the point at which angiogenesis occurs, in the growth and progression of tumours, is known as the angiogenic switch [9]. The pathways controlling this switch to the angiogenic phenotype in tumours are dependent on a net effect of stimulators and inhibitors of angiogenesis [10–12]. This involves cell migration, matrix degradation by various growth factors, and the proliferation of the endothelial cells [13–15]. Stimulators of angiogenesis include vascular endothelial growth factor (VEGF), platelet-derived endothelial growth factor (PD-ECGF), and angiopoietin [16–18]. Thrombospondin-1, VEGF inhibitor, and angiostatin are well-known inhibitors of angiogenesis [19, 20]. In a previous study, we examined the expression of PD-ECGF/TP and VEGF in PDV and PDB. PD-ECGF/TP was expressed in 41% of Paget cells in PDV and 55% in PDB. There was no significant difference in PD-ECGF/TP expression in PDV and PDB with or without DCIS or invasive disease. VEGF was not expressed by Paget cells [21].

Microvessel density (MVD) is a measure of tumour angiogenesis. Increased MVD has been shown to be associated with disease progression and metastasis in several cancers, including vulval, breast, and prostate cancers [22–24]. A variety of endothelial cell markers have been used to identify microvessels for the purpose of counting. The most commonly used include factor-VIII-related antigen (F8RA)/von Willebrand factor (vWF), CD31/PECAM-1, and CD34. F8RA forms part of the vWF complex and plays a critical role in the process of haemostasis [25]. CD31 (PECAM-1), a platelet-endothelial cell adhesion molecule, is a transmembrane glycoprotein involved in cell adhesion [26], and CD34 is a surface glycoprotein expressed in endothelial cells in lymphoid tissue [27]. This current study extends our previous studies on Paget's disease of the vulva and the breast. The aim was to establish whether angiogenesis, as correlated with microvessel density, is different in PDV and PDB with or without an underlying tumour. The identification of an association between these diseases and angiogenesis would increase our understanding of the biological processes involved and would help us to move closer in unravelling the pathogenesis of PDV and PDB.

2. Materials and Methods

2.1. Tissue Specimens. Ethical approval was granted by the Royal Free Hospital NHS Trust. Seventy-one cases of PDV, including 8 cases associated with invasive disease, and 34 cases of PDB, which included 12 cases with DCIS alone, 5 cases with both DCIS and invasive carcinoma, 6 with an underlying invasive carcinoma, and eleven cases of PDB without a DCIS or an underlying carcinoma (PDB alone), were analysed for the expression of microvessels using anti-von Willebrand factor antibody. These cases were retrieved from the Histopathology Department at the Royal Free Hampstead NHS Trust and from collaborators as listed in the acknowledgements. The cases were diagnosed and treated between 1984 and 2000.

2.1.1. Immunohistochemistry. Immunohistochemical staining was performed using the streptavidin-biotin-peroxidase technique. Briefly, sections were deparaffinised in xylene and rehydrated in different percentages of ethanol up to distilled water for 10 min. 3% hydrogen peroxide was placed on the sections to block endogenous peroxidase for 10 min. They were then placed in distilled water for 10 min at 37°C.

Antigen retrieval was performed using 12.5 mg of proteinase (bacterial protease Type 24, Sigma) in 100 mL of phosphate buffered saline (PBS) at 37°C for 10 mins. The tissue sections were then incubated at room temperature with monoclonal anti-human vWF antibody for 1 hr (1 : 40 dilution; clone F8/86, Dako, Ely, Cambs, UK), followed by incubation with the secondary antibody (biotinylated rabbit anti-mouse immunoglobulin E0354, Dako), dilution 1 : 400 for 45 min. All sections were then incubated with streptavidin-biotin-horseradish peroxidase complex (Dako), diluted 1 : 200 in Tris-buffered saline for 30 min. Antibody binding was visualised with a solution containing the chromogen 3,3′-diaminobenzidine (Sigma-Aldrich, Poole, Dorset, UK) for 8–12 min and then terminated with tap water. The sections were counterstained with Mayer's haematoxylin (Merck, Lutterworth, Leics, UK), dehydrated in methanol, cleared in xylene, and mounted in DPX. Human placenta was used as positive control, and for negative control, vWF was replaced with PBS. In this study, we used vWF as the endothelial cell marker of choice because of its consistent staining and the fact that it was less likely to react with other tissue components, such as macrophages, compared to CD31 and CD34 endothelial cell markers.

2.2. Microvessel Density Assessment. A single countable microvessel was considered as a brown staining endothelial cell or endothelial cell cluster that was separate from adjacent microvessels, tumour cells, and other connective tissue elements. Large vessels with lumina greater than approximately seven red blood cells were excluded from the count [28]. Blood vessels were detected by a method similar to Bosari et al. [28]. Briefly, areas of highest neovascularisation, that is, containing the highest number of capillaries and small venules per area (hot spots) were found by scanning the whole tissue section at low power (×40 and ×100) using a light microscope. Five fields in each section with the highest number of hot spots were selected. The highest vessel density (HVD) of five fields at ×200 field (0.74 mm^2 under the light microscope) and ×400 field (0.17 mm^2 under the light microscope) was recorded, and the average vessel density (AVD) was also recorded in these five fields at ×200 and ×400. This was repeated using the HVD and AVD of three fields. The area of HVD and AVD using five fields did not differ significantly from the values obtained using three fields and therefore the analysis was performed using three fields. Individual MVD was made at both ×200 and ×400 magnification within each hot spot. The MVD is confined to an area within 500 μm of dermal tissue just beneath the basement membrane of the epidermis and expressed as HVD/AVD per mm^2.

Sections were stained on 3 separate occasions to ensure reproducibility. Results were analysed by three independent

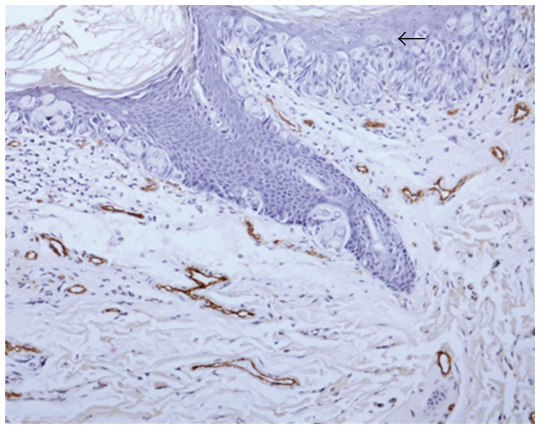

Figure 1: vWF expression demonstrating microvessels in PDB with DCIS (×200). Arrow : Paget cells.

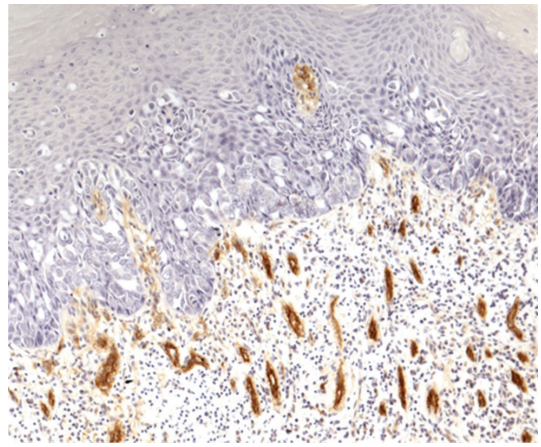

Figure 2: vWF expression demonstrating microvessels in PDV without invasive disease (×200).

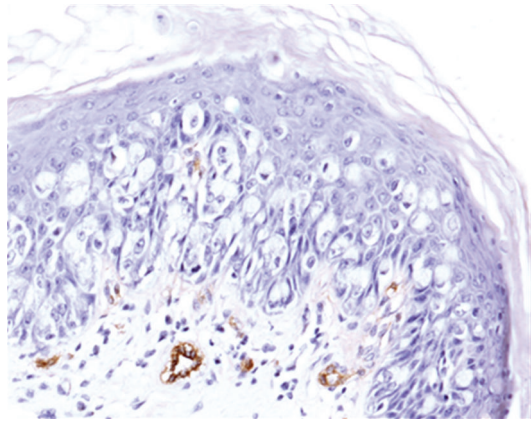

Figure 3: vWF expression demonstrating microvessels in PDV without invasive disease (×200).

observers (PEE, LFWTF, and JCC). In all cases, there was <5% variation in results between sections and observers.

2.3. Statistical Analysis. Statistical analysis was performed using the Mann-Whitney U test to compare MVD expression between invasive and noninvasive cases of PDV and cases of PDB with DCIS and invasive carcinoma. The SPSS v15 software was used to conduct the analysis. A P value of <0.05 was considered significant.

3. Results

The vascular endothelial cells were stained brown by the anti vWF antibody. Figures 1, 2, and 3 show the Paget cells and the surrounding stained microvessels in PDB and PDV. There were significant differences between PDB alone and PDB with DCIS, $P < 0.008$ at HVD ×400 and $P < 0.02$ at AVD ×400; and between PDB alone and PDB with invasive cancer, $P < 0.013$ at HVD ×400 and $P < 0.009$ at AVD ×400. The mean MVD ×400 was also higher in PDB with DCIS and invasive carcinoma compared to PDB alone but did not reach statistical significance. Similarly, the HVD and AVD ×200 magnification in cases of PDB with DCIS and PDB with invasive carcinoma were also higher compared to PDB alone. The mean HVD and AVD values in PDB are summarised in Table 1.

The mean HVD at 200 and 400 magnification in PDV without invasive disease was 28.4 and 7.0, respectively, and 20.3 and 8.6 in PDV with invasive disease. Table 2 demonstrates the mean values of the MVD in PDV. There appeared to be no significant difference in the MVD in intraepidermal PDV as compared with PDV associated with invasive disease.

4. Discussion

MVD has been used in several studies to investigate the role of angiogenesis in patients with cancer and has been shown to be a prognostic indicator for several tumours. The role of angiogenesis, as determined by MVD, has been examined in vulval lichen sclerosus, vulval intraepithelial neoplasia (VIN), and vulval cancer [29–31]. MVD was thought to be valuable prognostic marker for VIN 3 in determining progression to invasive disease [30]. Increased MVD was also associated with a poor prognosis in squamous cell carcinoma (SCC) of the vulva. It was not a useful parameter in determining potential malignant progression in vulval lichen sclerosus. In comparison, another study [32] did not demonstrate a positive correlation in vulval SCC with stage, survival, or pattern of invasion.

In breast cancer, there have also been conflicting results reported in the association with MVD and its role as a prognostic factor. It has been shown that intratumour MVD is an independent prognostic factor for breast carcinoma. The authors found a correlation between MVD and overall and relapse-free survival in patients with early-stage breast carcinoma [33]. Others have demonstrated the vessel density to be a significant prognostic indicator in node-negative and node-positive breast cancer [34]. A more recent study reported an increase in MVD between normal and benign hyperplastic breast tissue and between in situ and invasive carcinomas [35]. However, other studies have demonstrated a lower MVD in the breast carcinoma compared to the

Table 1: Mean values of the MVD in PDB.

Cases	*n*	HVD (×200)	AVD (×200)	HVD (×400)	AVD (×400)
PDB with DCIS	12	26.9 (13.7)	18.3 (12.3)	11.2 (3.1)	8.3 (3.1)
PDB with DCIS/invasive carcinoma	5	14.6 (10.0)	11.7 (8.9)	9.0 (4.6)	7.4 (3.8)
PDB with invasive carcinoma	6	20.8 (6.4)	15.3 (4.8)	17.2 (13.2)	14.3 (11.3)
PDB alone	11	19.1 (13.6)	13.9 (10.2)	7.2 (2.7)	5.1 (2.4)

n: number of cases. The SDs of the mean are given in brackets.

Table 2: Mean values of the MVD in PDV with and without invasive disease.

Cases	*n*	HVD (×200)	AVD (×200)	HVD (×400)	AVD (×400)
PDV without invasive disease	63	28.5 (16.4)	20.0 (14.04)	10.4 (5.9)	7.0 (3.8)
PDV with invasive disease	8	20.4 (19.5)	14.1 (13.3)	12.1 (9.4)	8.7 (5.4)

n: number of cases. The SDs of the mean are given in brackets.

adjacent normal breast tissue [36] and were unable to find a relationship between MVD and breast metastases [37]. The inconsistent results reported in these studies may be due to the different techniques and endothelial cell markers used to measure tumour angiogenesis. A double-labelling technique was used to quantify MVD using CD34 or vWF [36]. vWF was used as the only endothelial cell marker [36] and a further study utilised CD31 as the endothelial cell marker and the Chalkley method to assess MVD [37]. The Chalkley method measures the relative area of vessel profile in a high-density region of the tumour as compared to MVD, which measures the density of the vessels [38]. Hollingsworth et al. [39] described a method using vascular volume to assess MVD. Determination of vessel density by vascular volume represents an average of the entire section rather than focusing on areas of most intense neovascularisation and therefore does not reflect the angiogenic activity of tumour cells or metastatic potential. To our knowledge, no other study has investigated MVD in PDV and PDB. Our findings suggest that neovascularisation is an important factor in the development of PDB but not in PDV. MVD as assessed by HVD and AVD ×400 magnification may be a useful parameter to determine which cases of PDB will have DCIS or invasive carcinoma disease present. Identifying those cases with a low MVD may allow a more conservative approach in the surgical management of PDB.

A different mechanism may be involved in the growth and progression of PDV. It is possible that in PDV, Paget cells can migrate and progress to invasive disease by utilising the existing vasculature, without the need for the formation of new blood vessels. This could explain why there was no difference in the microvessel counts between PDV with or without underlying invasive disease. Tumour progression in the absence of neoangiogenesis has been described by several authors [40–42]. "Cooption", the utilisation of preexisting vasculature by tumours to obtain its blood supply and therefore to grow and progress, has been reported in malignant melanomas, brain metastases, and lung cancer. Döme et al. [40] demonstrated the incorporation of the existing host vascular plexus into a progressing malignant melanoma. Others have described growth of tumour cells in non small cell carcinoma of the lung without morphological evidence of neoangiogenesis [43] and the development of brain metastases, without the induction of sprouting angiogenesis, even in the presence of high levels of VEGF [41].

It is well documented that the growth and disease progression of many cancers is due in part to the loss of cell-cell adhesion. We have demonstrated that the cell adhesion molecule E-cadherin is significantly reduced ($P = 0.039$) in Paget's disease of the vulva cases with invasive disease when compared with Paget's disease of the vulva cases without invasive disease. E-cadherin expression was normal in PDB and there was no difference between those cases of PDB with or without DCIS or invasive disease [44]. These findings and the results from this current study demonstrate the critical steps involved in the pathogenesis of PDB and PDV may occur by different mechanisms.

In conclusion, this is the first study to assess MVD in PDV and PDB. MVD can be a useful parameter in determining the presence of PDB with or without DCIS or invasive disease. Additional work is needed to assess the relationship between MVD and other stimulators of angiogenesis in the pathogenesis of PDB and PDV. What impact the differences in the pathogenesis in PDB and PDV, as described in this study, have on the histogenesis of these two diseases remains to be clarified.

Acknowledgments

The authors would like to thank the following for their assistance in obtaining cases of PDV and PDB: Dr. C. Andrews (The General Infirmary, Leeds)), Dr. S. Andrews (Hope Hospital, Manchester), Dr. L. Brown (Leicester Royal Infirmary, Leicester), Dr. E. Courtauld (Farrer-Brown Laboratory, London), Dr. Paul Cross (Queen Elizabeth Hospital, Gateshead), Dr. A. Desai (Whittington Hospital, London), Dr. R. Dina (Hammersmith Hospital, London), Dr. A. Flanagan (St Mary's Hospital, London), Professor T. Krauz (Hammersmith Hospital London), Professor D. Lowe (St. Bartholomew's Hospital London), Dr. P. Millard (The John Radcliffe Hospital, Oxford), Dr. N. Nasseri (The Royal Marsden Hospital, London), Dr. J. Smith (The Northern General Hospital,

Sheffield), Dr. P. Trott (The London Clinic, London), Professor M. Wells (The Royal Hallamshire Hospital, Sheffield), Dr. G. Wilson (Manchester Royal Infirmary, Manchester), and Dr. M. Young (St. George's Hospital, London).

References

[1] J. P. Curtin, S. C. Rubin, W. B. Jones, W. J. Hoskins, and J. L. Lewis, "Paget's disease of the vulva," *Gynecologic Oncology*, vol. 39, no. 3, pp. 374–377, 1990.

[2] J. Lloyd and A. M. Flanagan, "Mammary and extramammary Paget's disease," *Journal of Clinical Pathology*, vol. 53, no. 10, pp. 742–749, 2000.

[3] L. Morandi, A. Pession, G. L. Marucci et al., "Intraepidermal cells of Paget's carcinoma of the breast can be genetically different from those of the underlying carcinoma," *Human Pathology*, vol. 34, no. 12, pp. 1321–1330, 2003.

[4] G. Marucci, C. M. Betts, R. Golouh, J. L. Peterse, P. Foschini, and V. Eusebi, "Toker cells are probably precursors of Paget cell carcinoma: a morphological and ultrastructural description," *Virchows Archiv*, vol. 441, no. 2, pp. 117–123, 2002.

[5] J. H. Willman, L. E. Golitz, and J. E. Fitzpatrick, "Vulvar clear cells of Toker: precursors of extramammary Paget's disease," *American Journal of Dermatopathology*, vol. 27, no. 3, pp. 185–188, 2005.

[6] B. Liegl, S. Leibl, M. Gogg-Kamerer, B. Tessaro, L. C. Horn, and F. Moinfar, "Mammary and extramammary Paget's disease: an immunohistochemical study of 83 cases," *Histopathology*, vol. 50, no. 4, pp. 439–447, 2007.

[7] B. Liegl and F. Moinfar, "'Toker cells' as origin of Paget's disease: fact or fiction?" *Histopathology*, vol. 52, no. 7, pp. 891–892, 2008.

[8] M. D. Lagios, P. R. Westdahl, M. R. Rose, and S. Concannon, "Paget's disease of the nipple. Alternative management in cases without or with minimal extent of underlying breast carcinoma," *Cancer*, vol. 54, no. 3, pp. 545–551, 1984.

[9] J. Folkman, K. Watson, D. Ingber, and D. Hanahan, "Induction of angiogenesis during the transition from hyperplasia to neoplasia," *Nature*, vol. 339, no. 6219, pp. 58–61, 1989.

[10] F. Rastinejad, P. J. Polverini, and N. P. Bouck, "Regulation of the activity of a new inhibitor of angiogenesis by a cancer suppressor gene," *Cell*, vol. 56, no. 3, pp. 345–355, 1989.

[11] N. P. Bouck, "Tumor angiogenesis: the role of oncogenes and tumor suppressor genes," *Cancer Cells*, vol. 2, no. 6, pp. 179–185, 1990.

[12] K. M. Dameron, O. V. Volpert, M. A. Tainsky, and N. P. Bouck, "Control of angiogenesis in fibroblasts by p53 regulation of thrombospondin-1," *Science*, vol. 265, no. 5178, pp. 1582–1584, 1994.

[13] R. F. Nicosia, R. Tchao, and J. Leighton, "Interactions between newly formed endothelial channels and carcinoma cells in plasma clot culture," *Clinical and Experimental Metastasis*, vol. 4, no. 2, pp. 91–104, 1986.

[14] J. Hamada, P. G. Cavanaugh, O. Lotan, and G. L. Nicolson, "Separable growth and migration factors for large-cell lymphoma cells secreted by microvascular endothelial cells derived from target organs for metastasis," *British Journal of Cancer*, vol. 66, no. 2, pp. 349–354, 1992.

[15] J. W. Rak, E. J. Hegmann, C. Lu, and R. S. Kerbel, "Progressive loss of sensitivity to endothelium-derived growth inhibitors expressed by human melanoma cells during disease progression," *Journal of Cellular Physiology*, vol. 159, no. 2, pp. 245–255, 1994.

[16] N. Ferrara and W. J. Henzel, "Pituitary follicular cells secrete a novel heparin-binding growth factor specific for vascular endothelial cells," *Biochemical and Biophysical Research Communications*, vol. 161, no. 2, pp. 851–858, 1989.

[17] F. Ishikawa, K. Miyazono, U. Hellman et al., "Identification of angiogenic activity and the cloning and expression of platelet-derived endothelial cell growth factor," *Nature*, vol. 338, no. 6216, pp. 557–562, 1989.

[18] J. Folkman and Y. Shing, "Angiogenesis," *The Journal of Biological Chemistry*, vol. 267, no. 16, pp. 10931–10934, 1992.

[19] B. L. Riser, J. Varani, K. O'Rourke, and V. M. Dixit, "Thrombospondin binding by human squamous carcinoma and melanoma cells: relationship to biological activity," *Experimental Cell Research*, vol. 174, no. 2, pp. 319–329, 1988.

[20] M. S. O'Reilly, L. Holmgren, Y. Shing et al., "Angiostatin: a novel angiogenesis inhibitor that mediates the suppression of metastases by a Lewis lung carcinoma," *Cell*, vol. 79, no. 2, pp. 315–328, 1994.

[21] P. E. Ellis, L. F. Wong Te Fong, K. J. Rolfe et al., "The role of vascular endothelial growth factor-A (VEGF-A) and platelet-derived endothelial cell growth factor/thymidine phosphorylase (PD-ECGF/TP) in Paget's disease of the vulva and breast," *Anticancer Research*, vol. 22, no. 2 A, pp. 857–861, 2002.

[22] A. Obermair, P. Kohlberger, D. Bancher-Todesca et al., "Influence of microvessel density and vascular permeability factor/vascular endothelial growth factor expression on prognosis in vulvar cancer," *Gynecologic Oncology*, vol. 63, no. 2, pp. 204–209, 1996.

[23] S. Tsutsui, M. Kume, and S. Era, "Prognostic value of microvessel density in invasive ductal carcinoma of the breast," *Breast Cancer*, vol. 10, no. 4, pp. 312–319, 2003.

[24] G. Kaygusuz, O. Tulunay, S. Baltaci, and O. Gogus, "Microvessel density and regulators of angiogenesis in malignant and nonmalignant prostate tissue," *International Urology and Nephrology*, vol. 39, no. 3, pp. 841–850, 2007.

[25] M. Franchini and G. Lippi, "Von Willebrand factor and thrombosis," *Annals of Hematology*, vol. 85, no. 7, pp. 415–423, 2006.

[26] H. M. DeLisser, P. J. Newman, and S. M. Albelda, "Molecular and functional aspects of PECAM-1/CD31," *Immunology Today*, vol. 15, no. 10, pp. 490–495, 1994.

[27] D. S. Krause, M. J. Fackler, C. I. Civin, and W. S. May, "CD34: structure, biology, and clinical utility," *Blood*, vol. 87, no. 1, pp. 1–13, 1996.

[28] S. Bosari, L. Arthur, R. Del-Ellis, B. Wiley, G. Heatley, and M. Silverman, "Microvessel quantification and prognosis in invasive breast carcinoma," *Human Pathology*, vol. 23, no. 7, pp. 755–761, 1992.

[29] D. Bancher-Todesca, A. Obermair, S. Bilgi et al., "Angiogenesis in vulvar intraepithelial neoplasia," *Gynecologic Oncology*, vol. 64, no. 3, pp. 496–500, 1997.

[30] J. Saravanamuthu, W. N. Reid, D. St George et al., "The role of angiogenesis in vulvar cancer, vulvar intraepithelial neoplasia, and vulvar lichen sclerosus as determined by microvessel density analysis," *Gynecologic Oncology*, vol. 89, no. 2, pp. 251–258, 2003.

[31] V. V. Nayha and F. G. Stenback, "Increased angiogenesis is associated with poor prognosis of squamous cell carcinoma of the vulva," *Acta Obstetricia et Gynecologica Scandinavica*, vol. 86, no. 11, pp. 1392–1397, 2007.

[32] F. Qureshi, A. Munkarah, M. Banerjee, and S. Jacques, "Tumour angiogenesis in vulvar saquamous cell carcinoma," *Gynecologic Oncology*, vol. 72, no. 1, pp. 65–70, 1999.

[33] N. Weidner, J. Folkman, F. Pozza et al., "Tumor angiogenesis: a new significant and independent prognostic indicator in early-stage breast carcinoma," *Journal of the National Cancer Institute*, vol. 84, no. 24, pp. 1875–1887, 1992.

[34] M. Toi, J. Kashitani, and T. Tominaga, "Tumor angiogenesis is an independent prognostic indicator in primary breast carcinoma," *International Journal of Cancer*, vol. 55, no. 3, pp. 371–374, 1993.

[35] J. E. Bluff, S. R. Menakuru, S. S. Cross et al., "Angiogenesis is associated with the onset of hyperplasia in human ductal breast disease," *British Journal of Cancer*, vol. 101, no. 4, pp. 666–672, 2009.

[36] A. Eberhard, S. Kahlert, V. Goede, B. Hemmerlein, K. H. Plate, and H. G. Augustin, "Heterogeneity of angiogenesis and blood vessel maturation in human tumors: implications for antiangiogenic tumor therapies," *Cancer Research*, vol. 60, no. 5, pp. 1388–1393, 2000.

[37] N. R. Hall, D. E. Fish, N. Hunt, R. D. Golding, P. J. Guilou, and J. R. T. Monson, "Is the relationship between angiogenesis and metastasis in breast cancer real?" *Surgical Oncology*, vol. 1, no. 3, pp. 223–229, 1992.

[38] S. Hansen, F. B. Sorensen, W. Vach, D. A. Grabau, M. Bak, and C. Rose, "Microvessel density compared with the Chalkley count in a prognostic study of angiogenesis in breast cancer patients," *Histopathology*, vol. 44, no. 5, pp. 428–436, 2004.

[39] H. C. Hollingsworth, E. C. Kohn, S. M. Steinberg, M. L. Rothenberg, and M. J. Merino, "Tumor angiogenesis in advanced stage ovarian carcinoma," *American Journal of Pathology*, vol. 147, no. 1, pp. 33–41, 1995.

[40] B. Döme, S. Paku, B. Somlai, and J. Tímár, "Vascularization of cutaneous melanoma involves vessel co-option and has clinical significance," *Journal of Pathology*, vol. 197, no. 3, pp. 355–362, 2002.

[41] B. Kusters, W. P. J. Leenders, P. Wesseling et al., "Vascular endothelial growth factor-A_{165} induces progression of melanoma brain metastases without induction of sprouting angiogenesis," *Cancer Research*, vol. 62, no. 2, pp. 341–345, 2002.

[42] W. P. J. Leenders, B. Kusters, K. Verrijp et al., "Antiangiogenic therapy of cerebral melanoma metastases results in sustained tumor progression via vessel co-option," *Clinical Cancer Research*, vol. 10, pp. 6222–6230, 2004.

[43] F. Pezzella, U. Pastorino, E. Tagliabue et al., "Non-small-cell lung carcinoma tumor growth without morphological evidence of neo-angiogenesis," *American Journal of Pathology*, vol. 151, no. 5, pp. 1417–1423, 1997.

[44] P. E. Ellis, S. Diaz Cano, M. Fear et al., "Reduced E-cadherin expression correlates with disease progression in Paget's disease of the vulva but not Paget's disease of the breast," *Modern Pathology*, vol. 21, no. 10, pp. 1192–1199, 2008.

Hindawi Publishing Corporation
Journal of Oncology
Volume 2012, Article ID 723541, 16 pages
doi:10.1155/2012/723541

Review Article

The Molecular Biology of Brain Metastasis

Gazanfar Rahmathulla,[1,2] Steven A. Toms,[3] and Robert J. Weil[1,2]

[1] *The Burkhardt Brain Tumor & Neuro-Oncology Center, Cleveland Clinic, Desk S-7, 9500 Euclid Avenue, Cleveland, OH 44195, USA*
[2] *Department of Neurosurgery, Neurological Institute, Cleveland Clinic, Cleveland, OH 44195, USA*
[3] *Division of Neurosciences, Department of Neurosurgery, Geisinger Medical Center, Danville, PA 17822, USA*

Correspondence should be addressed to Gazanfar Rahmathulla, rahmatg@ccf.org

Received 20 October 2011; Accepted 25 November 2011

Academic Editor: Sushant Kachhap

Metastasis to the central nervous system (CNS) remains a major cause of morbidity and mortality in patients with systemic cancers. Various crucial interactions between the brain environment and tumor cells take place during the development of the cancer at its new location. The rapid expansion in molecular biology and genetics has advanced our knowledge of the underlying mechanisms involved, from invasion to final colonization of new organ tissues. Understanding the various events occurring at each stage should enable targeted drug delivery and individualized treatments for patients, with better outcomes and fewer side effects. This paper summarizes the principal molecular and genetic mechanisms that underlie the development of brain metastasis (BrM).

1. Introduction

Brain metastases are the most frequently diagnosed intracranial neoplasms in adults, with an annual incidence estimated at 200,000 cases in the USA alone [1], an incidence 10 times greater than primary brain tumors [2]. Up to 20–40% of patients with adult systemic malignancies will develop brain metastases in the course of their disease; about 10–20% will be symptomatic [3, 4]. Improved treatment options for systemic disease, along with tools that permit less invasive screening, often when patients are asymptomatic, have increased patient survival, paradoxically escalating both its incidence and prevalence. A variety of systemic malignancies can metastasize to the central nervous system (CNS), although the majority of the lesions come from lung cancer (40–50%) followed by breast cancer (20–30%), melanoma (5–10%), lymphoma, and various other primary sites like the gastrointestinal tract (4–6%) and prostate [5, 6].

More than a century ago, Stephen Paget advanced his "seed and soil" hypothesis, which suggests that the occurrence of brain metastases is not random, but is secondary to certain tumor cells—"the seed"—having an attraction for the surrounding environment—"the soil" [7]. The hypothesis envisages three principles: first, that neoplasms are composed of heterogeneous subpopulations of cells, with different characteristics; second, that only a selectively "fit" subpopulation of cells will survive and multiply, invade, and migrate to other locations; finally, that colonization depends on tumor cell "seed" and host microenvironment "soil" interactions [8]. According to Ewing, circulatory patterns are responsible for the organ-specific spread between the primary tumor and their final destination [9]. Although complex, the metastatic process can be broadly divided into two main stages, the first being the migration of tumor cells from their primary tumor environment to various distant tissues and the second being the colonization of these tumor cells in their new location [10]. Underlying these two main stages are a number of cellular hallmarks taking place during the development and metastasis of human tumors [11]. The various molecular, genetic, and epigenetic changes that occur define the multistep dissemination process of the tumor, also known as the "metastatic cascade."

Most BrMs occur in the cerebral hemispheres (80%), followed by the cerebellum (15%) and the brainstem (5%), corresponding to vascular distribution and tissue volumes [12]. BrMs are a major cause of morbidity and mortality, with clinical features of the metastasis corresponding to the location, causing focal neurological deficits, or presenting

with nonspecific central nervous system features such as headache, cognitive impairment, and seizures [13]. The central nervous system (CNS) acts as a "safe haven," generally beyond the reach of nearly all chemotherapeutic agents. The blood brain barrier (BBB) prevents the entry of most chemotherapeutic agents, and so the brain can act as a refuge for metastatic tumors [14]. The microenvironment of the CNS is exceptional in having a high chloride content, enabling tumors which prefer this environment, such as neuroepithelial tumors like small cell cancer of the lung and melanoma, to colonize, while potentially inhibiting invasion by other cancer cell types without this predilection [15]. Treatments targeting metastatic intracranial disease include surgery, whole-brain radiation therapy (WBRT), stereotactic radiosurgery (SRS), alone or in combination with various targeted agents, and generalized chemotherapy [16]. Following WBRT, survival ranges from anywhere between 4 and 6 months and can be as long as 24 months [17]. Various combinations of surgery, SRS, WBRT, and chemotherapy have been used to improve overall survival, obtain good clinical outcomes, and prevent recurrence of disease.

This paper will focus on metastatic brain tumors describing the hallmarks acquired in the metastatic cascade, which finally brings cancer cells to their "safe haven" in the CNS. The mechanisms through which cancer cells escape their primary focus of origin, invade adjacent tissues making their way into the microvasculature (intravasation), evade cell death, and make their way to a distant site (extravasation), finally proliferating and colonizing this new location, are outlined. With further understanding of the various molecular events that occur in metastasis, future-targeted therapies may lead to prevention or a slowdown in the development of BrM and more effective and less toxic therapy (ies).

2. The Metastatic Process

The ability of cancer cells to sever their link to the primary tumor site and commence the metastatic process begins once specific functions have been acquired by an appropriate subset of cancer cells. The multistep cascade can be grouped into two stages: migration, which includes intravasation, dissemination, and extravasation, and colonization (Figures 1(a) and 1(b)). We will review below the underlying pathobiology within each stage.

2.1. Migration

2.1.1. Cellular Heterogeneity and Proliferation. The primary tumor consists of cancer cells which are genetically heterogeneous and have varying potentials to metastasize. These include the cell's ability to invade adjacent tissues, initiate (neo-) angiogenesis, disseminate, and adhere to new tissue substrates, while expressing an affinity for the CNS [3, 18]. Tumor cells have the ability to evade the structural organization present in normal tissues and cells. In spite of being exposed to various environmental pressures such as hypoxia and nutrient deprivation, low pH, poor blood supply, and immune and inflammatory mediators, a subset of tumor cells survive these pressures with the ability to metastasize to distant sites. Additionally, tumor cells are able to evade growth suppressors, which limit cell growth and proliferation, as well as circumvent inhibitors of cell proliferation such as cell cycle checkpoint and DNA damage control systems. Tumor cells can also resist apoptosis (programmed cell death) by the increased expression of antiapoptotic regulators (Bcl-2, Bcl-x_L), survival signals (lgf 1/2), and downregulating proapoptotic factors (Bax, Bim, and Puma) [19]. The primary tumor cells have the ability to acquire genetic and epigenetic mutations such as DNA methylation and histone modification, allowing the fittest group of cells to survive [10, 20]. Emerging evidence also suggests that microRNA (miRNA) species interactions with pseudogenes may modify gene expression in cancer [21]. Various genetic mutations result in the ability of tumor cells to commence the proliferative process, and a number of genes associated with this process are listed in Table 1. Clonal expansion of these surviving fit cells leads to an acquisition of further changes, making subsequent cell lines progressively more carcinogenic (Figure 2).

Observations within the primary tumor mass have revealed the presence of heterogeneous cell lines including cancer stem cells (CSCs), partially differentiated progenitor cells, and fully differentiated end-stage cells; these appear to recapitulate the same hierarchal patterns in normal tissue types but in an uncontrolled manner [22]. Present evidence suggests that these CSCs may be the primary drivers of the enhanced malignant potential of primary tumors, giving origin to their aggressive phenotypes with the ability to degrade the extracellular matrix (ECM), invade blood vessels and lymph nodes, migrate, extravasate, colonize, and renew themselves at their new locations [23, 24]. These CSCs can reside in clusters or niches, at two or more locations within the primary tumor cell mass [23, 24]. Thus, the key role a CSC plays in the metastatic cascade cannot be overstated, due to its ability to initiate tumor proliferation and "self-renew" itself at alternative tissue locations. Other observations reveal that, in addition to the abilities discussed, they are also motile and invasive and are resilient to the apoptotic process [25].

2.1.2. Epithelial-Mesenchymal Transition (EMT). The epithelial-mesenchymal transition (EMT), which is currently at the forefront of investigation by numerous groups, describes a temporary, reversible phenomenon wherein cells can dedifferentiate, migrate to a distant focus, and then redifferentiate back to their original cell, forming a new structure [26]. Signals activating the EMT can be intrinsic, such as gene mutations, and extrinsic, such as growth factor signaling. Transdifferentiation appears to be initiated by release of certain EMT-inducing transcription factors (EMT-TFs) that transform epithelial cells into mesenchymal derivatives, giving these cells the capacity to invade, resist apoptosis, and disseminate [11, 27]. Transforming growth factor β (TGFβ) [28], hepatocyte growth factor (HGF) [29], epidermal growth factor (EGF), insulin-like growth factor (IGF) [30], fibroblast growth factor (FGF), and members of the Notch signaling family [31] play a role in inducing the EMT pathway. More recent evidence indicates that the EMT program enables non-CSCs to derive characteristics of the

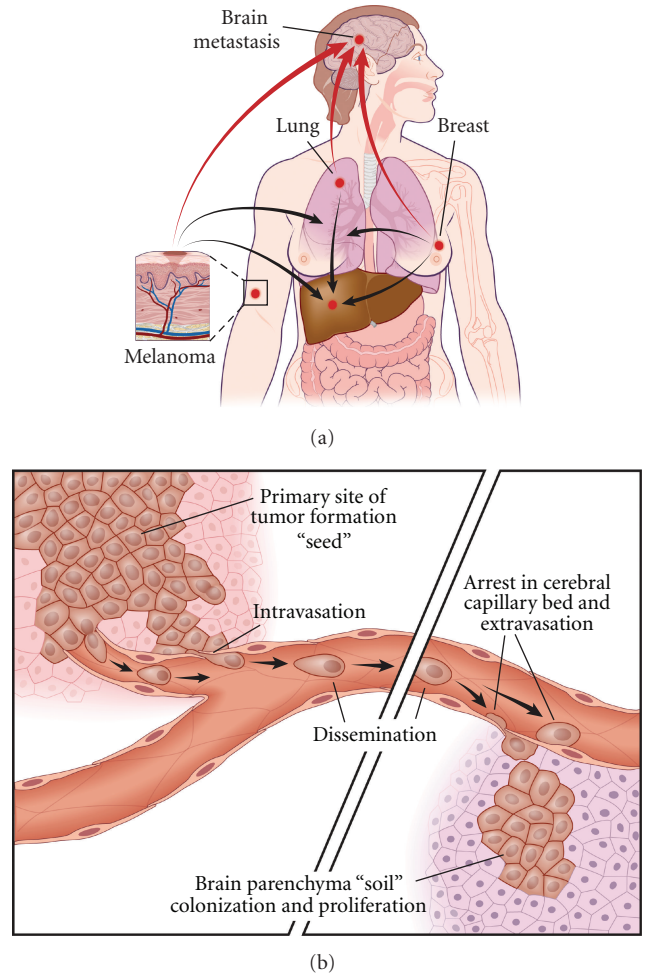

Figure 1: Schematics of the process of metastasis. (a) Formation of metastatic tumor cell lines at primary sites like breast, lung, and skin (melanoma) seen as the red nodes. Metastasis from these primary sites then spreads to the brain via the circulatory system (red arrows) and also to adjacent sites like the liver, bone, lung, and lymph nodes (black arrows). The inset shows the primary site of melanoma cells proliferating and migrating towards the vasculature, subsequently disseminating to secondary organ sites. (b) The metastatic tumor cells detach from the primary site and penetrate the adjacent parenchyma to reach the blood vessels. On reaching the vessels, the cells invade and enter the circulation (intravasation) and then disseminate within the vascular system (left half of figure). These cells eventually adhere to secondary sites "soil" to then extravasate out of the blood vessels and for colonies of metastatic cells (right half of figure).

CSC state, which enables them to invade and disseminate from the primary tumor to a distant, metastatic focus [32]. Some of these traits include the ability to loosen adherent junctions, express matrix-degrading enzymes, resist apoptosis, and to undergo morphological conversion. Using the EMT program, cancer cells can, transiently or for longer time frames, activate themselves and acquire attributes critical to survival and dissemination. To activate the EMT, a certain amount of crosstalk has to exist between the tumor cells and adjacent stromal cells, which are done by various EMT-TFs and signals from within the adjacent tumor stroma [11, 32].

2.1.3. Interactions with Tumor Stroma. Progression in cancer also involves activating a number of cells in the adjacent stroma via paracrine signaling [33]. These stromal cells, including endothelial cells, pericytes, fibroblasts, and leukocytes, provide a number of protumorigenic factors which sustain tumor growth. The two prominent cell types are the cancer-associated fibroblasts (CAFs) and the pericytes [34]. These cells produce growth factors, hormones, and cytokines that promote tumor proliferation. CAFs are known to express high amounts of TGFβ, HGF, EGF, FGF, canonical Wnt families, and cytokines like stromal-derived factor- (SDF-) 1α (CXL12) and interleukin-6 (IL-6) [35]. Invasion of cancer cells can be enhanced by stromal macrophages which supply matrix-degrading enzymes such as matrix metalloproteinases and cysteine cathepsin protease [36]. Experimental tumor models suggest that cancer cells release factors such as CSF-1, which stimulates macrophages in the tumor microenvironment, with the subsequent release of EGF, which promotes proliferation of the tumor mass [37]. In addition, CAFs are activated by various inflammatory mediators and induced to produce increased quantities of VEGF, FGF-2, among other cytokines and growth

Table 1: Genes associated with increased metastatic potential.

Genes	Cancer site (primary)	Role and implications	OMIM no.	Chromosome location
RHoC	Melanoma	Regulates remodeling of actin cytoskeleton during morphogenesis and motility. Important in tumor cell invasion	165380	1p21-p13
LOX	Breast Head and neck cancer	Increases invasiveness of hypoxic human cancer cells through cell matrix adhesion and focal adhesion kinase activity	153455	5q23.1-q23.2
VEGF	Lung Breast Melanoma Colon	Angiogenic growth factor Inhibition decreases brain metastasis formation; reduces blood vessel formation and cell proliferation; increases apoptosis	192240	6p21.1
CSF1	Breast Lung	Stimulate macrophage proliferation and subsequent release of growth factors	120420	1p13.3
ID1	Breast Lung	Involved in matrix remodeling, intracellular signaling, and angiogenesis	600349	20q11.21
TWIST1	Breast Gastric Rhabdomyosarcoma Melanoma Hepatocellular	Causes loss of E-cadherin-mediated cell-cell adhesion, activates mesenchymal markers, and induces cell motility by promoting epithelial-mesenchymal transition	601622	7p21.1
MET	Renal cell cancer	Affects a wide range of biological activity depending on the cell target, varying from mitogenesis, morphogenesis, and motogenesis	164860	7q31.2
MMP-9	Colorectal Breast Melanoma Chondrosarcoma	Extracellular matrix degradation, tissue remodeling	120361	20q13.12
NEDD9	Melanoma	Acquisition of a metastatic potential	602265	6p24.2
LEF1	Lung	Transcriptional effecter—WNT pathway; predilection for brain metastasis Knockdown inhibits brain metastasis, decreases colony formation; *in vitro decreases invasion*	153254	4q25
HOXB9	Lung Breast	Homeobox gene family; critical for embryonic segmentation and patterning. Also a TCF4 target Knockdown *in vitro* decreased invasion and colony formation; *in vivo* appears to inhibit brain metastasis	142964	17q21.32
BMP4	Lung Colorectal	Plays an essential role in embryonic development and may be an essential component of the epithelial-mesenchymal transition	112262	14q22.2
STAT3	Melanoma	Cell signaling transcription factor Reduction suppresses brain metastasis; decreases angiogenesis *in vivo* and cellular invasion *in vitro*	102582	17q21.2

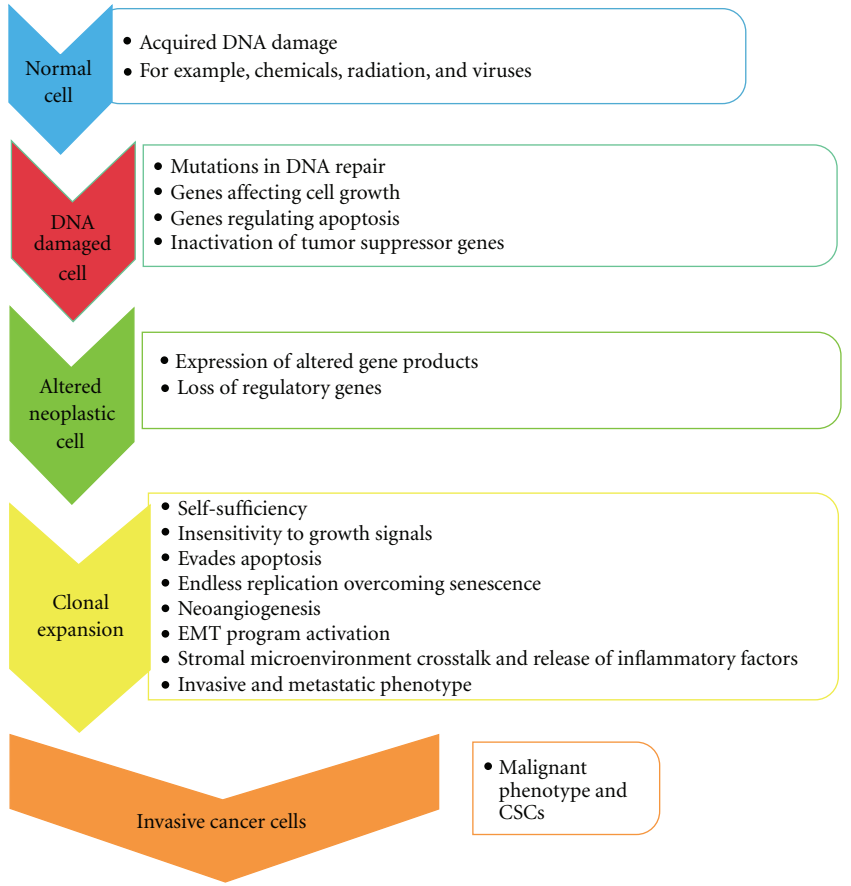

Figure 2: Schematic of the metastatic cascade. Cascade of events taking place at the primary site during oncogenesis, illustrating the steps creating the neoplastic cell line followed by clonal expansion and survival of the fittest cells, becoming the invasive and metastatic phenotype.

factors, which recruits endothelial progenitor cells thereby promoting angiogenesis [38, 39]. This dynamic stromal environment further stresses the tumor cells, potentially enhancing additional genomic instability, and heterogeneity and epigenetic dysregulation [40].

2.1.4. Local Invasion. Once the phenotypically aggressive clone has developed, spread of the tumor consists of a series of two sequential steps: namely, invasion of the extracellular matrix (ECM), with penetration into the vasculature and hematogenous dissemination to the CNS. Tumor expansion causes adjacent ECM compression and modifies lymphatic and blood vessel flow, eventually leading to basement membrane (BM) thinning. Combined with the various molecular and cellular events, this leads to eventual tumor metastasis.

To reach the circulation, tumor cells must penetrate the BM, traverse the extracellular connective tissue matrix (ECM) tissue, and then breach the vascular basement membrane (VBM) to enter the circulation. The process is dependent on a number of protein complexes that regulate cellular interactions and proteolytic enzymes, with degradation of the ECM, which permits extravasation.

2.1.5. E-Cadherin-Catenin Complex (ECCC), Integrins, and Other Molecules. The E-cadherin-catenin molecular complex is essential to maintain a normal and tumoral cytoarchitecture. It is a necessary mediator of cell-cell adhesion that, among other functions, determines the polarity of normal (and tumor) cells and their organization into tissues [41]. Cadherin molecules are integral cell membrane glycoproteins that interact in a homophilic manner with one another. They have a stable extracellular fragment and possess a cytoplasmic undercoat protein of one or more proteins called catenins. In the process of tumor metastasis, tumor clones become discohesive, fail to adhere to one another, and develop a more disordered cytoarchitecture, which allows these cells to separate from the tumor mass. E-cadherin maintains cell adhesion by anchoring its cytoplasmic domain to actin cytoskeleton via α-catenin and β-catenin. Infiltrating malignancies have mutations in the genes for α- and β-catenins and E-cadherin, thus decreasing the expression of this complex. This has been correlated with invasion, metastasis, and an unfavorable prognosis. Furthermore, DNA hypermethylation of the promoter region of *E-cadherin* can diminish or silence its expression, thereby disturbing ECCC function, and is a common event in many metastatic cancers [42]. N-cadherin is another molecule connected to the cellular cytoskeleton via α-catenin and β-catenin in a manner similar to E-cadherin. One of the hallmarks of the EMT described above is

a cadherin switch, with loss of epithelial E-cadherin and gain of mesenchymal N-cadherin functions. This induces loss of epithelial cellular affinity, while at the same time increasing the affinity of cells for the mesenchymal cells like fibroblasts. Gain-of-function mutations in *N-cadherin* also trigger increased migration and invasion in tumors [43].

Integrins are another family of major adhesion and signaling receptor proteins linking the ECM to the cellular actin cytoskeletal structure called focal adhesions and play an important role in mediating cell migration and invasion [44]. They trigger a variety of signal transduction pathways and regulate cytoskeletal organization, specific gene expression, control of growth, and apoptosis. Animal models of human nonsmall cell lung cancer (NSCLC) have shown that blocking $\alpha_3\beta_1$ integrin significantly decreases brain metastasis [45]. Additionally, Carbonell et al. have shown that blocking the β_1 integrin subunit prevents adhesion to the VBM and attenuates the development of metastasis [46]. Integrins induce the release of a key mediator in signaling known as focal adhesion kinase (FAK). FAK is a ubiquitously expressed nonreceptor cytoplasmic tyrosine kinase, thought to play a key role in migration and proliferation, by providing abnormal signals for survival, EMT, invasion, and angiogenesis [47]. FAK may also play an important role in the regulation of CSCs. Dephosphorylation and inhibition of FAK at the Y397 locus via the activated Ras (rat sarcoma) oncogene promote tumor migration by facilitating focal adhesion at the leading edge of tumor cells [15, 48].

The ability of tumor cells to escape the primary site is dependent on their ability to remodel the ECM. This remodeling occurs by breaking down or degrading the ECM via proteolytic enzymes, thus creating a pathway for invasion. The advancing edge of tumor cells posses the ability to carry out this proteolytic activity by releasing signals that promote cell proliferation and angiogenesis in the metastatic cascade. Neurotrophins (NTs) promote brain invasion by enhancing the production of heparinase, which is an ECM proteolytic enzyme. Heparinase is a β-d-glucuronidase that cleaves the heparin sulfate chain of the ECM. It is the prominent heparin sulfate degradative enzyme [49] and is known to destroy both the ECM and the BBB [3]. Evidence suggests the presence of NTs at the tumor-brain interface in melanomas, and reports have suggested a role for the p75 NT receptor in brain metastasis [50].

Matrix metalloproteinases (MMPs) are members of a family of zinc-dependent endopeptidases that function at physiological pH and help remodeling human connective tissue at low levels. About 25 human family members have been identified, and they have been grouped according to their substrate on which they act, namely, collagenases, stromelysins, matrilysins, and gelatinases [51]. They also play a critical role in the EMT and tumor microenvironment [52]. Cytokines and inducers present on the surface of tumor cells in the ECM regulate their expression. Once these MMPs are induced and stimulated, they aid in breakdown of type I collagen, fibronectin, and laminin in the ECM [53] and enhance tumor cell migration. MMP activity correlates with invasiveness, metastasis, and poor prognosis [54]. In one study of brain metastasis, MMP-2 was identified in all metastases regardless of site of origin. Moreover, MMP-2 activity correlated inversely with survival [55]. In a murine tumor model, the incidence of brain metastasis was reduced by 75% when compared to the wild type following the use of tissue inhibitor of metalloprotease1 (TIMP-1), which suggests that inhibitors of MMPs suppress BrMs [56].

The urokinase-type plasminogen activator (uPA) system consists of uPA, its receptor (uPAR), and plasminogen. The uPA binds to the receptor uPA-R (CD87), the activity of which is regulated by the action of plasminogen activator inhibitor type 1 and 2 (PAI-1/2) on the cell membrane and causes urokinase to convert plasminogen to plasmin. The proteolytic activity of plasmin then degrades components of the ECM including fibrin, fibronectin, proteoglycans, and laminin. Further, plasmin activates other proteolytic enzymes with resultant local invasion and migration [57]. As far back as 1994, researchers have found that there is a high level of uPA in metastatic tumors, that uPA correlates with necrosis and edema, and that there is an inverse correlation with a tumor's levels of uPA and survival [58]. Additionally, high levels of uPA and absent tissue plasminogen activator (tPA) correlate with aggressiveness and decreased survival [58].

More recent evidence describes the role of "invadopodia," which are three-dimensional protrusive processes, compared to the two-dimensional lamellipodia and filopodia, in metastatic invasion [59]. Invadopodia appear to share a number of structural and functional features with filopodia, but spatially focus proteolytic secretion, remodeling the ECM matrix and establishing tracts supporting subsequent invasion [60]. Integrins play a major role in organizing the components, triggering the formation of invadopodia. $\alpha_3\beta_1$ activation promotes Src-dependent tyrosine phosphorylation of p190RhoGAP, via RhoGTPases family, which activates invadopodia and invasion [61]. Integrins also appear to focus proteolytic activity to the region of these processes, as in melanoma cells, where collagen-induced $\alpha_3\beta_1$ association with the serine protease Seprase (surface-expressed protease) enhances the activity of matrix-degrading enzymes focally at the invadopodia [62]. Numerous cancer cell lines such as melanoma, breast cancer, glioma, and head and neck cancer have shown the presence of invadopodia. A number of other molecules, such as EGF, HGF, or TGF-β, can induce their formation as well [63]. The release of tumor-released chemokines such as CSF-1 and PIGF attract tumor-associated macrophages (TAM) to the microenvironment, which in turn release multiple factors stimulating invadopodia [64]. In addition, a family of proteins called aquaporins may also facilitate migration. Aquaporin-dependent tumor angiogenesis and metastases enhance water transport in the lamellipodia of migrating cells [65]. Studies on brain-specific breast metastasis reveal that increased expression of *KCNMA1*, a gene encoding for a big conductance type potassium channel (BKCa) that is upregulated in breast cancer, leads to greater invasiveness and transendothelial migration [66].

2.1.6. Genetic Alterations. Several known tumor suppressor genes (TSGs) that function at the level of escape and

migration/intravasation are worth exploring and are enumerated in Table 2. The best known of these is the *KiSS1* gene on chromosome 1. *KiSS1* encodes metastin, which is a ligand of the orphan G protein couples receptor hOT7T175. Lee et al. [67] have found that the forced expression of *KiSS1* suppressed both melanoma and breast metastasis. Other authors have found an inverse correlation between *KiSS1* expression and melanoma progression [68].

KAI1 (CD82), a TSG on chromosome 11p11.2, regulates adhesion, migration, growth, and differentiation of tumor cell lines. *KAI1* expression is inversely correlated with prostate cancer progression [69] as well as breast [26, 27] and melanoma metastasis [28]. Additionally, *KAI1* is known to be associated with the epidermal growth factor receptor (EGFR), discussed later in this paper, and is thought to affect the Rho GTPase pathway [29] resulting in suppression of lamellipodia formation and migration [30].

Hypermethylation of the TSG *Drg1* inhibits both liver metastasis and colorectal carcinoma invasion [70]. Conversely, overexpression of *Drg1* has been linked to resistance to irinotecan chemotherapy [71]. Finally, in a murine model of breast cancer metastasis, the Notch signaling pathway was found to be activated via increased Jag2 mRNA levels, thereby, creating a cell line that was both more migratory and more invasive in collagen assays. Additionally, inactivation of the Notch pathway significantly decreased tumor cell migratory and invasive activity [72]. In addition to the suppressor genes responsible for invasion and metastasis, there are a number of promoter genes responsible for invasion and metastasis as well, a few of which are enumerated in Table 3. Genetic activation or inactivation of promoter/suppressor genes in human cancer can be the result of mutations, deletions, loss of heterozygosity, multiplication, and translocation [73]. The same genes that are responsible for normal cellular functioning, signaling, signal transduction, modulating, and mediating cellular response are frequently the genes that enhance invasion and metastasis when altered by genetic or epigenetic dysfunction [74, 75].

These changes within the primary tumor microenvironment give rise to an "active seed" ready to implant itself in a fertile environmental "soil" (Figure 3). These cellular modifications enable the next steps of migration, namely, dissemination and extravasation.

2.1.7. Dissemination. Once a cancer cell has breached its microenvironment and arrived at the vasculature (brain metastasis) or lymphatic system (other sites), the tumor cell must survive its exposure to high shear forces and varied stress patterns. Tumor cells respond by reenforcing their cytoskeleton and increasing the ability to adhere to the vascular wall [76]. More recent experimental evidence suggests shear induces a paradoxical enhancement of adhesion to the VBM via activation of Src [77] and FAK phosphorylation seen in colon cancer cell lines [78]. On adhering to endothelium of target tissue, the tumor cells behave like macrophages, creating pseudopodia, and penetrating the cell-cell junctions, driven by dynamic remodeling of the cellular cytoskeleton [60]. There are a subset of circulating tumor cells which maintain their physical plasticity and, although much larger in diameter (20–30 μ) than lung capillaries (~8 μ), can survive the sieving action of lung capillaries. These cells can be found either growing as clumps in the lung or colonizing other organ sites [10]. Cancer cells in circulation appear to attract platelets because of their expressed surface tissue proteins, and these protect the cells from the immune system [79]. Once these mobile cancer cells get lodged in a secondary organ tissue site, there are two pathways for colonization. One is mediated by cellular diapedesis, extravasation, and proliferation of the tumor cell mass, whereas the other consists of accumulation of tumor cells within the site of obstruction in the foreign tissue vascular bed, wherein they proliferate, prior to their rupture into the adjacent stroma where they begin to grow [80].

2.2. Colonization

2.2.1. Organ-Specific Infiltration. Subsequent to intravasation and dissemination, special mechanisms are necessary to extravasate and colonize secondary sites. The metastatic deposits occur in certain organ tissues because of the influence of hematogenous dynamics, for example, colon cancer metastasis preferentially metastasizing to the liver because of mesenteric circulation and large vascular sinusoids [81]. The overexpression of the cell adhesion molecule, metadherin, in breast cancer makes it easier for tumor cells to target and adhere to endothelial lining in the lung parenchyma [82], making it possible for these endothelial-adhesive interactions to enhance the possibility of brain metastasis. Although the exact causes of preferential metastatic sites have not been clearly elucidated, one theory states that direct neurotropic interactions with yet undiscovered brain homing mechanisms result in BrM. "Vascular co-option," a term put forward by Carbonell et al., describes the ability of metastatic cells to grow along the preexisting vessels much before overt secondaries are detected. Once adherent to the VBM, tumor cells can extravasate into the parenchyma, the VBM thus being the "soil" for BrM (Figure 4) [46]. Saito et al. demonstrated that the pia-glial membrane along the external surface of blood vessels serves as a scaffold for the angiocentric spread of metastatic cells [83].

In a mouse model of CNS metastasis, tumor cells function like macrophages within the vasculature and during extravasation, expressing CD11b, Iba1, F4/80, CD68, CD45, and CXCR, which are proteins normally expressed specifically by macrophages [84]. The ability of tumor cells to mimic macrophages may enable them to evade the immune system while in the vasculature.

2.2.2. The BBB, Function of the Brain Microenvironment, and Brain Metastasis. Passage of tumor cells across the BBB occurs via mechanisms which have not yet been delineated fully. Recently, three proteins that mediate breast metastasis to the brain and lungs have been described, namely, cyclooxygenase 2 or COX2 (also known as PTGS2), EGFR, ligand and heparin binding epidermal growth factor (HBEGF). These proteins facilitate extravasation through nonfenestrated blood vessels and enhance colonization [85]. Other molecules targeting organ specific colonization may

Table 2: Representative metastasis and invasion suppressor genes.

Gene	Cancer/metastatic tumor	Function(s) of protein	OMIM no.	Chromosome Location
NM23	Breast, colon, melanoma	A histidine kinase. Nm23 phosphorylates KSR and can lead to decreased ERK 1/2 activation. appears to play a role in normal development and differentiation	156490	17q21.3
MKK4	Breast, ovarian, and prostate	A mitogen-activated protein kinase (MAPKK) that phosphorylates p38 and Jun (JNK) kinases	601335	17p11.2
BRMS1	Breast, melanoma	Functions in gap-junction communication	606259	11q13.1-q13.2
KiSS1	Breast, melanoma	A G-protein coupled receptor ligand, also known as metastin.	603286	1q32
KAI1 (CD82)	Bladder, breast, lung, pancreas, and prostate	Interact with beta-catenin-reptin and histone deacetylases. It may desensitize EGFR activity, also known as kangai	600623	11p11.2
CD44	Breast, colon, lung, melanoma, prostate	An integral cell membrane glycoprotein that affects cell adhesion. Decreased expression due in part to hypermethylation	107269	11pter-p13
CRSP3	Melanoma	A transcriptional coactivator that may work through the enhancer binding factor Sp1	605042	
RHOGDI2	Bladder, breast, colon, kidney, liver, lung, and prostate	Regulates function of Rho and Rac, GTP-binding proteins of the Ras superfamily		11p11.2
VDUP1	Melanoma	A differentiation factor via thioredoxin inhibition	606599	1q21
PTEN/MMAC1	Breast, colon, endometrial, germ cell, kidney, lung, melanoma, and thyroid	A homologue of cytoskeletal tension, leading to invasion and metastasis through interaction with actin filaments at focal adhesions	601728	10q23.31
VHL	Renal cell, pheochromocytoma, and hemangioblastoma	Encodes protein products playing an essential role in microtubule stability, orientation, tumor suppression, cilia formation, signaling of cytokines, and extracellular matrix assembly	608537	3p25.3
TIMP2	Melanoma	Protease inhibitor plays a role in preventing excessive ECM disruption	188825	17q25.3
SMAD4	Pancreatic cancer, colorectal, and prostate	Transcription factor, pivotal role in signal transduction of TGFβ	600993	18q21.2
RRM1	Lung	Cell cycle regulator	180410	11p15.4
PTPN11	Lung, colon, thyroid, and melanoma	Regulates tyrosine phosphatase, proliferation, differentiation, motility, and apoptosis of cells	176876	12q24.1
CDH1	Gastric, breast	Cellular adherens junctional protein	192090	16q22.1
CASP8	Gastric, breast, lung, and PNETs	Apoptotic cascade via aspartate-specific cysteine proteases	601763	2q33

Definitions: EGFR: epidermal growth factor; ERK: extracellular signal-regulated kinase; JNK: Jun-terminal kinase; KSR: kinase suppressor of Ras. OMIM no.: Online Mendelian Inheritance in Man Identification number (http://www.ncbi.nlm.nih.gov/), which provides detailed information and references for these genes, their protein products, and potential functions.

Table 3: Representative metastasis and invasion promoter genes.

Gene	Cancer/metastatic tumor	Function(s) of protein	OMIM no.	Chromosome location
ERBB2 (HER2)	Breast	Receptor tyrosine kinase, critical component of IL6, and cytokine signaling	164870	17q21.1
TIAM1	Lymphomas, renal cell cancer, colon, prostate, and breast	Activates Rho-like GTPase Rac1, Tiam1Rac1 signaling which affects invasion in numerous ways	600687	21q22.1
SRC	Colorectal, breast, melanoma, and lung	Critical role in cellular signal transduction pathways, regulating cell division, motility, adhesion, angiogenesis, and survival	190090	20q12-q13
S100A4	Colorectal Breast Gastric cancers	Increases endothelial cell motility and induces angiogenesis, increases invasive properties through deregulation of the extracellular matrix	114210	1q21
MTA1	Breast Ovary Lung Gastrointestinal Colorectal	Nucleosome remodeling and deacetylating (NuRD) complex serves multiple functions in cellular signaling, chromosome remodeling and transcription processes, that are important in the progression, invasion, and growth of metastatic epithelial cells	603526	14q32.3
KRAS	Pancreatic Lung Colorectal	Encode GDP/GTP-binding proteins involved in signal transduction during cellular proliferation, differentiation, and senescence	190070	12p12.1
HRAS	Bladder Renal Thyroid	Small GTPase growth promoting factor	190020	11p15.5

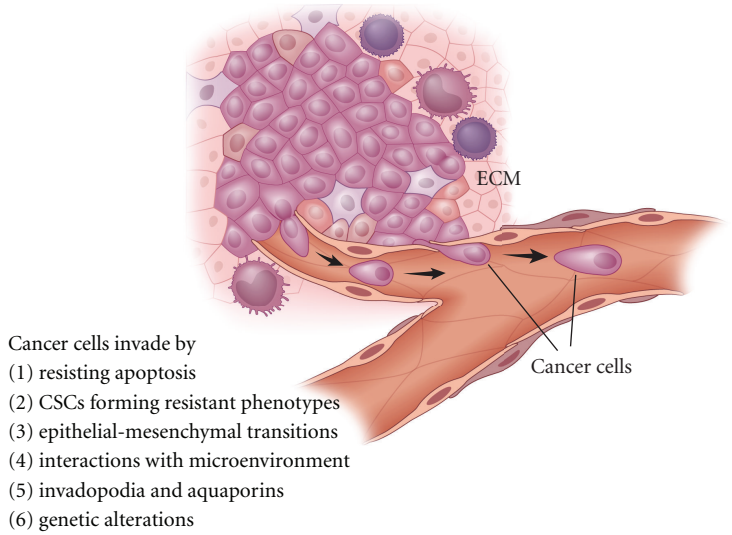

Figure 3: Invasion and migration. Subsets of cancer cells at the primary site develop an invasive phenotype; survive environmental pressures such as hypoxia and nutrient deprivation, low pH, poor blood supply, immune, and inflammatory mediators, gaining the ability to metastasize to distant sites. These cancer cells can evade growth suppressors and circumvent inhibitors of cell proliferation to intravasate and disseminate to various other sites.

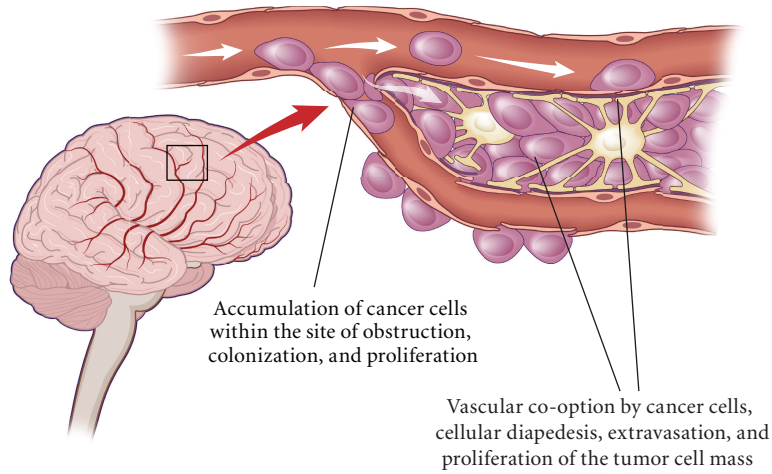

Figure 4: Colonization of metastatic tumor cells in the brain. Overexpression of the adhesion molecules makes it easy for tumor cells to target and adhere to endothelial lining in the parenchyma, making it possible for these endothelial-adhesive interactions to enhance the possibility of brain metastasis. Direct neurotropic interactions with brain homing mechanisms result in BrM. "Vascular co-option" is the ability of metastatic cells to grow along the preexisting vessels, and once adherent to the VBM, tumor cells can extravasate into the parenchyma, the VBM thus being the "soil" for BrM.

also be expressed by the cancer cell [86]. These molecules include ezrin (an intracellular protein necessary for the survival of osteosarcoma cells in the lung) and serine-threonine kinase 11 (STK11, or LKB1, a metastasis suppressor which regulates *NEDD9* in lung cancer) [87].

2.2.3. Neoangiogenesis and Proliferation. A key component of both primary and secondary (metastatic) tumor growth at any site is angiogenesis [8]. Experimental systems, using breast or melanoma cell lines to model BrM, have revealed that growth may occur by utilizing preexisting vasculature, or co-opting these vessels rather than inducing new vessel formation (neoangiogenesis) [46, 88, 89]. Kusters et al. [90], using a melanoma cell line in a murine metastatic brain tumor model, showed that growth of the metastatic tumor up to 3 mm could occur without inducing the angiogenic switch [91]. Carbonell et al. have also shown that β_1 integrin, expressed by the metastatic tumor cell line, is the key molecule to co-opt adjacent blood vessels to the growing tumor.

Various angiogenic factors have been scrutinized as viable targets for treatment. Vascular endothelia growth factor (VEGF) is the most commonly recognized angiogenic factor. VEGF expression in breast cancer plays a role in metastasis and inhibition with a tyrosine kinase receptor inhibitor-reduced growth and angiogenesis [92]. *SSecks* (Src-suppressed C kinase substrate) has been observed to decrease VEGF expression. This protein also stimulates proangiogenic angiopoietin 1 and regulates bran angiogenesis and tight junction creation, thus helping to regulate BBB differentiation [93].

MMP-9/gelatinase B complex, a member of the MMP family, and PAI-1, a uPA cell surface receptor, may play roles in angiogenesis [94]. The role in angiogenesis and uniqueness of Plexin D1 expression was explored in tumor cells and vasculogenesis. Neoplastic cells expressed Plexin D1 as well as tumor vasculature, while its expression in nonneoplastic tissue was restricted to a small subset of activated macrophages, which suggests that Plexin D1 may play a significant role in tumor angiogenesis [95]. Overexpression of hexokinase 2 (HK2), which plays a key role in glucose metabolism and apoptosis, may also influence BrM in breast and other cancers. Researchers at the National Cancer Institute found that both mRNA and protein levels of HK2 are elevated in brain metastatic derivative cell lines compared to the parental cell line *in vitro*. Knockdown of expression reduced cell proliferation, which implies that HK2 contributes to the proliferation and growth of breast cancer metastasis. Finally, increased expression of HK2 is associated with poor survival after craniotomy [96, 97].

At least two tumor suppressor genes that function at the proliferation level of the metastatic cascade have been described. The first, *NM23*, regulates cell growth by encoding for a nucleotide diphosphate protein kinase that interacts with menin, a TSG encoded by *MEN1* [98]. NM23 is thought to reduce signal transduction and thereby decrease anchorage independent colonization, invasion, and motility [99]. In melanoma, decreased expression is correlated with increased brain metastasis [100]. Another tumor suppressor gene, *BrMS1*, located at 11q13 is altered in many melanomas and breast cancers. BrMS1 prevents disseminated tumor cell growth by restoring the normal gap junction phenotype

and maintaining cell-to-cell communication in the primary tumor [101]. Seraj et al. [102] found an inverse correlation between the expression of BrMS1 and the metastatic potential in melanoma.

2.2.4. Cascade-Nonspecific Contributors to Metastasis. There are certain molecular contributions that cannot be attributed to a specific step in the cascade, either because they are active at every level or, as in most cases, their true function is yet to be discovered (see Tables 1 and 2). These molecular entities are on the forefront of cancer research and are worth addressing. *Zeb-1*, the zinc finger E-box homeobox transcription factor, is overexpressed in metastatic cancers. This overexpression leads to epithelial-mesenchymal transition and increased metastasis. Mutation of *Zeb-1* leads to decreases in the proliferation of progenitor cells in mutant mice. This mutation may be a target for metastatic prevention at the progenitor level [103].

Several other genetic markers have been located that pertain to metastasis in particular. A deletion of the 4q arm in lung (both small and nonsmall cell) metastasis to the brain and bone has been documented [104]. Additionally, in NSCLC, overexpression of *CDH2* (N-cadherin), *KIFC1*, and *FALZ* is highly predictive of metastasis to the brain in early and advanced lung cancer. Therefore, these genes may be used to predict a high risk of metastasis early in the diagnosis [105]. In prostate cancer, increased expression of *KLF6-SV1,* the Kruppel-like factor tumor suppressor gene, predicts poorer survival and is correlated with increased metastasis to the lymphatic system, the brain, and bone [106]. Finally, overexpression of homeoprotein Six-1, a transcriptional regulator, increased TGF-β signaling and metastasis in breast cancer with significantly shortened relapse times [107]. Gaining a better understanding of the role(s) of these genes and others will be important to deeper knowledge of the metastatic cascade.

2.2.5. Overview of microRNAs (miRNAs) and Their Emerging Role in Oncogenesis. Recent evidence has established an important role of microRNAs in cell and tissue development, proliferation and motility via their ability to repress mRNA translation or induce mRNA degradation [108]. The dysregulated expression of a single miRNA can cause a cascade of silencing events capable of eliciting disease development in humans, which includes cancer [109]. Breast cancer is found to possess aberrant regulation of several miRNAs [110]. They also play a prominent role in expression of EMT-related genes. Finally, pseudogenes, which encode RNAs that do not have to produce proteins but can compete for microRNA binding, may play a role in tumorigenesis and metastasis. Poliseno et al. [111]. Recently described the functional relationship between the mRNAs produced by the *PTEN* tumor suppressor gene and its pseudogene *PTENP1*. *PTENP1* regulates cellular levels of PTEN and can exert a growth-suppressive role and the *PTENP1* locus is lost in several human tumors, including prostate and colon cancer. They also showed that other cancer-related genes possess pseudogenes, including oncogenic *KRAS*. While the role of miRNAs and psuedogenes in metastasis is beyond the scope of this summary, several recent, excellent reports detail this emerging field [21, 111, 112].

3. Conclusion

The metastatic cascade, from its initiation to its completion in the brain, is an extremely complex, multistep process. For patients, the progression in the metastatic cascade to brain colonization is becoming both an increasingly treatable and yet simultaneously and increasingly prevalent feature of their disease, with consequent morbidity. As more evidence regarding the molecular and genetic factors that contribute to the cascade appears, targeting this ominous disease with multiple therapeutic strategies comes closer.

Knowledge of the metastatic process may lead to better detection and treatment of brain metastases. The goal however will be to utilize all the information gained at the genetic and molecular level to stop cancer, at the primary proliferative stage, preventing the initiation of the metastatic cascade and subsequent development of brain metastasis.

Abbreviations

AKAP12:	A-kinase anchor protein 12
ARHGDIB(RhoGD12):	Rho GDP dissociation inhibitor beta
BBB:	Blood brain barrier
BKCa:	Big conductance type potassium channel
BrMS1:	Breast cancer metastasis suppressor 1
CASP8:	Caspase8
CDH1:	Cadherin 1
CD11b:	Cluster of differentiation molecule 11b
CD45:	Cluster of differentiation 45
CD44:	cluster of differentiation 44
CD6:	Cluster of differentiation 68
CDH2:	Neutral cadherin (N-cadherin), when overexpressed with FALZ and KlFC1 genes) predicts metastasis to brain
COX2:	Cyclooxygenase 2 (also known as PTGS2)
CRSP3:	Cofactor required for Sp1 transcriptional activation subunit 3
CXCR:	Chemokine receptor
CD87:	uPA binds to the receptor uPA-R
CNS:	Central nervous system
CXCL12/CXCR4:	Chemokine/receptor system
CXCR7:	Alternate receptor to CXCL12
CSF-1:	Colony stimulating factor-1
Drg-1:	Differentiation-related, putative metastatic suppressor gene
ECM:	Extracellular matrix
EGFR:	Epidermal growth factor receptor
ERBB2(HER2):	Avian erythroblastic leukemia homolog 2

F4/80: Transmembrane protein present on cell surface of mouse
FALZ: Overexpression with CDH2 and KlFC1 genes predicts metastasis to the brain
FAK: Focal adhesion kinase
HBEGF: Heparin binding epidermal growth factor
HSP27: Heat shock protein
HK2: Hexokinase 2
HOXB9: homeobox B9
HRAS: Harvey rat sarcoma viral oncogene homolog
Iba1: Ionized calcium binding adaptor molecule 1
KAI1 (CD82) gene: Tumor suppressor gene
KCNMA1: tumor suppressor gene
KIFC1: Overexpression with CDH2 and FALZ genes predicts metastasis to brain
KISS-1: Gene that encodes metastin
KLF6-SV1: Kruppel-like factor tumor suppressor gene
KRAS: Kirsten rat sarcoma viral oncogene homolog
LEF1: Lymphoid enhancing factor 1
MIB-1: Mindbomb homolog 1 labeling index
MMAC1: Multiple advanced cancers
MMPs: Matrix metalloprotease
MEN1: Multiple endocrine neoplasia type 1
MTA1: Metastasis-associated protein 1
NM23(NME1): Metastasis suppressor gene also known as NDP kinase
NSCLC: Nonsmall cell lung cancer
NTs: Neurotrophins
PAI-1/2: plasminogen activator inhibitor type 1 and 2
PTEN: Chromosome 10
PIGF: Phosphatidylinositol glycan, class F
PTPN11: Protein-tyrosine phosphatase, nonreceptor type 11
PTEN: Phosphatase and tensin homologue deleted on chromosome 10
Ras: Oncogene (rat sarcoma) gene
RRM1: Ribonucleotide reductase, M12 subunit
sHSP: Small heat shock protein
SSecks: Src-suppressed C kinase substrate
Six-1: Homeoprotein transcriptional regulator
ST6GALNAC5: α2,6-sialyltransferase
S100A4: S100 calcium-binding protein A4
SMAD4: Sma- and Ma-related protein 4
SRC: Rous sarcoma virus protein
TIAM1: T-cell lymphoma invasion and metastasis 1
TIMP2: Tissue inhibitor of metalloproteinase 2
TCF: T-cell factor pathway
TGF: Transforming growth factor
TIMP-1: Tissue inhibitor of metalloprotease 1
tPA: Tissue plasminogen activator
uPA: Urokinase-type plasminogen activator
uPA-R (CD87): Urokinase-type plasminogen activator receptor
VBM: Vascular basement membrane
VEGF: Vascular endothelial growth factor
VDUP: Vitamin D3-upregulated protein
VHL: Von Hippel-Lindau tumor suppressor
WNT: Wingless integration gene
Zeb-1: Zinc finger E-box-binding homeobox 1
OMIM no.: Online Mendelian Inheritance in Man Identification Number (http://www.ncbi.nlm.nih.gov/), which provides detailed information and references for these genes, their protein products, and potential functions.

Conflict of Interests

Each author declares that he or she has no conflict of interests.

Acknowledgments

This work was supported in part by Grant no. W81XWH-062-0033 from the U.S. Department of Defense Breast Cancer Research Program, to R. J. Weil. The authors wish to thank the Melvin Burkhardt chair in neurosurgical oncology and the Karen Colina Wilson research endowment within the Brain Tumor and Neuro-oncology Center at the Cleveland Clinic Foundation for additional support and funding.

References

[1] I. T. Gavrilovic and J. B. Posner, "Brain metastases: epidemiology and pathophysiology," *Journal of Neuro-Oncology*, vol. 75, no. 1, pp. 5–14, 2005.

[2] R. A. Patchell, "The management of brain metastases," *Cancer Treatment Reviews*, vol. 29, no. 6, pp. 533–540, 2003.

[3] M. Nathoo, A. Chahlavi, G. H. Barnett, and S. A. Toms, "Pathobiology of brain metastases," *Journal of Clinical Pathology*, vol. 58, no. 3, pp. 237–242, 2005.

[4] S. H. Landis, T. Murray, S. Bolden, and P. A. Wingo, "Cancer statistics, 1998," *Ca-A Cancer Journal for Clinicians*, vol. 48, no. 1, pp. 6–29, 1998.

[5] P. Y. Wen and J. S. Loeffler, "Brain metastases," *Current Treatment Options in Oncology*, vol. 1, no. 5, pp. 447–458, 2000.

[6] S. H. Kim, S. T. Chao, S. A. Toms et al., "Stereotactic radiosurgical treatment of parenchymal brain metastases from prostate adenocarcinoma," *Surgical Neurology*, vol. 69, no. 6, pp. 641–646, 2008.

[7] S. Paget, "The distribution of secondary growths in cancer of the breast. 1889," *Cancer and Metastasis Reviews*, vol. 8, no. 2, pp. 98–101, 1989.

[8] I. J. Fidler, S. Yano, R. D. Zhang, T. Fujimaki, and C. D. Bucana, "The seed and soil hypothesis: vascularisation and

brain metastases," *Lancet Oncology*, vol. 3, no. 1, pp. 53–57, 2002.
[9] J. Ewing, *Neoplastic Diseases*, WB Saunders, 1922.
[10] C. L. Chaffer and R. A. Weinberg, "A perspective on cancer cell metastasis," *Science*, vol. 331, no. 6024, pp. 1559–1564, 2011.
[11] D. Hanahan and R. A. Weinberg, "Hallmarks of cancer: the next generation," *Cell*, vol. 144, no. 5, pp. 646–674, 2011.
[12] J. Y. Delattre, G. Krol, H. T. Thaler, and J. B. Posner, "Distribution of brain metastases," *Archives of Neurology*, vol. 45, no. 7, pp. 741–744, 1988.
[13] E. L. Chang, J. S. Wefel, M. H. Maor et al., "A pilot study of neurocognitive function in patients with one to three new brain metastases initially treated with stereotactic radiosurgery alone," *Neurosurgery*, vol. 60, no. 2, pp. 277–283, 2007.
[14] P. R. Lockman, R. K. Mittapalli, K. S. Taskar et al., "Heterogeneous blood-tumor barrier permeability determines drug efficacy in experimental brain metastases of breast cancer," *Clinical Cancer Research*, vol. 16, no. 23, pp. 5664–5678, 2010.
[15] K. D. Beasley and S. A. Toms, "The molecular pathobiology of metastasis to the brain: a review," *Neurosurgery Clinics of North America*, vol. 22, no. 1, pp. 7–14, 2011.
[16] A. F. Eichler, E. Chung, D. P. Kodack, J. S. Loeffler, D. Fukumura, and R. K. Jain, "The biology of brain metastases-translation to new therapies," *Nature Reviews Clinical Oncology*, vol. 8, no. 6, pp. 344–356, 2011.
[17] M. P. Mehta, P. Rodrigus, C. H. J. Terhaard et al., "Survival and neurologic outcomes in a randomized trial of motexafin gadolinium and whole-brain radiation therapy in brain metastases," *Journal of Clinical Oncology*, vol. 21, no. 13, pp. 2529–2536, 2003.
[18] A. C. Chiang and J. Massagué, "Molecular basis of metastasis," *The New England Journal of Medicine*, vol. 359, no. 26, pp. 2752–2823, 2008.
[19] M. R. Junttila and G. I. Evan, "P53 a Jack of all trades but master of none," *Nature Reviews Cancer*, vol. 9, no. 11, pp. 821–829, 2009.
[20] P. A. Jones and S. B. Baylin, "The Epigenomics of Cancer," *Cell*, vol. 128, no. 4, pp. 683–692, 2007.
[21] L. Salmena, L. Poliseno, Y. Tay, L. Kats, and P. P. Pandolfi, "A ceRNA hypothesis: the rosetta stone of a hidden RNA language?" *Cell*, vol. 146, no. 3, pp. 353–358, 2011.
[22] L. E. Ailles and I. L. Weissman, "Cancer stem cells in solid tumors," *Current Opinion in Biotechnology*, vol. 18, no. 5, pp. 460–466, 2007.
[23] P. Marcato, C. A. Dean, P. Da et al., "Aldehyde dehydrogenase activity of breast cancer stem cells is primarily due to isoform ALDH1A3 and its expression is predictive of metastasis," *Stem Cells*, vol. 29, no. 1, pp. 32–45, 2011.
[24] E. Quintana, M. Shackleton, M. S. Sabel, D. R. Fullen, T. M. Johnson, and S. J. Morrison, "Efficient tumour formation by single human melanoma cells," *Nature*, vol. 456, no. 7222, pp. 593–598, 2008.
[25] R. Pang, W. L. Law, A. C. Y. Chu et al., "A subpopulation of CD26+ cancer stem cells with metastatic capacity in human colorectal cancer," *Cell Stem Cell*, vol. 6, no. 6, pp. 603–615, 2010.
[26] M. Yilmaz and G. Christofori, "EMT, the cytoskeleton, and cancer cell invasion," *Cancer and Metastasis Reviews*, vol. 28, no. 1-2, pp. 15–33, 2009.
[27] J. P. Thiery, H. Acloque, R. Y. J. Huang, and M. A. Nieto, "Epithelial-mesenchymal transitions in development and disease," *Cell*, vol. 139, no. 5, pp. 871–890, 2009.
[28] J. Zavadil and E. P. Böttinger, "TGF-β and epithelial-to-mesenchymal transitions," *Oncogene*, vol. 24, no. 37, pp. 5764–5774, 2005.
[29] P. Savagner and V. Arnoux, "Epithelio-mesenchymal transition and cutaneous wound healing," *Bulletin de l'Academie Nationale de Medecine*, vol. 193, no. 9, pp. 1981–1992, 2009.
[30] T. R. Graham, H. E. Zhau, V. A. Odero-Marah et al., "Insulin-like growth factor-I—dependent up-regulation of ZEB1 drives epithelial-to-mesenchymal transition in human prostate cancer cells," *Cancer Research*, vol. 68, no. 7, pp. 2479–2488, 2008.
[31] K. G. Leong, K. Niessen, I. Kulic et al., "Jagged1-mediated Notch activation induces epithelial-to-mesenchymal transition through Slug-induced repression of E-cadherin," *Journal of Experimental Medicine*, vol. 204, no. 12, pp. 2935–2948, 2007.
[32] S. A. Mani, W. Guo, M. J. Liao et al., "The epithelial-mesenchymal transition generates cells with properties of stem cells," *Cell*, vol. 133, no. 4, pp. 704–715, 2008.
[33] K. Pietras and A. Östman, "Hallmarks of cancer: interactions with the tumor stroma," *Experimental Cell Research*, vol. 316, no. 8, pp. 1324–1331, 2010.
[34] A. Östman and M. Augsten, "Cancer-associated fibroblasts and tumor growth—bystanders turning into key players," *Current Opinion in Genetics and Development*, vol. 19, no. 1, pp. 67–73, 2009.
[35] N. A. Bhowmick, E. G. Neilson, and H. L. Moses, "Stromal fibroblasts in cancer initiation and progression," *Nature*, vol. 432, no. 7015, pp. 332–337, 2004.
[36] K. Kessenbrock, V. Plaks, and Z. Werb, "Matrix metalloproteinases: regulators of the tumor microenvironment," *Cell*, vol. 141, no. 1, pp. 52–67, 2010.
[37] B. Z. Qian and J. W. Pollard, "Macrophage diversity enhances tumor progression and metastasis," *Cell*, vol. 141, no. 1, pp. 39–51, 2010.
[38] A. Orimo, P. B. Gupta, D. C. Sgroi et al., "Stromal fibroblasts present in invasive human breast carcinomas promote tumor growth and angiogenesis through elevated SDF-1/CXCL12 secretion," *Cell*, vol. 121, no. 3, pp. 335–348, 2005.
[39] K. Pietras, J. Pahler, G. Bergers, and D. Hanahan, "Functions of paracrine PDGF signaling in the proangiogenic tumor stroma revealed by pharmacological targeting," *PLoS Medicine*, vol. 5, no. 1, article 019, pp. 0123–0138, 2008.
[40] R. G. Bristow and R. P. Hill, "Hypoxia and metabolism: hypoxia, DNA repair and genetic instability," *Nature Reviews Cancer*, vol. 8, no. 3, pp. 180–192, 2008.
[41] S. Hirohashi and Y. Kanai, "Cell adhesion system and human cancer morphogenesis," *Cancer Science*, vol. 94, no. 7, pp. 575–581, 2003.
[42] R. M. Bremnes, R. Veve, F. R. Hirsch, and W. A. Franklin, "The E-cadherin cell-cell adhesion complex and lung cancer invasion, metastasis, and prognosis," *Lung Cancer*, vol. 36, no. 2, pp. 115–124, 2002.
[43] J. Hulit, K. Suyama, S. Chung et al., "N-cadherin signaling potentiates mammary tumor metastasis via enhanced extracellular signal-regulated kinase activation," *Cancer Research*, vol. 67, no. 7, pp. 3106–3116, 2007.
[44] R. O. Hynes, "Integrins: bidirectional, allosteric signaling machines," *Cell*, vol. 110, no. 6, pp. 673–687, 2002.
[45] T. Yoshimasu, T. Sakurai, S. Oura et al., "Increased expression of integrin $\alpha 3\beta 1$ in highly brain metastatic subclone of a human non-small cell lung cancer cell line," *Cancer Science*, vol. 95, no. 2, pp. 142–148, 2004.

[46] W. S. Carbonell, O. Ansorga, N. Sibson, and R. Muschel, "The vascular basement membrane as "soil" in brain metastasis," *PLoS ONE*, vol. 4, no. 6, Article ID e5857, 2009.

[47] X. Zhao and J. -L. Guan, "Focal adhesion kinase and its signaling pathways in cell migration and angiogenesis," *Advanced Drug Delivery Reviews*, vol. 63, no. 8, pp. 610–615, 2011.

[48] Y. Zheng and Z. Lu, "Paradoxical roles of FAK in tumor cell migration and metastasis," *Cell Cycle*, vol. 8, no. 21, pp. 3474–3479, 2009.

[49] D. Marchetti and G. L. Nicolson, "Human heparanase: a molecular determinant of brain metastasis," *Advances in Enzyme Regulation*, vol. 41, pp. 343–359, 2001.

[50] D. Marchetti, R. Aucoin, J. Blust, B. Murry, and A. Greiter-Wilke, "p75 neurotrophin receptor functions as a survival receptor in brain-metastatic melanoma cells," *Journal of Cellular Biochemistry*, vol. 91, no. 1, pp. 206–215, 2004.

[51] S. Zucker, J. Cao, and W. T. Chen, "Critical appraisal of the use of matrix metalloproteinase inhibitors in cancer treatment," *Oncogene*, vol. 19, no. 56, pp. 6642–6650, 2000.

[52] E. C. Finger and A. J. Giaccia, "Hypoxia, inflammation, and the tumor microenvironment in metastatic disease," *Cancer and Metastasis Reviews*, vol. 29, no. 2, pp. 285–293, 2010.

[53] K. Hotary, X. Y. Li, E. Allen, S. L. Stevens, and S. J. Weiss, "A cancer cell metalloprotease triad regulates the basement membrane transmigration program," *Genes and Development*, vol. 20, no. 19, pp. 2673–2686, 2006.

[54] I. Stamenkovic, "Extracellular matrix remodelling: the role of matrix metalloproteinases," *Journal of Pathology*, vol. 200, no. 4, pp. 448–464, 2003.

[55] J. Jäälinojä, R. Herva, M. Korpela, M. Höyhtyä, and T. Turpeenniemi-Hujanen, "Matrix metalloproteinase 2 (MMP-2) immunoreactive protein is associated with poor grade and survival in brain neoplasms," *Journal of Neuro-Oncology*, vol. 46, no. 1, pp. 81–90, 2000.

[56] A. Krüger, O. H. Sanchez-Sweatman, D. C. Martin et al., "Host TIMP-1 overexpression confers resistance to experimental brain metastasis of a fibrosarcoma cell line," *Oncogene*, vol. 16, no. 18, pp. 2419–2423, 1998.

[57] K. Danø, N. Behrendt, G. Høyer-Hansen et al., "Plasminogen activation and cancer," *Thrombosis and Haemostasis*, vol. 93, no. 4, pp. 676–681, 2005.

[58] A. K. Bindal, M. Hammoud, Wet Ming Shi, S. Z. Wu, R. Sawaya, and J. S. Rao, "Prognostic significance of proteolytic enzymes in human brain tumors," *Journal of Neuro-Oncology*, vol. 22, no. 2, pp. 101–110, 1994.

[59] H. Yamaguchi, J. Wyckoff, and J. Condeelis, "Cell migration in tumors," *Current Opinion in Cell Biology*, vol. 17, no. 5, pp. 559–564, 2005.

[60] S. Kumar and V. M. Weaver, "Mechanics, malignancy, and metastasis: the force journey of a tumor cell," *Cancer and Metastasis Reviews*, vol. 28, no. 1-2, pp. 113–127, 2009.

[61] R. Buccione, G. Caldieri, and I. Ayala, "Invadopodia: specialized tumor cell structures for the focal degradation of the extracellular matrix," *Cancer and Metastasis Reviews*, vol. 28, no. 1-2, pp. 137–149, 2009.

[62] V. V. Artym, A. L. Kindzelskii, W. T. Chen, and H. R. Petty, "Molecular proximity of seprase and the urokinase-type plasminogen activator receptor on malignant melanoma cell membranes: dependence on β1 integrins and the cytoskeleton," *Carcinogenesis*, vol. 23, no. 10, pp. 1593–1602, 2002.

[63] D. Oxmann, J. Held-Feindt, A. M. Stark, K. Hattermann, T. Yoneda, and R. Mentlein, "Endoglin expression in metastatic breast cancer cells enhances their invasive phenotype," *Oncogene*, vol. 27, no. 25, pp. 3567–3575, 2008.

[64] J. Wyckoff, W. Wang, E. Y. Lin et al., "A paracrine loop between tumor cells and macrophages is required for tumor cell migration in mammary tumors," *Cancer Research*, vol. 64, no. 19, pp. 7022–7029, 2004.

[65] A. S. Verkman, "Aquaporins: translating bench research to human disease," *Journal of Experimental Biology*, vol. 212, no. 11, pp. 1707–1715, 2009.

[66] D. Khaitan, U. T. Sankpal, B. Weksler et al., "Role of KCNMA1 gene in breast cancer invasion and metastasis to brain," *BMC Cancer*, vol. 9, article no. 258, 2009.

[67] J. H. Lee, M. E. Miele, D. J. Hicks et al., "KiSS-1, a novel human malignant melanoma metastasis-suppressor gene," *Journal of the National Cancer Institute*, vol. 88, no. 23, pp. 1731–1737, 1996.

[68] F. Shirasaki, M. Takata, N. Hatta, and K. Takehara, "Loss of expression of the metastasis suppressor gene KiSS1 during melanoma progression and its association with LOH of chromosome 6q16.3-q23," *Cancer Research*, vol. 61, no. 20, pp. 7422–7425, 2001.

[69] J. T. Dong, H. Suzuki, S. S. Pin et al., "Down-regulation of the KAI1 metastasis suppressor gene during the progression of human prostatic cancer infrequently involves gene mutation or allelic loss," *Cancer Research*, vol. 56, no. 19, pp. 4387–4390, 1996.

[70] R. J. Guan, H. L. Ford, Y. Fu, Y. Li, L. M. Shaw, and A. B. Pardee, "Drg-1 as a differentiation-related, putative metastatic suppressor gene in human colon cancer," *Cancer Research*, vol. 60, no. 3, pp. 749–755, 2000.

[71] M. A. Shah, N. Kemeny, A. Hummer et al., "Drg1 expression in 131 colorectal liver metastases: correlation with clinical variables and patient outcomes," *Clinical Cancer Research*, vol. 11, no. 9, pp. 3296–3302, 2005.

[72] D. H. Nam, H. M. Jeon, S. Kim et al., "Activation of Notch signaling in a xenograft model of brain metastasis," *Clinical Cancer Research*, vol. 14, no. 13, pp. 4059–4066, 2008.

[73] M. Mareel, M. J. Oliveira, and I. Madani, "Cancer invasion and metastasis: interacting ecosystems," *Virchows Archiv*, vol. 454, no. 6, pp. 599–622, 2009.

[74] L. J. Stafford, K. S. Vaidya, and D. R. Welch, "Metastasis suppressors genes in cancer," *International Journal of Biochemistry and Cell Biology*, vol. 40, no. 5, pp. 874–891, 2008.

[75] L. Dollé, H. T. Depypere, and M. E. Bracke, "Anti-invasive and anti-metastasis strategies: new roads, new tools and new hopes," *Current Cancer Drug Targets*, vol. 6, no. 8, pp. 729–751, 2006.

[76] P. F. Davies, J. A. Spaan, and R. Krams, "Shear stress biology of the endothelium," *Annals of Biomedical Engineering*, vol. 33, no. 12, pp. 1714–1718, 2005.

[77] V. Thamilselvan, D. H. Craig, and M. D. Basson, "FAK association with multiple signal proteins mediates pressure-induced colon cancer cell adhesion via a Src-dependent PI3K/Akt pathway," *FASEB Journal*, vol. 21, no. 8, pp. 1730–1741, 2007.

[78] A. Von Sengbusch, P. Gassmann, K. M. Fisch, A. Enns, G. L. Nicolson, and J. Haier, "Focal adhesion kinase regulates metastatic adhesion of carcinoma cells within liver sinusoids," *American Journal of Pathology*, vol. 166, no. 2, pp. 585–596, 2005.

[79] B. Nieswandt, M. Hafner, B. Echtenacher, and D. N. Männel, "Lysis of tumor cells by natural killer cells in mice is impeded

by platelets," *Cancer Research*, vol. 59, no. 6, pp. 1295–1300, 1999.

[80] E. Sahai, "Illuminating the metastatic process," *Nature Reviews Cancer*, vol. 7, no. 10, pp. 737–749, 2007.

[81] P. F. Lalor, W. K. Lai, S. M. Curbishley, S. Shetty, and D. H. Adams, "Human hepatic sinusoidal endothelial cells can be distinguished by expression of phenotypic markers related to their specialised functions in vivo," *World Journal of Gastroenterology*, vol. 12, no. 34, pp. 5429–5439, 2006.

[82] D. M. Brown and E. Ruoslahti, "Metadherin, a cell surface protein in breast tumors that mediates lung metastasis," *Cancer Cell*, vol. 5, no. 4, pp. 365–374, 2004.

[83] N. Saito, T. Hatori, N. Murata et al., "Comparison of metastatic brain tumour models using three different methods: the morphological role of the pia mater," *International Journal of Experimental Pathology*, vol. 89, no. 1, pp. 38–44, 2008.

[84] L. C. Huysentruyt, P. Mukherjee, D. Banerjee, L. M. Shelton, and T. N. Seyfried, "Metastatic cancer cells with macrophage properties: evidence from a new murine tumor model," *International Journal of Cancer*, vol. 123, no. 1, pp. 73–84, 2008.

[85] P. D. Bos, X. H. F. Zhang, C. Nadal et al., "Genes that mediate breast cancer metastasis to the brain," *Nature*, vol. 459, no. 7249, pp. 1005–1009, 2009.

[86] C. Khanna, X. Wan, S. Bose et al., "The membrane-cytoskeleton linker ezrin is necessary for osteosarcoma metastasis," *Nature Medicine*, vol. 10, no. 2, pp. 182–186, 2004.

[87] H. Ji, M. R. Ramsey, D. N. Hayes et al., "LKB1 modulates lung cancer differentiation and metastasis," *Nature*, vol. 448, no. 7155, pp. 807–810, 2007.

[88] D. P. Fitzgerald, D. Palmieri, E. Hua et al., "Reactive glia are recruited by highly proliferative brain metastases of breast cancer and promote tumor cell colonization," *Clinical and Experimental Metastasis*, vol. 25, no. 7, pp. 799–810, 2008.

[89] W. P. J. Leenders, B. Küsters, and R. M. W. De Waal, "Vessel co-option: how tumors obtain blood supply in the absence of sprouting angiogenesis," *Endothelium*, vol. 9, no. 2, pp. 83–87, 2002.

[90] B. Kusters, J. R. Westphal, D. Smits et al., "The pattern of metastasis of human melanoma to the central nervous system is not influenced by integrin $\alpha v\beta 3$ expression," *International Journal of Cancer*, vol. 92, no. 2, pp. 176–180, 2001.

[91] J. Folkman and D. Hanahan, "Switch to the angiogenic phenotype during tumorigenesis," *Princess Takamatsu Symposia*, vol. 22, pp. 339–347, 1991.

[92] S. K. Lee, S. Huang, W. Lu, D. C. Lev, and J. E. Price, "Vascular endothelial growth factor expression promotes the growth of breast cancer brain metastases in nude mice," *Clinical and Experimental Metastasis*, vol. 21, no. 2, pp. 107–118, 2004.

[93] W. Xia, P. Unger, L. Miller, J. Nelson, and I. H. Gelman, "The Src-suppressed C kinase substrate, SSeCKS, is a potential metastasis inhibitor in prostate cancer," *Cancer Research*, vol. 61, no. 14, pp. 5644–5651, 2001.

[94] G. Bergers, R. Brekken, G. McMahon et al., "Matrix metalloproteinase-9 triggers the angiogenic switch during carcinogenesis," *Nature Cell Biology*, vol. 2, no. 10, pp. 737–744, 2000.

[95] I. Roodink, J. Raats, B. Van Der Zwaag et al., "Plexin D1 expression is induced on tumor vasculature and tumor cells: a novel tarqet for diagnosis and therapy?" *Cancer Research*, vol. 65, no. 18, pp. 8317–8323, 2005.

[96] D. Palmieri, D. Fitzgerald, S. M. Shreeve et al., "Analyses of resected human brain metastases of breast cancer reveal the association between up-regulation of hexokinase 2 and poor prognosis," *Molecular Cancer Research*, vol. 7, no. 9, pp. 1438–1445, 2009.

[97] R. J. Weil, D. C. Palmieri, J. L. Bronder, A. M. Stark, and P. S. Steeg, "Breast cancer metastasis to the central nervous system," *American Journal of Pathology*, vol. 167, no. 4, pp. 913–920, 2005.

[98] H. Yaguchi, N. Ohkura, T. Tsukada, and K. Yamaguchi, "Menin, the multiple endocrine neoplasia type 1 gene product, exhibits GTP-hydrolyzing activity in the presence of the tumor metastasis suppressor nm23," *The Journal of Biological Chemistry*, vol. 277, no. 41, pp. 38197–38204, 2002.

[99] T. Ouatas, M. Salerno, D. Palmieri, and P. S. Steeg, "Basic and translational advances in cancer metastasis: Nm23," *Journal of Bioenergetics and Biomembranes*, vol. 35, no. 1, pp. 73–79, 2003.

[100] M. Sarris, R. A. Scolyer, M. Konopka, J. F. Thompson, C. G. Harper, and S. C. Lee, "Cytoplasmic expression of nm23 predicts the potential for cerebral metastasis in patients with primary cutaneous melanoma," *Melanoma Research*, vol. 14, no. 1, pp. 23–27, 2004.

[101] M. J. Seraj, R. S. Samant, M. F. Verderame, and D. R. Welch, "Functional evidence for a novel human breast carcinoma metastasis suppressor, BRMS1, encoded at chromosome 11q13," *Cancer Research*, vol. 60, no. 11, pp. 2764–2769, 2000.

[102] M. J. Seraj, M. A. Harding, J. J. Gildea, D. R. Welch, and D. Theodorescu, "The relationship of BRMS1 and RhoGDI2 gene expression to metastatic potential in lineage related human bladder cancer cell lines," *Clinical and Experimental Metastasis*, vol. 18, no. 6, pp. 519–525, 2000.

[103] Y. Liu, S. El-Naggar, D. S. Darling, Y. Higashi, and D. C. Dean, "Zeb1 links epithelial-mesenchymal transition and cellular senescence," *Development*, vol. 135, no. 3, pp. 579–588, 2008.

[104] M. Wrage, S. Ruosaari, P. P. Eijk et al., "Genomic profiles associated with early micrometastasis in lung cancer: relevance of 4q deletion," *Clinical Cancer Research*, vol. 15, no. 5, pp. 1566–1574, 2009.

[105] H. Grinberg-Rashi, E. Ofek, M. Perelman et al., "The expression of three genes in primary non-small cell lung cancer is associated with metastatic spread to the brain," *Clinical Cancer Research*, vol. 15, no. 5, pp. 1755–1761, 2009.

[106] G. Narla, A. DiFeo, Y. Fernandez et al., "KLF6-SV1 overexpression accelerates human and mouse prostate cancer progression and metastasis," *Journal of Clinical Investigation*, vol. 118, no. 8, pp. 2711–2721, 2008.

[107] D. S. Micalizzi, K. L. Christensen, P. Jedlicka et al., "The Six1 homeoprotein induces human mammary carcinoma cells to undergo epithelial-mesenchymal transition and metastasis in mice through increasing TGF-β signaling," *Journal of Clinical Investigation*, vol. 119, no. 9, pp. 2678–2690, 2009.

[108] C. Blenkiron and E. A. Miska, "miRNAs in cancer: approaches, aetiology, diagnostics and therapy," *Human Molecular Genetics*, vol. 16, no. 1, pp. R106–R113, 2007.

[109] M. K. Wendt, T. M. Allington, and W. P. Schiemann, "Mechanisms of the epithelial-mesenchymal transition by TGF-β," *Future Oncology*, vol. 5, no. 8, pp. 1145–1168, 2009.

[110] T. Dalmay and D. R. Edwards, "MicroRNAs and the hallmarks of cancer," *Oncogene*, vol. 25, no. 46, pp. 6170–6175, 2006.

[111] L. Poliseno, L. Salmena, J. Zhang, B. Carver, W. J. Haveman, and P. P. Pandolfi, "A coding-independent function of gene

and pseudogene mRNAs regulates tumour biology," *Nature*, vol. 465, no. 7301, pp. 1033–1038, 2010.

[112] N. M.A. White, E. Fatoohi, M. Metias, K. Jung, C. Stephan, and G. M. Yousef, "Metastamirs: a stepping stone towards improved cancer management," *Nature Reviews Clinical Oncology*, vol. 8, no. 2, pp. 75–84, 2011.

Hindawi Publishing Corporation
Journal of Oncology
Volume 2012, Article ID 340380, 7 pages
doi:10.1155/2012/340380

Review Article

A Proposal of a Practical and Optimal Prophylactic Strategy for Peritoneal Recurrence

Masafumi Kuramoto,[1] Shinya Shimada,[1] Satoshi Ikeshima,[1] Akinobu Matsuo,[1] Hiroshi Kuhara,[1] Kojiro Eto,[1] and Hideo Baba[2]

[1] *Department of Surgery, Yatsushiro Social Insurance General Hospital, 2-26 Matsuejo, Yatsushiro, Kumamoto 866-8660, Japan*
[2] *Department of Gastroenterological Surgery, Graduate School of Medical Sciences, Kumamoto University, Honjo 1-1-1, Kumamoto 860-8556, Japan*

Correspondence should be addressed to Masafumi Kuramoto, kuramoto@yatsushiro-gh.jp

Received 14 October 2011; Accepted 4 November 2011

Academic Editor: Sushant Kachhap

Peritoneal metastasis, which often arises in patients with advanced gastric cancer, is well known as a miserable and ill-fated disease. Once peritoneal metastasis is formed, it is extremely difficult to defeat. We advocated EIPL (extensive intraoperative peritoneal lavage) as a useful and practical adjuvant surgical technique for those gastric cancer patients who are likely to suffer from peritoneal recurrence. In this paper, we review the effect of EIPL therapy on prevention of peritoneal recurrence on patients with peritoneal free cancer cells without overt peritoneal metastasis (CY+/P−) through the prospective randomized study, and we verified its potential as an optimal and standard prophylactic therapeutic strategy for peritoneal recurrence.

1. Introduction

Significant advances in surgical technique and perioperative management have dramatically improved the survival of patients with advanced gastric cancer; nevertheless, peritoneal metastasis is still the most common cause of tumor progression, and the prognosis of those patients with peritoneal recurrence remains extremely poor [1–5]. The median survival time (MST) of such patients is reported to be 3–6 months [6], and a standard regimen against peritoneal metastasis of gastric cancer has not yet been established [7–10].

In patients with serosal invasion, about half develop peritoneal recurrence and die of this disease during the first 2 years of followup, even if curative resection is performed [11, 12]. Further, it has been reported that the survival time of patients with cytology-positive peritoneal lavage fluid and without macroscopic peritoneal dissemination (CY+/P−) of gastric cancer was almost the same as that of patients with overt peritoneal metastasis [13], and the 5-year survival rate of patients with CY+/P− is only 2% [14]. Once peritoneal metastasis develops, it is quite impossible for patients to survive. The results of several randomized clinical trials which have been published before on perioperative intraperitoneal chemotherapy for patients with CY+/P− or peritoneal metastasis have not shown any significant demonstrations of improvement in survival as compared with surgery alone, especially in patients with peritoneal metastasis [3, 8, 15–18].

It is already generally accepted that peritoneal metastasis is completed by the implantation of peritoneal free cancer cells exfoliated from serosa-invasive tumors. Consequently, it is considered important to prevent peritoneal metastasis before the fixation and progression of free cancer cells on the peritoneum of patients with advanced gastric cancer. This is because the presence of intraperitoneal free cancer cells without macroscopic dissemination could possibly mean a condition where the implantation of cancer cells on the peritoneal wall has not yet occurred. The situation of CY+/P− might be the last opportunity for surgeons to undertake surgical intervention to rescue such patients, and therefore, a reliable and appropriate standard prophylactic treatment needs to be established to prevent CY+/P− gastric cancer developing into peritoneal metastasis.

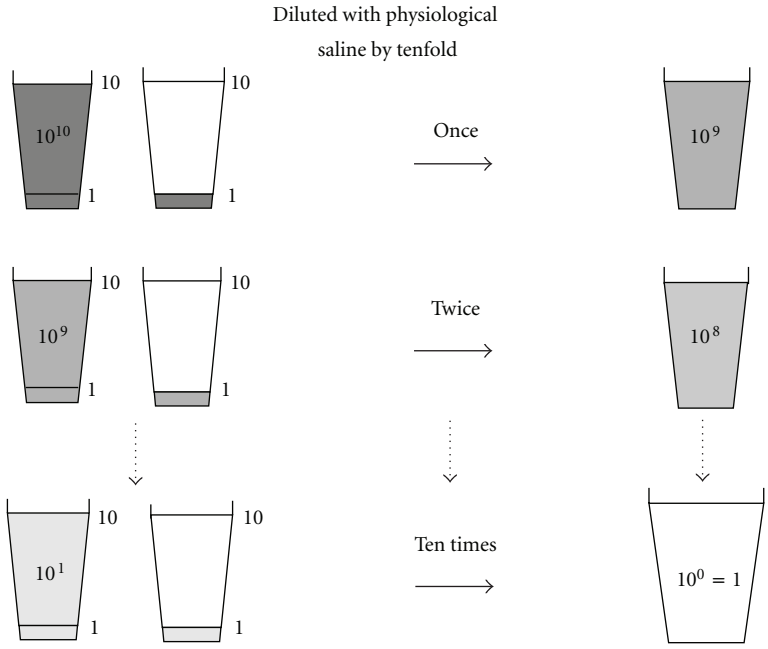

Figure 1: Schema of "limiting dilution method." This method is expected to lead to a logarithmic reduction of numerous cancer cells to zero.

From this point of view, we have been advocating the adoption of "extensive intraoperative peritoneal lavage" (EIPL) as a useful intraoperative technique for an adjuvant therapy to avoid the implantation of cancer cells on the intraperitoneal wall after a potentially curative resection, combined with intraperitoneal chemotherapy (EIPL-IPC). EIPL is very simple and can be performed anywhere and anytime. Also, it has quite an amazing power of reducing the number of intraperitoneal free cancer cells efficiently to potentially zero, analyzed by a detection system of cancer cells using real-time reverse transcriptase-polymerase chain reaction (RT-PCR), and intraperitoneal chemotherapy subsequent to EIPL could play an important role in eradicating any remaining cancer cells. We have confirmed the clinical effectiveness of EIPL by ultrarapid quantitative RT-PCR protocol. Quite a few intraperitoneal free cancer cells could be detected in the washing lavage fluid after 6 to 8 washes. Finally, our recent prospective randomized control study clearly revealed that EIPL-IPC therapy significantly improved the 5-year survival of advanced gastric cancer patients with CY+/P− [19].

In this article, we reviewed the efficacy and advantage of our new adjuvant intraoperative method to reduce the peritoneal recurrence, and clarified the feasibility and validity of adopting this method as the standard prophylactic strategy for the prevention of peritoneal metastasis in advanced gastric cancer patients.

2. Conventional Treatment of CY+ Gastric Cancer

To date, many studies on positive intraperitoneal free cancer cells (CY+) in patients with advanced gastric cancer without overt peritoneal metastasis have been conducted to assess whether CY+ could be a predictive factor. Although most of the studies succeeded in showing the validity of CY+ as a reliable predictive factor, there are not yet any reports concerning drastic and effective therapies for patients with CY+ [20–27]. As mentioned already, the simple existence of free cancer cells in the peritoneal cavity is apparently different from that of peritoneal dissemination; moreover, the status of CY+/P− includes the condition where peritoneal metastasis has not yet occurred. So, we have been focusing on devising a beneficial method that could improve the survival of CY+ patients surgically.

3. EIPL (Extensive Intraoperative Peritoneal Lavage)

We have proposed that EIPL is a quite formidable method for reducing the number of intraperitoneal free cancer cells to potentially zero, just like the so-called "limiting dilution" approach [28]. Briefly, the peritoneal cavity is extensively stirred and washed after the potentially curative operation, which is followed by the complete aspiration of the fluid. This procedure is done 10 times using 1 L of physiological saline. 10 washes of a 1 : 10 dilution result in just 1 cancerous cell from 10^{10} cells in the abdominal cavity (Figure 1). Furthermore, sufficient stirring and washing of the abdominal cavity would remove the cancer cells which merely adhere to the peritoneum. EIPL was performed in five cases of serosa-invasive gastric cancer with CY+/P−, and its efficacy was evaluated by the ultrarapid quantitative RT-PCR protocol, which made it possible to detect mRNA of CEA and CK20 intraoperatively by performing all steps of

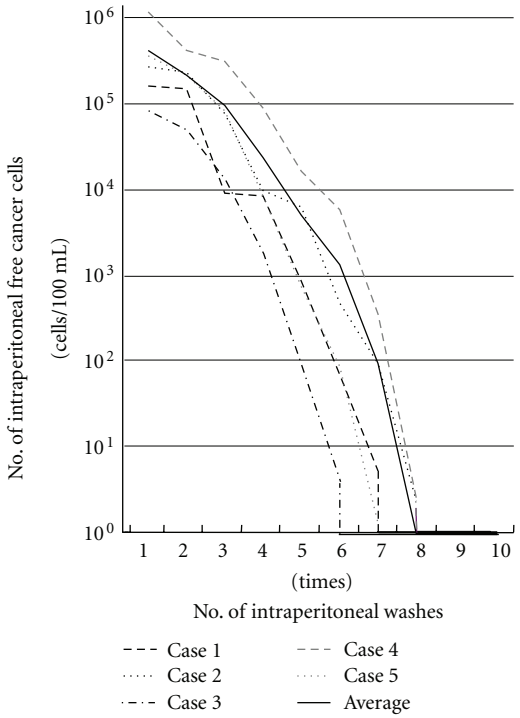

Figure 2: Changes in numbers of intraperitoneal free cancer cells in five gastric cancer patients with CY+ treated by EIPL therapy. The numbers of free cancer cells in 100 mL of samples from the lavage fluid using 1 liter of saline were measured by ulra-rapid RT-PCR. The free cancer cells were serially diluted by 6 to 8 liters of saline and disappeared in washing fluid after that.

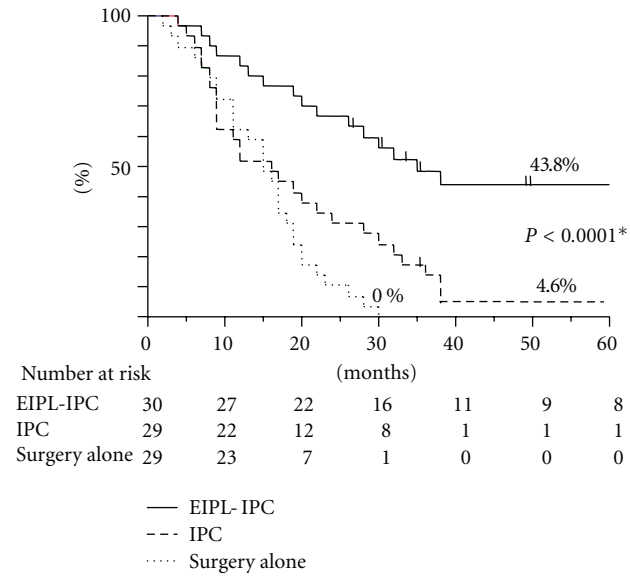

Figure 3: The survival curves for the 88 patients stratified according to the treatments. *By log-rank test.

the procedure in only about 70 minutes. Sequential washing of intraperitoneal free cancer cells of $3.8 \times 10^5 \pm 1.4 \times 10^5$/100 mL of lavage decreased the number to 2.8 ± 1.5 cells by 6 to 8 washes. Free cancer cells were not detected in the fluid after that (Figure 2). On the other hand, $2.8 \times 10^4 \pm 4.5 \times 10^4$ of intraperitoneal free cancer cells still remained in 100 mL of the lavage when not treated with EIPL. Our preliminary subset analysis based on 22 consecutive patients with CY+/P− who underwent curative surgical treatment for advanced gastric cancer, and who were followed up for 2 years or until death, has shown a statistically significant improvement of a 2-year survival rate when treated with EIPL as compared with when not treated with EIPL [29].

4. Clinical Adoption of EIPL-IPC Therapy

Based on our pioneering study, we have advocated EIPL-IPC (intraperitoneal chemotherapy) therapy. After the EIPL treatment, cisplatin (CDDP) is administrated into the abdominal cavity at a dose of 100 mg/body and the solution is drained 1 hour after the injection. In this way, even if only a few cancer cells were to remain, these cells might find it difficult to survive and/or to disseminate due to the effects of IPC.

To clarify the distinct survival effects of EIPL-IPC therapy, we designed a prospective randomized multicenter trial for advanced gastric cancer patients with CY+/P−.

A total of 88 gastric cancer patients with CY+/P− from 1522 patients with advanced gastric cancer at multicenters were enrolled in this study, and were randomly allocated to three groups: surgery alone group, surgery plus intraperitoneal chemotherapy (IPC) group, and surgery plus EIPL and IPC (EIPL-IPC) group. Peritoneal lavage for the surgery alone group and the IPC group was done with 3 liters of saline (1 liter, three times) before the closure of the abdominal wall or IPC, respectively.

The overall 5-year survival rate of patients with EIPL-IPC was 43.8%, and this data was significantly higher than that of the IPC group (4.6%, $P < 0.0001$) and the surgery alone group (0%, $P < 0.0001$), as shown in Figure 3.

Among various recurrent patterns, the EIPL-IPC group had a significantly lower incidence of peritoneal recurrence than either of the other groups. Univariate and multivariate analyses clearly revealed that EIPL was the most significant impact factor.

The results of this study far exceeded our expectations and showed a remarkably better prognosis than previous studies on gastric cancer patients with CY+/P−. For example, a study on the median survival time (MST) of 91 patients with CY+/P− who had potentially curative operations stated survival to be only 386 days [30], and the 5-year overall survival rate has been 13% [31]. In our study, the surgery alone group as well as the IPC group also showed similar results to the reports just cited. Surprisingly, however, in the EIPL-IPC group the overall 5-year survival rate and MST were 42.1% and 35 months, respectively, remarkably significant improvement of both survival and MST. These results were convincing and are promising enough to serve

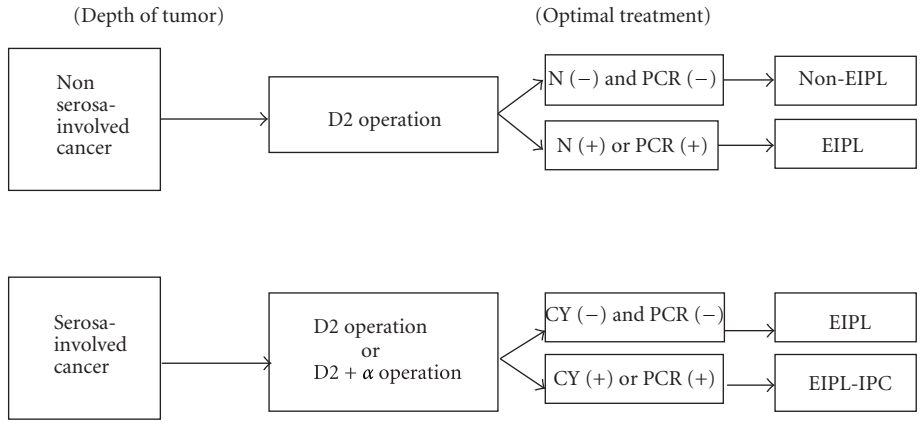

Figure 4: A practical and optimal treatment protocol for advanced gastric cancer. D2 operation: gastrectomy with dissection of group 1 and 2 lymph node [37], N(+): positive lymph node metastasis through operation, N(−): no evidence of lymph node metastasis, PCR: real-time reverse transcriptase-polymerase chain reaction, EIPL: extensive intraoperative peritoneal lavage, IPC: intraperitoneal chemotherapy.

as a solid basis on which to build strong confidence in and high expectations for employing the EIPL-IPC therapy.

5. Further Application of EIPL Therapy

5.1. Application to CY−/P− Gastric Cancer. Despite neither the apparent existence of abdominal free cancer cells nor overt peritoneal metastasis, approximately half of patients with serosa-involved gastric cancer developed peritoneal recurrence after curative operations [27]. In addition, some nonserosa-involved gastric cancers advance to peritoneal recurrence, even though a curative operation has been performed [5, 32–34]. We elucidated the mechanisms of peritoneal recurrence after curative operations for patients with nonserosa-involved gastric cancer.

CEA and CK20 mRNA in the peritoneal lavage samples from 63 patients with nonserosa-involved gastric cancer which were obtained just after laparotomy and after lymph node dissection were examined by an ultrarapid quantitative RT-PCR system [28]. In the peritoneal lavage samples from nonserosa-involved cases after lymph node dissection, CEA or CA20 mRNA were detected in 16 of 63 patients (25.4%) despite no detection of either CEA or CA20 mRNA just after laparotomy. These were not evident in the mucosal (M) tumor, but were detected in three (14.3%), six (46.2%), and seven (53.8%) patients with submucosal (SM), muscularis propria (MP), and subserosal (SS) tumors, respectively. These data suggested the existence of free cancer cells in the peritoneal cavity after lymph node dissection with non-serosa-involved gastric cancer patients. Moreover, our previous study on 1272 gastric cancer patients revealed that 1/257 cases (0.4%) of SM and 6/136 cases (4.4%) of MP developed peritoneal recurrences after potentially curative resections [34]. Among them, 86% of the patients had lymph node metastasis and/or lymphatic invasion. Our results demonstrated that lymph node dissection would be a main factor for spreading viable free cancer cells into the peritoneal cavity. Thus, we came to an assurance that lymph node dissection itself is a cause of peritoneal dissemination, seeding viable cancer cells from the lymphatic vessels to the abdominal cavity. As there should be a low risk of the completion of peritoneal metastasis in such cases with non-serosal-involved gastric cancer, EIPL therapy will demonstrate its effectiveness to the maximum on the prevention of peritoneal recurrences after curative operations.

5.2. Application to Other Abdominal Organ Cancers. We applied EIPL therapy to the miserable disease of pancreatic cancer, where peritoneal recurrence is frequently found and yields a high mortality rate [35]. EIPL therapy was performed consecutively on 15 patients of 39 patients with invasive ductal adenocarcinoma of the pancreas who underwent curative surgical treatment. The peritoneal recurrence rate of the EIPL group was significantly lower than that of the non-EIPL group (6.7% versus 45.8%, $P = 0.013$) and the EIPL therapy was the independent negative risk factor for peritoneal recurrence. On the basis of such attractive data, EIPL therapy is considered to be applicable to various abdominal cancers which are likely to seed in abdominal cavities.

6. Proposal of EIPL Therapy as a Standard Therapeutic Strategy for Prevention of Peritoneal Recurrence

Lymphatic and peritoneal metastasis is well known to be high in advanced gastric cancer while hematogenous metastasis is relatively low [1, 36, 37]. Above all, peritoneal metastasis is the most common cause of tumor progression and death even if curative surgery is performed [1–5]. Once peritoneal metastasis is formed, it becomes extremely difficult for patients to survive through to a cure, though the survival time has become somewhat longer by excellent means

including intravenous and/or intraperitoneal chemotherapy. Several studies have suggested that chemotherapy could possibly result in much better prognosis than would be expected from aggressive surgery for gastric cancer patients with CY+/P−, just like patients with peritoneal metastasis [20, 21, 38, 39]. On the other hand, there is a report which has demonstrated that radical surgery as well as adjuvant chemotherapy should be performed for CY+/P− patients in cases of no lymph node metastasis [40]. This demonstrates that appropriate standard regimens for patients who are likely to progress toward peritoneal metastasis, including CY+/P− patients, has not yet been established.

As already mentioned, the situation of CY+/P− means the condition where the implantation of free cancer cells derived from the primary tumor has not yet occurred. We suppose there should be apparent differences between the conditions of CY+/P− and peritoneal metastasis which would require different management strategy. Therefore, it is considered reasonable and relevant to focus on devising some effective surgical measures to prevent peritoneal recurrence, accompanied by appropriate and respectable radical resection. Although the Dutch report has described the high postoperative morbidity and mortality after gastrectomy with D2 lymph node dissection [41], radical resections with D2 lymphadenectomy appear to be feasible and safe for patients in Japan [20, 21, 38, 39]. In our study, operative morbidity and mortality were 1.5% and 0.5%, respectively. These results show that potential benefits of D2 operations would outweigh the risk of morbidity and mortality after the radical operation. Complete extirpation of gastric cancer with a sufficient resection margin from the tumor and removal of metastatic lymph nodes is the only measure that could bring the hope of cure for patients with gastric cancer [1, 36, 37, 42, 43], therefore, advanced gastric cancer should be treated with radical resection even if it is accompanied by CY+/P− because our novel EIPL-IPC regimen would have the power to cancel the CY+ condition.

Lastly, we strongly advocate the adoption of the new treatment protocol for advanced gastric cancer as shown in Figure 4. In case of positive lymph node metastasis through operation or positive molecular detections of CEA and CA20 mRNA in the lavage fluid after lymph node dissection, EIPL is performed even for the patients with non-serosa-involved cancer. Except for overt peritoneal metastasis, all patients with serosa-involved cancer undergo EIPL in principle and IPC therapy is added to the patients with CY+ or PCR (+) in the lavage fluid just after laparotomy. After the proper tumor resection and lymphadenectomy, EIPL (or EIPL-IPC) therapy serves an extremely important role for gastric cancer patients with high peritoneal recurrence risk such as serosal invasion and lymph node metastasis. The innovative EIPL-IPC therapy is very practical and its theoretical basis creates high expectations as to the effects of cytoreduction, potentially to zero. Furthermore, EIPL therapy is simple, not time-consuming, inexpensive, and it is not curtailed by place or time, so it can easily be performed anytime, anywhere. Also, it does not require the use of any special techniques or devices. In addition, a point worthy of special mention is that EIPL itself only has minimal risk for patients.

7. Conclusion

In conclusion, we reviewed clinical studies concerning EIPL therapy, and very favorable results convinced us to advocate EIPL therapy as an optimal treatment protocol for advanced gastric cancer patients. It is our fervent wish that EIPL therapy be adopted as the standard prophylactic strategy for peritoneal recurrence.

References

[1] D. C. Balfour, "Factor of significance in the prognosis of cancer of the stomach," *Annals of Surgery*, vol. 105, no. 5, pp. 733–740, 1973.

[2] Y. Kodera, H. Nakanishi, Y. Yamamura et al., "Prognostic value and clinical implications of disseminated cancer cells in the peritoneal cavity detected by reverse transcriptase-polymerase chain reaction and cytology," *International Journal of Cancer*, vol. 79, no. 4, pp. 429–433, 1998.

[3] M. Ikeguchi, S. Matsumoto, S. Yoshioka et al., "Laparoscopic-assisted intraperitoneal chemotherapy for patients with scirrhous gastric cancer," *Chemotherapy*, vol. 51, no. 1, pp. 15–20, 2005.

[4] M. Hiratsuka, T. Iwanaga, H. Furukawa et al., "Important prognostic factors in surgically treated gastric cancer patients," *Japanese Journal of Cancer and Chemotherapy*, vol. 22, no. 5, pp. 703–708, 1995.

[5] C. H. Yoo, S. H. Noh, D. W. Shin, S. H. Choi, and J. S. Min, "Recurrence following curative resection for gastric carcinoma," *British Journal of Surgery*, vol. 87, no. 2, pp. 236–242, 2000.

[6] Y. Kitamura, K. Hayashi, T. Sasagawa, H. Oguma, and K. Takasaki, "Pilot study of S-1 in patients with disseminated gastric cancer," *Drugs under Experimental and Clinical Research*, vol. 29, no. 3, pp. 125–130, 2003.

[7] C. Kunisaki, H. Shimada, H. Akiyama et al., "Therapeutic outcomes of continuous hyperthermic peritoneal perfusion against advanced gastric cancer with peritoneal carcinomatosis," *Hepato-Gastroenterology*, vol. 53, no. 69, pp. 473–478, 2006.

[8] C. Kunisaki, H. Shimada, M. Nomura, H. Akiyama, M. Takahashi, and G. Matsuda, "Lack of efficacy of prophylactic continuous hyperthermic peritoneal perfusion on subsequent peritoneal recurrence and survival in patients with advanced gastric cancer," *Surgery*, vol. 131, no. 5, pp. 521–528, 2002.

[9] S. Ishizone, F. Maruta, H. Saito et al., "Efficacy of S-1 for patients with peritoneal metastasis of gastric cancer," *Chemotherapy*, vol. 52, no. 6, pp. 301–307, 2006.

[10] L. Suhsien, E. M. Bart, G. M. Stuart, E. Newman, R. S. Berman, and S. P. Hiotis, "Results following resection for stage IV gastric cancer; are better outcomes observed in selected patient subgroups?" *Journal of Surgical Oncology*, vol. 95, no. 2, pp. 118–122, 2007.

[11] U. Ribeiro, J. J. Gama-Rodrigues, A. V. Safatle-Ribeiro et al., "Prognostic significance of intraperitoneal free cancer cells obtained by laparoscopic peritoneal lavage in patients with gastric cancer," *Journal of Gastrointestinal Surgery*, vol. 2, no. 3, pp. 244–249, 1998.

[12] M. Ikeguchi, A. Oka, S. Tsujitani, M. Maeta, and N. Kaibara, "Relationship between area of serosal invasion and intraperitoneal free cancer cells in patients with gastric cancer," *Anticancer Research*, vol. 14, no. 5, pp. 2131–2134, 1994.

[13] T. Boku, Y. Nakane, T. Minoura et al., "Prognostic significance of serosal invasion and free intraperitoneal cancer cells in gastric cancer," *British Journal of Surgery*, vol. 77, no. 4, pp. 436–439, 1990.

[14] E. Bando, Y. Yonemura, K. Taniguchi et al., "Intraoperative lavage for cytological examination in 1,297 patients with gastric carcinoma," *American Journal of Surgery*, vol. 178, no. 3, pp. 256–262, 1999.

[15] W. J. Cunliffe and P. H. Sugarbaker, "Gastrointestinal malignancy: rationale for adjuvant therapy using early postoperative intraperitoneal chemotherapy," *British Journal of Surgery*, vol. 76, no. 10, pp. 1082–1090, 1989.

[16] T. Sautner, F. Hofbauer, D. Depisch, R. Schiessel, and R. Jakesz, "Adjuvant intraperitoneal cisplatin chemotherapy does not improve long-term survival after surgery for advanced gastric cancer," *Journal of Clinical Oncology*, vol. 12, no. 5, pp. 970–974, 1994.

[17] A. Hagiwara, T. Takahashi, O. Kojima et al., "Prophylaxis with carbon-adsorbed mitomycin against peritoneal recurrence of gastric cancer," *Lancet*, vol. 339, no. 8794, pp. 629–631, 1992.

[18] J. H. Cheong, J. Y. Shen, C. S. Song et al., "Early postoperative intraperitoneal chemotherapy following cytoreductive surgery in patients with very advanced gastric cancer," *Annals of Surgical Oncology*, vol. 14, no. 1, pp. 61–68, 2007.

[19] M. Kuramoto, S. Shimada, S. Ikeshima et al., "Extensive intraoperative peritoneal lavage as a standard prophylactic strategy for peritoneal recurrence in patients with gastric carcinoma," *Annals of Surgery*, vol. 250, no. 2, pp. 242–246, 2009.

[20] C. C. Wu, J. T. Chen, M. C. Chang et al., "Optimal surgical strategy for potentially curable serosa-involved gastric carcinoma with intraperitoneal free cancer cells," *Journal of the American College of Surgeons*, vol. 184, no. 6, pp. 611–617, 1997.

[21] N. Hayes, J. Wayman, V. Wadehra, D. Scott, S. Raimes, and S. Griffin, "Peritoneal cytology in the surgical evaluation of gastric carcinoma," *British Journal of Cancer*, vol. 79, no. 3-4, pp. 520–524, 1999.

[22] T. Fujimoto, B. Zhang, S. Minami, X. Wang, Y. Takahashi, and M. Mai, "Evaluation of intraoperative intraperitoneal cytology for advanced gastric carcinoma," *Oncology*, vol. 62, no. 3, pp. 201–208, 2002.

[23] H. R. Rosen, G. Jatzko, S. Repse et al., "Adjuvant intraperitoneal chemotherapy with carbon-adsorbed mitomycin in patients with gastric cancer: results of a randomized multicenter trial of the Austrian Working Group for Surgical Oncology," *Journal of Clinical Oncology*, vol. 16, no. 8, pp. 2733–2738, 1998.

[24] R. Hamazoe, M. Maeta, and N. Kaibara, "Intraperitoneal thermochemotherapy for prevention of peritoneal recurrence of gastric cancer: final results of a randomized controlled study," *Cancer*, vol. 73, no. 8, pp. 2048–2052, 1994.

[25] Y. Yonemura, I. Ninomiya, M. Kaji et al., "Prophylaxis with intraoperative chemohyperthermia against peritoneal recurrence of serosal invasion-positive gastric cancer," *World Journal of Surgery*, vol. 19, no. 3, pp. 450–455, 1995.

[26] W. Yu, I. Whang, I. Suh, A. Averbach, D. Chang, and P. H. Sugarbaker, "Prospective randomized trial of early postoperative intraperitoneal chemotherapy as an adjuvant to resectable gastric cancer," *Annals of Surgery*, vol. 228, no. 3, pp. 347–354, 1998.

[27] S. Fujimoto, M. Takahashi, T. Mutou, K. Kobayashi, and T. Toyosawa, "Successful intraperitoneal hyperthermic chemoperfusion for the prevention of postoperative peritoneal recurrence in patients with advanced gastric carcinoma," *Cancer*, vol. 85, no. 3, pp. 529–534, 1999.

[28] T. Marutsuka, S. Shimada, K. Shiomori et al., "Mechanisms of peritoneal metastasis after operation for non-serosa-invasive gastric carcinoma: an ultrarapid detection system for intraperitoneal free cancer cells and a prophylactic strategy for peritoneal metastasis," *Clinical Cancer Research*, vol. 9, no. 2, pp. 678–685, 2003.

[29] S. Shimada, E. Tanaka, T. Marutsuka et al., "Extensive intraoperative peritoneal lavage and chemotherapy for gastric cancer patients with peritoneal free cancer cells," *Gastric Cancer*, vol. 5, no. 3, pp. 168–172, 2002.

[30] Y. Kodera, Y. Yamamura, Y. Shimizu et al., "Peritoneal washing cytology: prognostic value of positive findings in patients with gastric carcinoma undergoing a potentially curative resection," *Journal of Surgical Oncology*, vol. 72, no. 2, pp. 60–65, 1999.

[31] R. Rosenberg, H. Nekarda, P. Bauer, U. Schenck, H. Hoefler, and J. R. Siewert, "Free peritoneal tumour cells are an independent prognostic factor in curatively resected stage IB gastric carcinoma," *British Journal of Surgery*, vol. 93, no. 3, pp. 325–331, 2006.

[32] S. Abe, H. Yoshimura, H. Tabara et al., "Curative resection of gastric cancer: limitation of peritoneal lavage cytology in predicting the outcome," *Journal of Surgical Oncology*, vol. 59, no. 4, pp. 226–229, 1995.

[33] F. Bozzetti, G. Bonfanti, and A. Morabito, "A multifactorial approach for the prognosis of patients with carcinoma of the stomach after curative resection," *Surgery Gynecology and Obstetrics*, vol. 162, no. 3, pp. 229–234, 1986.

[34] S. Shimada, Y. Yagi, K. Shiomori et al., "Characterization of early gastric cancer and proposal of the optimal therapeutic strategy," *Surgery*, vol. 129, no. 6, pp. 714–719, 2001.

[35] K. Yamamoto, S. Shimada, M. Hirota, Y. Yagi, M. Matsuda, and H. Baba, "EIPL (extensive intraoperative peritoneal lavage) therapy significantly reduces peritoneal recurrence after pancreatectomy in patients with pancreatic cancer," *International Journal of Oncology*, vol. 27, no. 5, pp. 1321–1328, 2005.

[36] K. Maruyama, "The most important prognostic factor for gastric cancer patients. A study using univariate and multivariate analyses," *Scandinavian Journal of Gastroenterology*, vol. 22, no. 133, pp. 63–68, 1987.

[37] Japanese Research Society for Gastric Cancer. Japanese Classification of Gastric Carcinoma, 1st English Edition. Tokyo, Japan, Kanehara, 1999.

[38] Y. Yamamura, S. Ito, Y. Mochizuki, H. Nakanishi, M. Tatematsu, and Y. Kodera, "Distribution of free cancer cells in the abdominal cavity suggests limitations of bursectomy as an essential component of radical surgery for gastric carcinoma," *Gastric Cancer*, vol. 10, no. 1, pp. 24–28, 2007.

[39] T. Mori, Y. Fujiwara, Y. Sugita et al., "Application of molecular diagnosis for detection of peritoneal micrometastasis and evaluation of preoperative chemotherapy in advanced gastric carcinoma," *Annals of Surgical Oncology*, vol. 11, no. 1, pp. 14–20, 2004.

[40] H. Saito, K. Kihara, H. Kuroda, T. Matsunaga, S. Tatebe, and M. Ikeguchi, "Surgical outcomes for gastric cancer patients with intraperitoneal free cancer cell, but no macroscopic peritoneal metastasis," *Journal of Surgical Oncology*, vol. 104, no. 5, pp. 534–537, 2011.

[41] J. Bonenkamp, I. Songun, J. Hermans et al., "Randomised comparison of morbidity after D1 and D2 dissection for gastric cancer in 996 Dutch patients," *Lancet*, vol. 345, no. 8952, pp. 742–748, 1995.

[42] L. E. Harrison, M. S. Karpeh, and M. F. Brennan, "Extended lymphadenectomy is associated with a survival benefit for node-negative gastric cancer," *Journal of Gastrointestinal Surgery*, vol. 2, no. 2, pp. 126–131, 1998.

[43] H. Zhang, C. Liu, D. Wu et al., "Does D3 surgery offer a better survival outcome compared to D1 surgery for gastric cancer? A result based on a hospital population of two decades as taking D2 surgery for reference," *BMC Cancer*, vol. 10, article 308, 2010.